Annu. Rev. Astron. Astrophys. 2000. 38:379–425

GAMMA-RAY BURST AFTERGLOWS

Jan van Paradijs,[1*] Chryssa Kouveliotou,[2] and Ralph A. M. J. Wijers[3]

[1]*Astronomical Institute 'Anton Pannekoek', University of Amsterdam, Kruislaan 403, 1098 SJ Amsterdam, The Netherlands and Department of Physics, University of Alabama in Huntsville, Huntsville, AL 35899*

[2]*Universities Space Research Association, NASA Marshall Space Flight Center, SD–50, Huntsville, AL 35812; e-mail: chryssa.kouveliotou@iss.msfc.nasa.gov*

[3]*Department of Physics & Astronomy, State University of New York, Stony Brook, NY 11794-3800; e-mail: rwijers@astro.sunysb.edu*

Key Words gamma-ray bursts, compact objects, cosmology, particle acceleration, shocks, supernovae

■ **Abstract** The discovery of counterparts in X-ray and optical to radio wavelengths has revolutionized the study of γ-ray bursts, until recently the most enigmatic of astrophysical phenomena. We now know that γ-ray bursts are the biggest explosions in nature, caused by the ejection of ultrarelativistic matter from a powerful energy source and its subsequent collision with its environment. We have just begun to uncover a connection between supernovae and γ-ray bursts, and are finally constraining the properties of the ultimate source of γ-ray burst energy. We review here the observations that have led to this breakthrough in the field; we describe the basic theory of the fireball model and discuss the theoretical understanding that has been gained from interpreting the new wealth of data on γ-ray bursts.

Ik zie een ster
en onder mij
zakt de aarde langzaam weg.

I see a star
and beneath me
the Earth slowly falls away.

1. INTRODUCTION

The very first model of γ-ray bursts was proposed by Colgate (1968, 1974) even before γ-ray bursts had been discovered; the model invoked γ-ray emission by accelerated particles at the breakout of a shock from a supernova progenitor's photosphere.

*deceased

Cosmic γ-ray bursts (GRBs) were first reported in 1973 by Klebesadel et al (1973), who in their discovery paper pointed out the lack of evidence for a connection between GRBs and supernovae as proposed by Colgate. It is an interesting twist of history that a quarter-century later, observations of the low-energy afterglows of GRBs have provided evidence that at least some GRBs originate from a probably rare type of supernova. The return to a discarded GRB model that preceded the discovery of GRBs is part of the flood of results that have become available since the initial discoveries of X-ray (Costa et al 1997b), optical (van Paradijs et al 1997), and radio (Frail et al 1997c) afterglows of GRBs. The review of these results is the subject of this paper.

Cavallo & Rees (1978) and Schmidt (1978) realized that the very small sizes (implied by a short variability time, δt) and high fluxes of GRBs ($F_\gamma \lesssim 10^{-4}$ erg/cm^2 s) implied a high photon density at the source. This, in turn, implied that photon-photon scattering would prevent emission of the observed MeV photons for any GRB population more distant than ~1 kpc (unless the source were expanding ultrarelativistically). Cavallo & Rees (1978) formalized the salient source properties into a single *compactness parameter* given by

$$\theta_* = \frac{L\sigma_{\rm T}}{m_{\rm p}c^3R} \simeq \frac{F_\gamma d^2 \sigma_{\rm T}}{m_{\rm p}c^4\delta t} \sim 1 F_{\gamma-4} d^2_{\rm kpc}/(\delta t)_{\rm ms} \sim 10^{12} F_{\gamma-4} d^2_{\rm Gpc}/(\delta t)_{\rm ms}, \quad (1)$$

where $F_{\gamma-4} = F_\gamma/10^{-4}$ erg cm^{-2} s^{-1}, $\sigma_{\rm T}$ is the Thompson electron scattering cross section, $m_{\rm p}$ is the proton mass; L, d are the luminosity and distance of the GRB source, respectively; and $R = c\delta t$ is the radius of the emitting region. Barring relativistic expansion, $\theta_* \gtrsim 1$ implies that the source is optically thick for $\gamma\gamma$ interactions, and cannot be a copious emitter of high-energy photons. The preceding numerical values therefore suggest that nonrelativistic GRB sources would have to be in the Galaxy, and conversely, extragalactic GRBs would have to come from very relativistic sources.

Early indications against a Euclidean space distribution of GRBs was the apparent lack of very weak GRBs (Fishman et al 1978). This result anticipated by about a decade the discussion on the GRB distance scale in the early and mid-1990s. A detailed discussion of this issue, in particular the extent to which this result reflected instrumental effects, was given by Hurley (1986).

In spite of this uncertainty, by the mid-1980s there was a general belief that GRBs originate from galactic neutron stars—a belief that was supported by the cyclotron lines in the spectra of some GRBs reported by the Ginga team (Murakami et al 1988, Fenimore et al 1988), and by line features near 500 keV reported by the Konus team (Mazets et al 1981).

A galactic disc population of neutron stars was firmly excluded as the source of GRBs, based on the results of the first 6 months of BATSE observations, which showed that the GRB sky distribution is isotropic and that there is a strong lack of very faint GRBs (Meegan et al 1992). With the increasing number of GRBs detected with BATSE, the isotropy has become strongly established (Briggs et al 1996). The lack of very faint GRBs shows up as a turnover in the cumulative log $N(>P)$ distribution (here P is the GRB peak flux); for the brightest bursts,

the slope of the distribution follows the Euclidean value of $-3/2$, but below $P \sim 5$ ph/cm^2 s ($\sim 10^{-6}$ ergs/cm^2 s) the slope decreases and becomes as low as ~ -0.6 at the faint end of the distribution (see Paciesas et al 1999 for a review; also Figure 19).

The statistical properties of GRBs are naturally explained if their typical distances are measured in Gpc (the cosmological distance scale; Paczyński 1986, Usov & Chibisov 1975), across which inhomogeneity in the distribution of luminous matter is averaged out (see Condon 1999 for a sky map of extragalactic radio sources nicely illustrating this point). The turnover in the log $N(>P)$ is the direct consequence of the effect of cosmological redshift on the observed GRB *rates* (downward shift of the low P end of the curve) and the GRB *peak fluxes* (leftward shift of the low P end of the curve).

However, there was a countervailing view that GRBs arise from neutron stars in a large galactic corona (Shklovskii & Mitrofanov 1985, Brainerd 1992, Podsiadlowski et al 1995, Lamb 1995, Bulik et al 1998), whose size had to be several 100 kpc to mask the offset of the Earth from the galactic center (Shklovskii & Mitrofanov 1985), but not much larger to avoid seeing excess GRBs from M31 (Hakkila et al 1994).

For several years, the GRB distance was the subject of a lively debate (see e.g. Lamb 1995, Paczyński 1995), but this debate did not lead to a consensus. It was generally felt that setting the distance scale would require the identification of possibly long-lived GRB counterparts in other wavebands (Fishman & Meegan 1995).

Independent of which of the two contending distance scales were correct, the compactness problem was severe, and by analogy to e.g. BL Lac objects and other superluminal AGN sources, appeared to require relativistic outflow of the GRB source (Cavallo & Rees 1978). Reviving the idea already hinted at by Cavallo & Rees, Rees & Mészáros (1992) suggested that γ-ray bursts can be produced if part of a relativistic bulk flow is converted back into high-energy photons through particle acceleration in a relativistic shock between the outflow and the circumsource medium. This basic mechanism has been developed into the fireball model, which provides the background of current discussions on GRBs.

Early attempts to find GRB counterparts employed several approaches, some of which are as follows:

1. Archival plate searches for optical transients in small GRB error boxes obtained from the IPN network of satellites through triangulation (Hurley et al 2000a,b). Schaefer et al (1981, 1984) reported the discovery of such transients in the error boxes of several GRBs after extensive searches in the Harvard plate archives. However, Żytkow (1990) and Greiner et al (1990) have argued, on the basis of an analysis of the 3-D distribution of the image in the plate emulsions, that these events are likely plate defects (but see Schaefer 1990).
2. Deep imaging observations (optical, X-ray, and radio) of small error boxes. The aim of these observations was to find out if particular objects appear in

these error boxes with a statistically significant excess, which might qualify them as possible GRB counterparts. These searches were not successful, i.e. they did not lead to a convincing detection of a source population connected to GRBs. For example, some error boxes were conspicuously devoid of host galaxies (Schaefer 1992, Band et al 1999), which was taken as evidence against extragalactic origin of GRBs or as a problem with specific extragalactic models (Schaefer 1992, Band et al 1999)—though correlations with extragalactic objects were also claimed (e.g. Larson et al 1996, Kolatt & Piran 1996) but disputed (Schaefer 1998, Hurley et al 1997).

3. Simultaneous sky coverage using wide-field optical meteor search cameras (see e.g. Hudec et al 1999, Greiner et al 1993, Krimm et al 1996). In none of the simultaneous photographic images was an optical event detected; the corresponding magnitude limit (for optical flashes lasting as long as the GRB) is $\sim$5th magnitude (McNamara et al 1995).

Extensive summaries of the early attempts to find GRB counterparts have been given by McNamara et al (1995) and Frail & Kulkarni (1995). In hindsight, the lack of success of these early attempts is now understood as a result of these observations being either too late or not sensitive enough.

A breakthrough in the search for GRB counterparts occurred in early 1997, as the result of the first rapidly available (typically within a few hours) accurate (of order several arcminutes) GRB error boxes produced by the two Wide Field Cameras (WFCs; Jager et al 1995) on the Italian-Dutch satellite BeppoSAX (Boella et al 1997). These WFCs are coded-mask cameras with a full field of view of $40^\circ \times 40^\circ$ and a resolution of several arcminutes. GRBs are detected as transient events in the WFC ratemeter (2–20 keV). Trigger information that a GRB occurred is usually provided by the Gamma Ray Burst Monitor (GRBM) on BeppoSAX (Feroci et al 1997), and occassionally by other instruments (e.g. BATSE). In several cases, scans of a BATSE GRB error box with the Proportional Counter Array (PCA) of the Rossi X-ray Timing Explorer (RXTE) have produced relatively accurate GRB error boxes (Takeshima et al 1998; see also Section 5).

This review of the rapid increase in our understanding of GRBs during the last two and a half years thus describes to a large extent the success story of BeppoSAX. To many, the impact of BeppoSAX came as a surprise; however, the direct use of the WFCs for accurate GRB locations was an integral part of the scientific goals of this instrument from the very beginning (see e.g. Hurley 1986). Rapid follow-up observations of these error boxes have unambiguously shown that γ-ray bursts originate from the high-redshift universe.

The review is structured as follows. In Section 2 we provide a brief description of the developments in our understanding of the pure γ-ray aspects of GRBs. In Section 3 we give a very brief description of a simple version of the fireball model, because this provides the current framework of virtually all discussions of GRBs. This is done in the hope that it will guide the description of the observations, although we realize that in a sense we are prejudicial. Yet we feel the overall evidence

for the baseline model is strong enough to proceed this way. In Section 4 we describe the main results of low-energy afterglow studies in the form of highlights. Numerical information and a very short narrative on individual GRB afterglow observations are collected in Section 5, in tabular form. In Section 6 we contrast the results of the afterglow observations with those expected from the simplest fireball models, and discuss the complexities of the GRB emitter that may explain the various discrepancies between the two. In Section 7 we briefly discuss the connection of GRB to host galaxies and cosmological aspects of γ-ray burst follow-up observations, among them a possible connection with the star formation rate history. We briefly mention some implications of the GRB association with galaxies and supernovae for the central engine. In Section 8 we close our review with some comments regarding the impact of GRB follow-up observations on our understanding of the origin of γ-ray bursts, and likely developments in the near future.

2. PROMPT γ-RAY EMISSION

A comprehensive review on γ-ray bursts was written by Fishman & Meegan in 1995. In the five years that have elapsed, BATSE has recorded an additional 1000 GRBs, with a grand total of over 2704 events. The isotropy and inhomogeneity of their distribution is now firmly established, as well as the GRB hardness-duration correlation and bimodal duration distribution (Paciesas et al 1999). The line detection paucity is still a hard fact (Briggs 1999), as is the non-detection of any GRB repeater (Paciesas et al 1999).

With almost 3000 events at hand, the next step in the pure γ-ray field was obtaining elaborate statistics, i.e. statistics on GRB properties that required the use of advanced (sometimes copious) analyses and/or model simulations and fits. This section describes some of the new results that have appeared in the last three years in the literature. Selection criteria applied were the broader impact of the result and its significance in improving our understanding of the physical mechanisms responsible for the production of the prompt γ-ray emission.

2.1 Faint (Untriggered) GRBs

Kommers et al (2000a,b) recently completed a search of six years of archival BATSE data for GRBs that were too faint to activate the real-time on-board burst trigger system (untriggered bursts). They found 873 untriggered events, 551 of which were faint—i.e. below the BATSE detection threshold (their detection efficiency falls below 50% at peak fluxes of 0.16 ph/cm^2 s). The events thus collected have peak fluxes a factor of $\sim$2 lower than those detected with the nominal BATSE trigger criteria.

The latest BATSE $\log N - \log P$ flattens below $P = 0.6$ ph/cm^2 s (Paciesas et al 1999; see Figure 19). The efficiency calculations of Pendleton et al (1998) show that this is a real effect and not an instrumental artifact. The combined faint + BATSE GRB cumulative $\log N - \log P$ distribution also exhibits a dramatic

flattening consistent with the triggered burst results, an indication that few faint bursts have remained undetected with BATSE in the triggered or untriggered mode. However, Stern et al (1999) find no indication of a turnover in a similar study; the discrepancy appears to lie in the trigger efficiency calculation. Kommers et al (2000a) extended the GRB peak flux distribution ($\log N - \log P$) to ~ 0.18 ph/cm^2 s and fitted it with several cosmological models with power-law luminosity distributions. Their results favor models in which the redshift distribution of the GRB rate approximately traces the star formation rate of the Universe.

2.2 A Hubble Relationship for GRBs?

Norris et al (2000) analyzed two samples of GRBs: (1) seven events (six of which have known redshifts) observed with BATSE and BeppoSAX that also have optical or radio counterparts, and (2) the 174 brightest long duration (over 2 s) GRBs. In particular, they computed cross-correlation lags between low (25–50 keV) and high (100–300 keV and >300 keV) energy bands and examined their dependence on burst γ/X peak flux ratio and peak luminosity. They find that the spectral lags and the burst peak intensities are *anticorrelated* in both samples. For the bursts with known redshifts, the connection is well fitted by a power-law, $L_{53} = 1.3 \times (\tau/0.01s)^{-1.15}$ (Figure 1).

A similar claim is made by Ramirez-Ruiz & Fenimore (1999), who have found a relationship between burst variability and absolute burst luminosity. If these results stand the test of time, they may provide a unique way of determining burster distances using the prompt γ-ray data, thus significantly expanding the distance

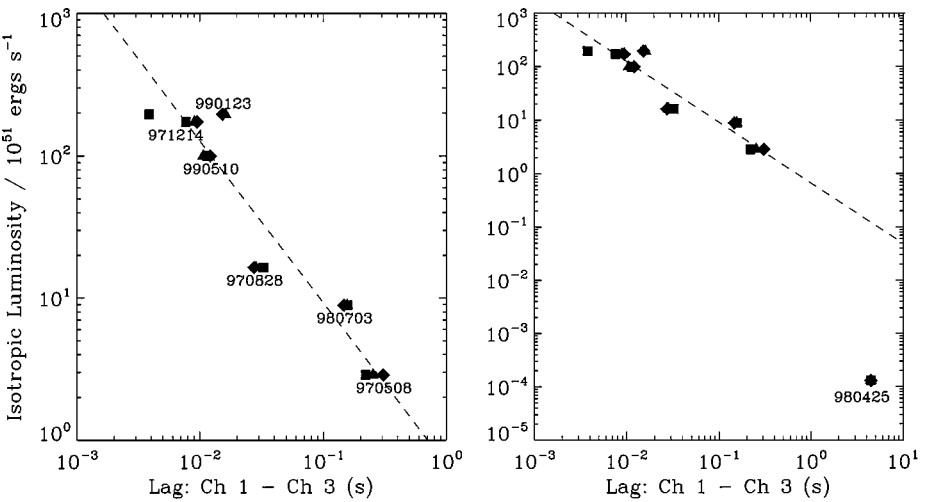

Figure 1 Spectral lag versus luminosity for GRBs with known redshifts. The right panel has an expanded luminosity range to include GRB 980425 (Norris et al 2000).

sample and enabling deep cosmological probing. However, the interpretation of the duration differences between bright and dim bursts previously attributed to cosmological time dilation (Norris et al 1994) has now become very unclear.

2.3 Prompt Gamma-ray "Afterglows"?

Costa et al (1997b) have shown that the BeppoSAX NFI X-ray afterglow light curve of GRB 970228 smoothly joins with the WFC prompt emission, indicating a gradual evolution between prompt and afterglow emission. Similarly, Connors & Hueter (1998) report distinct X-ray afterglow emission from GRB 780506, starting $\sim$2 min after the main event and lasting for about 30 min. Burenin et al (1999) found a power-law decay in one GRANAT/SIGMA burst, albeit with a considerably flatter decay index ($\delta = -0.7$) than a normal ($\delta = -1.0$) afterglow.

Giblin et al (1999) have found evidence in the BATSE data for a prompt high-energy (25–300 keV) afterglow component from GRB 980923. After 40 s of variable emission, the γ-ray light-curve decays with a power-law index, $\delta = -1.81(2)$, in a smooth tail lasting $\sim$400 s. An abrupt change in spectral shape is found when the tail becomes noticeable (Figure 2). More important, Giblin et al (1999) showed that the spectral evolution in the tail mimics that of a cooling synchrotron spectrum, similar to the spectral evolution of the low-energy afterglows of GRBs. Currently, Connaughton (2000) is working on a statistical analysis of GRB tail emission; her results indicate that high-energy tails are prevalent in long GRBs, albeit at low intensity levels. If confirmed, these results will provide evidence for a continuation of the emission during the GRB, and will constrain the emission models.

2.4 TeV Prompt Emission?

Atkins et al (2000) detected photons with energies greater than a few hundred GeV in one out of 54 BATSE searched events with the Milagrito detector, GRB 970417a. The excess has a chance probability of 2.8×10^{-5} of being a background fluctuation, and 1.5×10^{-3} of being a chance coincidence. If this result stands, this would be the highest energy emission ever associated with a GRB—a result that could provide a theoretical challenge for some GRBs because the fluence of GRB 970417a above 50 GeV is an order of magnitude higher than its sub-MeV fluence.

3. BASIC THEORY OF FIREBALLS AND BLAST WAVES

Here we give a brief overview, starting from first principles, of the evolution of spherical blast waves, to set the context for the subsequent discussion of the observations. More complex effects are discussed later (Section 6) in broad terms. Much more about theoretical developments, including many of the technical details, can be found in the review by Piran (1999).

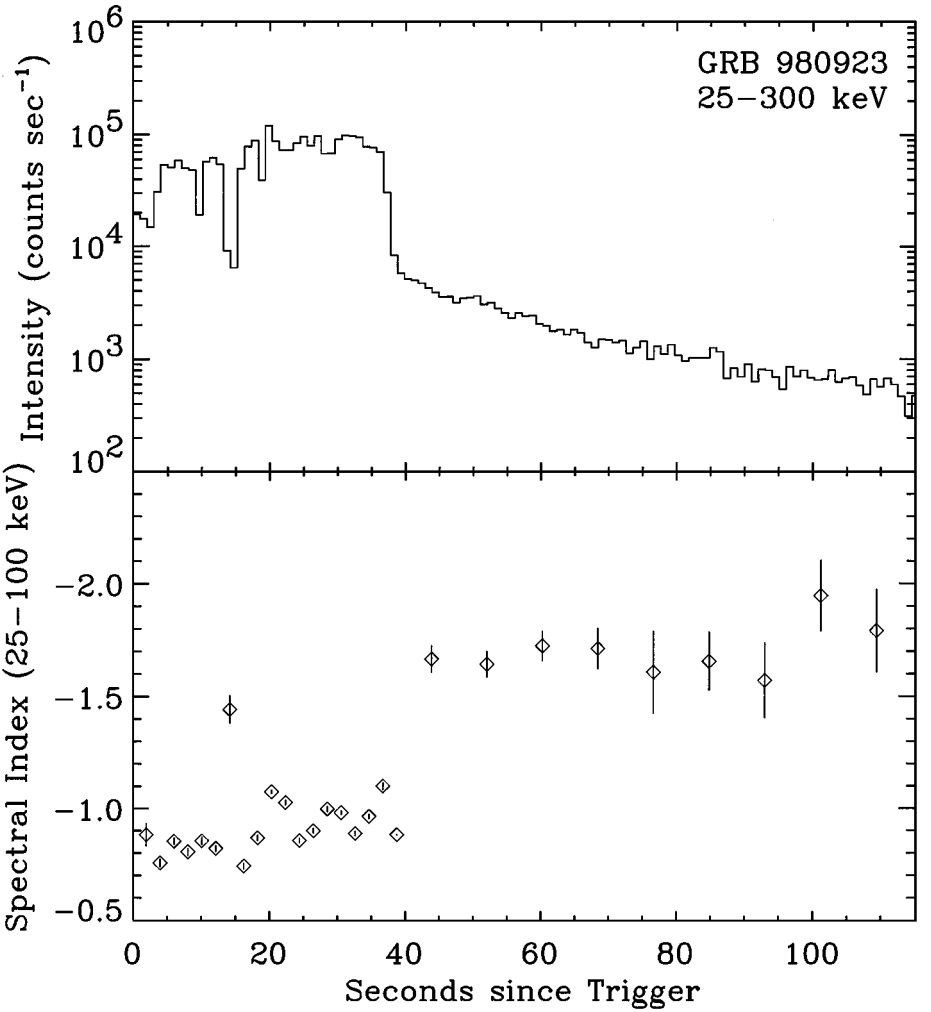

Figure 2 Time history of GRB 980923 (25–300 keV) plotted logarithmically to indicate the first part of the 400 s long tail (*upper panel*). The high-energy photon spectral index as a function of time is shown in the *bottom panel*. Note the abrupt change of the spectral index when the tail begins (Giblin et al 1999).

3.1 Dynamics

As the simplest possible model of gamma-ray burst dynamics, we consider the release of a large amount of energy into a small volume, and follow the resulting explosion. This gives a scenario much like a normal supernova, except that we choose parameters so that the exploding fireball is ultrarelativistic; consequently,

Lorentz contractions play an important role in setting the typical size, duration, and characteristic photon energy to values very different from those of a supernova.

Let us consider the release of an energy $E = 10^{52}\,E_{52}$ erg into a sphere with radius $r_{\rm in}$. A rest mass M_0 of baryons is entrained in the volume, and the energy-to-mass ratio in the initial fireball is thus $\eta = E/M_0c^2$. The evolution from these initial conditions in the context of gamma-ray bursts was pioneered by Cavallo & Rees (1978). It depends on one other parameter, the optical depth, τ, of the fireball. For energy primarily in MeV photons, this will be dominated by photon-photon scattering and pair production, so that $\tau \sim E\sigma_{\rm T}/r_{\rm in}^2 m_{\rm p}c^2$ ($\sigma_{\rm T}$ is the Thompson cross section; see Cavallo & Rees 1978). Given energies appropriate for cosmological GRBs, the optical depth is very high. This means the internal energy can only be converted into kinetic energy, and an adiabatically expanding explosion is initiated.[1] A phase of acceleration now begins, and we can derive the rest-frame temperature T′ and bulk Lorentz factor Γ of the exploding fireball from thermodynamics and energy conservation. Adiabatic expansion dictates that $T'V^{\gamma_a - 1} = const.$, so that the temperature decreases with fireball radius as $T' \propto R^{-1}$ (V is the source volume and γ_a the adiabatic index of the gas; $\gamma_a = 4/3$ for an ultrarelativistic gas). The total internal plus kinetic energy in the frame of an external observer equals $E = \Gamma M_0\,(kT'/m_{\rm p} + c^2)$. For relativistic temperatures, the first term dominates, so that $E \propto \Gamma T' = {\rm const}$. Combined with the thermodynamic relation, we then find that $\Gamma \propto R$. The bulk Lorentz factor of the gas thus increases linearly with radius, until it saturates at a value $\Gamma_0 \sim \eta$, at a radius $r_{\rm c} \sim \eta r_{\rm in}$. Beyond $r_{\rm c}$, the now cold shell coasts along at constant Lorentz factor. Because all the matter in it has moved with $v \simeq c$ since the beginning, it is all piled up in a thin shell with thickness R/Γ^2 near the leading edge (Mészáros & Rees 1993).

As with supernovae, the coasting (or ballistic) phase ends when the energy contained in material swept up by the shell becomes a significant fraction of the total energy. The shell drives a blast wave into the ambient medium, with Lorentz factor $\gamma = \Gamma\sqrt{2}$ (Blandford & McKee 1976); the qualitative evolution of this system is easily understood in the case where the shocked ambient gas does not radiate. While the first material is swept up, the shock moves with Lorentz factor $\gamma \sim \gamma_0 \gg 1$. The shock jump conditions (Blandford & McKee 1976) imply that the rest-frame thermal energy of the mass, m, swept through the shock is γmc^2. In our frame, this energy is blueshifted, so that $E_{\rm s} \sim \gamma^2 mc^2$. This means that about half the initial explosion energy, $E \sim \gamma_0 M_0 c^2$, resides in the swept-up mass when $m \sim m_{\rm dec} = M_0/\gamma_0$, at which point the kinetic energy loss of the shell begins to be significant and the shell deceleration starts in earnest. This is much sooner than in the non-relativistic case, where $m_{\rm dec} \sim M_0$. Well beyond this point, the shocked gas dominates the mass and energy of the expanding system, and thus

[1] Ironically, Cavallo & Rees already recognized and discussed the evolution in this opaque limit. At the time, however, GRBs were believed to be very nearby, and consequently they emphasized the behavior of far lower-energy Galactic versions of the model.

$E \simeq E_s \propto \gamma^2 m = const.$, so γ slowly decreases as $\gamma \propto m^{-1/2}$. For the simplest case of a uniform ambient medium, we then have the standard result for a self-similar relativistic blast wave: $\gamma \propto r^{-3/2}$.

To get the corresponding observer times, we need to introduce the kinematic relation between radius and observer time for a relativistically approaching shell (Rees 1964):

$$dt = dr/2\gamma^2 c. \tag{2}$$

Before serious deceleration, we may set $\gamma = \gamma_{0,2}$ and omit the differentials. For a pure hydrogen medium with number density $n = \rho/m_p$ we then get the radius and observer time of the onset of deceleration (Rees & Mészáros 1992):

$$r_{dec} = \left(3E_0/4\pi\gamma_0^2 n m_p c^2\right)^{1/3} = 3.8 \times 10^{16} \left(E_{52}/n\right)^{1/3} \gamma_{0,2}^{-2/3} \text{ cm} \tag{3}$$

$$t_{dec} = r_{dec}/2\gamma_0^2 c = 63 \left(E_{52}/n\right)^{1/3} \gamma_{0,2}^{-8/3} \text{ s}. \tag{4}$$

Compared with the supernova case, deceleration takes place at somewhat smaller radii, but most starkly within seconds rather than centuries; this is caused by the higher speed of the ejecta, but even more by the two Lorentz factors in Equation 2. The relativistic phase ends and turns into the usual supernova behavior (Sedov 1969 Ch. IV, Taylor 1950) when the energy per particle approaches $m_p c^2$. At that time the Lorentz factor corrections disappear, and we may estimate the size simply as ct, hence

$$t_{NR} = \left(3E_0/4\pi n m_p c^5\right)^{1/3} = 1.2 \left(E_{52}/n\right)^{1/3} \text{yr}. \tag{5}$$

As we see from the preceding qualitative discussion, the relativistic self-similar phase can span many orders of magnitude in time. We now derive the evolution for the blast wave more precisely and generally, following Huang et al (1999; see also Katz & Piran 1997). We assume that material passing through the shock quickly radiates a fraction ϵ of the post-shock thermal energy, and retains the rest as thermal energy. The total (kinetic plus thermal) energy of the burst is then $E = (\gamma - 1)(M_0 + m)c^2 + (1 - \epsilon)\gamma U$, and the radiated energy is $dE_{rad} = \epsilon\gamma(\gamma - 1)c^2\, dm$ (Panaitescu & Mészáros 1998a, Blandford & McKee 1976). From the shock jump conditions, one finds $U = (\gamma - 1)mc^2$, which in combination with $dE = dE_{rad}$ gives

$$\frac{d\gamma}{dm} = -\frac{\gamma^2 - 1}{M_0 + \epsilon m + 2(1 - \epsilon)\gamma m}. \tag{6}$$

For fully radiative ($\epsilon = 1$) and fully adiabatic ($\epsilon = 0$) blast waves, one can write analytic solutions for the expansion. Equation 6 differs somewhat from the sometimes quoted

$$\frac{d\gamma}{dm} = -\frac{\gamma^2 - 1}{M}, \tag{7}$$

in which M is the total rest-frame mass (inclusive of mass equivalent of internal energy; Chiang & Dermer 1999, Katz 1994b). For $\epsilon = 1$, the forms are equivalent, but the adiabatic form of Equation 7 is only valid in the ultrarelativistic case: its solution near $\gamma = 1$ should yield the classical Sedov-Taylor solution but does not. Equation 6 does yield the Sedov-Taylor solution in the non-relativistic limit.

3.1.1 Fully Radiative Case, $\epsilon = 1$ The equation of motion is easily integrated to give (Blandford & McKee 1976, Huang et al 1999, Katz & Piran 1997)

$$\left(\frac{\gamma - 1}{\gamma + 1}\right)\left(\frac{\gamma_0 + 1}{\gamma_0 - 1}\right) = \left(\frac{M_0 + m_0}{M_0 + m}\right)^2, \tag{8}$$

where $\gamma_0 \sim \eta/2$, $m_0 \sim M_0/\eta$ are the initial conditions of the deceleration. The ultrarelativistic limit is obtained for $M_0 \gg m$, since the deceleration starts in that limit, and the large radiative losses mean that the shock comes to a halt after having swept up only a few times m_0. Expanding Equation 8, we obtain $\gamma m = M_0$, i.e. $\gamma \propto m^{-1}$. For a uniform ambient medium, this gives the well-known $\gamma \propto r^{-3}$. Inserting this into the kinematic relation between radius and observer time (Equation 2), we find that $\gamma \propto t^{-3/7}$ and $r \propto t^{1/7}$: the Lorentz factor decreases substantially at very slowly changing radius. In the non-relativistic limit, the solution becomes $\beta \propto m^{-1}$, which for a uniform medium is the snowplow (radiative) phase of supernova remnant expansion.

3.1.2 Adiabatic Case, $\epsilon = 0$ The equation of motion for this case is easily integrated to give $\gamma M_0 + (\gamma^2 - 1)m = const.$ To interpret this result, we subtract M_0 and multiply by c^2, and note that the result is the sum of thermal and bulk kinetic energies of the blast wave, hence

$$(\gamma - 1)M_0c^2 + (\gamma^2 - 1)mc^2 = E_{\rm K0}, \tag{9}$$

where $E_{\rm K0}$ is a constant. In the ultrarelativistic limit ($m \gg M_0/\gamma$ and $\gamma \gg 1$), this implies $\gamma^2 m = const.$ For a uniform ambient medium, this then gives $\gamma \propto r^{-3/2}$ as derived qualitatively above. With the kinematic r–t relation, this then gives $\gamma \propto t^{-3/8}$ and $r \propto t^{1/4}$. This demonstrates that although the self-similar relativistic case can cover 6–7 orders of magnitude in time, the range in radii it covers is not nearly as large. In the non-relativistic limit ($\gamma \sim 1, m \gg M_0$) we get $\beta \propto r^{-3/2}$, which is the proper Sedov-Taylor solution.

The above relations define (the limiting cases of) the dynamical behavior of the blast wave. Unfortunately, the great distances make the blast waves unresolved on the sky, so we cannot directly test the relations between r, t, and β, γ. [The scintillation size determination of GRB 970508 (Frail et al 1997c) is the one exception to this.] Therefore, we will have to describe the flux and spectrum of radiation from the expanding shock before we can find direct tests of our model from data.

3.2 Radiation

The material behind the shock has relativistic temperatures; because energy transfer between particles in two-body collisions becomes less efficient with increasing temperature, many common emission mechanisms fare poorly in the shock-heated gas. The one mechanism that does well with relativistic particles is synchrotron radiation—provided a significant magnetic field is present. These efficiency considerations made synchrotron emission a favored model early on. By now, its dominant importance has been confirmed for the afterglow phase of the burst, and we will develop the theory for this case. The origin of the burst emission is less clear; although it could be synchrotron emission, its nature is still the subject of lively debate (Section 6.4).

3.3 The Afterglow Emission

In the afterglow, rest frame densities of particles and photons are quite small, and the electron scattering optical depth will typically be 10^{-5} or less. This means that optical depth effects can be neglected for now, and that two-body encounters are not efficient in producing radiation. Let us therefore consider synchrotron emission, which, as we will see, provides very good fits to the afterglow spectra and light curves. The first precise prediction of this emission was made by Mészáros & Rees (1997). The relations between the observable synchrotron spectra and shock parameters have been derived in a number of papers (Rees & Mészáros 1992, Paczyński and Rhoads 1993, Waxman 1997c, Granot et al 1999b, Wijers & Galama 1999). Here we omit details, and follow the notation and coefficients of Wijers & Galama (1999).

The formation of magnetic fields and acceleration of particles at and in the wake of a relativistic shock front are not yet well understood. For now, we summarize our ignorance of the post-shock parameters in as few parameters as possible. The post-shock conditions are related to the pre-shock ones by jump conditions (Blandford & Mckee 1976), which in the ultrarelativistic limit ($\gamma \gg 1$) can be approximated as

$$n' = 4\gamma n; \qquad U' = 4\gamma^2 n m_\mathrm{p} c^2, \tag{10}$$

where primed quantities are in the rest frame of the shock, n is the number density, and U is the energy density. (Strictly speaking, if the medium is not pure hydrogen, n denotes the nucleon density.) We assume that the energy density in magnetic field and relativistic electrons are a fixed fraction, ϵ_B and ϵ_e, respectively, of the post-shock total energy density. For the magnetic field, this means

$$B' = \sqrt{8\pi\epsilon_B U'} = \gamma c \sqrt{32\pi\epsilon_B n m_\mathrm{p}}. \tag{11}$$

For the electrons, we have to specify a shape of the energy distribution as well as a total energy. In many acceleration mechanisms, the electron Lorentz factor distribution becomes a power law above some minimum Lorentz factor γ_m and

extends to much higher energies. For a power-law index p we can integrate this simple distribution and relate the Lorentz factor distribution to the total energy in relativistic electrons. We can then relate the minimum electron Lorentz factor to the energy fraction in these electrons:

$$\gamma_{\rm m} = \frac{2}{1+X}\frac{m_{\rm p}}{m_{\rm e}}\frac{p-2}{p-1}\epsilon_e\gamma, \tag{12}$$

where X is the hydrogen fraction by mass and the first term is (to good approximation) the electron-to-nucleon number ratio in the ambient gas.

The calculation of the synchrotron radiation spectrum given the electron energy and magnetic field is lengthy, but standard [see Rybicki & Lightman (1979), Ch. 7 for a general treatment, and Wijers & Galama (1999) for an example of application to GRBs]. Figure 3 illustrates the schematic shape of the spectrum from radio to X rays for the typical adiabatic case from hours to weeks into the afterglow. The spectrum at late times is divided up into four regions. At very low frequencies the spectrum is self-absorbed and follows a blackbody shape, $F \propto \nu^2$. This region ends at the self-absorption frequency, $\nu_{\rm a}$, characteristically a few GHz, above which we find the standard low-frequency synchrotron slope $F \propto \nu^{1/3}$, up to the peak frequency $\nu_{\rm m}$. This frequency corresponds to the minimum-energy electrons; the flux at this point, from which the spectrum is usually anchored, is denoted as $F_{\rm m}$. Above this, the slope of the spectrum depends on the electron energy index p in the usual way: $F \propto \nu^{-(p-1)/2}$. Finally, at very high energy, the injected electrons cool more rapidly than the characteristic time of the source (the expansion time), and thus the spectrum becomes steeper by a power $1/2$ at a third characteristic frequency $\nu_{\rm c}$, the cooling frequency. Schematically, for a uniform ambient medium, we find:

$$\begin{aligned}
\nu_{\rm a} &= f_{\rm a}(\epsilon_{\rm e}, \epsilon_B, n, E, p, z)\ {\rm Hz} \\
\nu_{\rm m} &= f_{\rm m}(\epsilon_{\rm e}, \epsilon_B, n, E, p, z)\, t^{-3/2}\ {\rm Hz} \\
\nu_{\rm c} &= f_{\rm c}(\epsilon_{\rm e}, \epsilon_B, n, E, p, z)\, t^{-1/2}\ {\rm Hz} \\
F_{\rm m} &= f_{\rm F}(\epsilon_{\rm e}, \epsilon_B, n, E, p, z)\ {\rm Hz}
\end{aligned} \tag{13}$$

The detailed forms of the coefficients can be derived (Wijers & Galama 1999b, Granot et al 1999b) but are somewhat uncertain. The main reasons are that the derivations usually assume a uniform medium behind the shock, as opposed to the true self-similar shock structure (Blandford & McKee 1976). Also, emission from the shell is strongly forward-beamed within an angle $1/\gamma$ of the radial direction, which means we need to average the spectrum properly over the shell rather than just take the point on our line of sight as representative. All these effects, along with proper radiation transport, can be accounted for with enough patience, and some numerical work has been done on parts of the problem. Generally, they lead to much smoother changes between regimes, and to changes of order unity in the

coefficients of Equation 13. There are also some true physical uncertainties—e.g. some assumption must be made about the pitch angle distribution of electrons relative to the field (here we take them to be isotropic, and to remain so even during cooling). These depend on the mechanisms of field formation and electron acceleration in the shock, about which little is yet known (but see later sections). The time dependence of the frequencies means that at very early times, typically minutes after the burst, we can have $\nu_c < \nu_m$, in which case the shape and evolution of the spectrum are different (Cohen et al 1998). Likewise, at very late times we may have $\nu_m < \nu_a$, which changes the evolution and shape of the radio spectrum. This may be so late that other effects, such as the blast turning non-relativistic, also play a role, preventing a clear-cut observation of either effect by itself. The bulk of current afterglow data are hours to weeks after the burst, however, where the spectrum and time evolution of Figure 3 and Equation 13 apply.

Despite some uncertainties in the coefficients, a number of very important inferences and tests of the model can be obtained from these relations. First, we note that for a burst with known redshift Equation 13 has four measurable quantities and four unknowns (p also follows from the measured spectrum). Therefore, the blast wave properties can be derived from a complete spectrum, and this has been accomplished in a few cases (Section 4). Also, because the spectrum evolves to

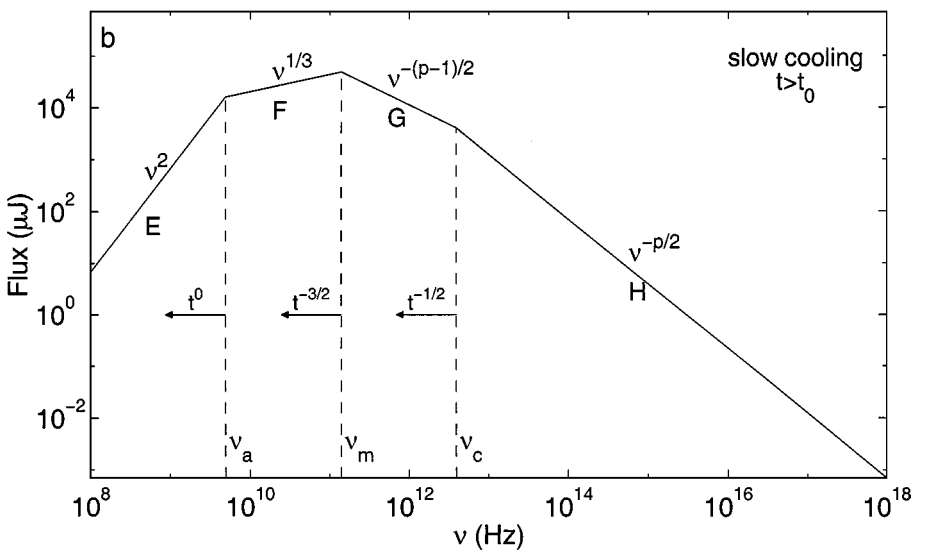

Figure 3 The piecewise power-law schematic shape of blast wave synchrotron spectra for later afterglow evolution (Sari et al 1998). The characteristic break frequencies and their time evolution are indicated, as is the spectral slope in each regime. This can be directly compared with the observed spectrum of GRB 970508 (Figure 12).

lower frequencies with time, one can sample in a given waveband and see the spectral breaks pass by. In this way, Frail et al (2000) have been able to measure the physical parameters of GRB 980703.

Second, if ϵ_e and/or ϵ_B were not constant, then the time dependencies of the measurable variables would change. Hence the observation that many afterglows follow the simple model predictions seems to justify the a priori uncertain ansatz that the electron and field energy densities scale like equipartition values—i.e. they are constant fractions of the total shock energy density. Given that sometimes $\epsilon_B \ll 1$ (e.g. in GRB 980703: Vreeswijk et al 1999, Bloom et al 1998b; and in GRB 990123: Galama et al 1999), the apparent good validity of this scaling is somewhat remarkable.

Third, now that we have the shape of the spectrum and the evolution of the breaks, we can compute the time evolution in any fixed observed waveband as well (Mészáros et al 1994, Wijers et al 1997, Sari et al 1998, Mészáros & Rees 1997, Mészáros et al 1998). Below ν_m, the spectral shape is independent of the electron spectrum, and its evolution has no free parameters; flux should increase as $t^{1/2}$ at all these frequencies. Above ν_m, the a priori unknown p enters. Recent theoretical calculations of particle acceleration in relativistic shocks (Gallant & Achterberg 1999, Gallant et al 1999) give $p \sim 2.3$–2.4, in good agreement with the observed range of 2–2.5. But observational precision is often much better, so the theoretical prediction is not yet accurate enough. Because observations often give both the spectral index and the time decay rate over a range of frequencies and times, however, this is only one parameter for two measured power-law indices. Therefore, this still leaves one test of the model. In practice, what one does is fit a model of the form $F(\nu, t) \propto \nu^{-\beta} t^{-\delta}$ to the data, and determine β and δ. Since $\beta = \beta(p)$ and $\delta = \delta(p)$, we then have a theoretical relation $\beta = \beta(\delta)$, which we may test with the fit to the data. A good summary of the scaling relations in the various spectral regimes for spherical fireballs is given by Sari, Piran, and Narayan (1998).

It must be noted first, though, that the relation is different for each dynamical evolution model of the blast wave, and also depends on whether our observed frequency is above or below ν_c. Therefore, unless we have other data from which to decide on the appropriate regime, our prediction will in fact consist of a few possible relations. In practice, the various possible predictions of β for a given δ differ only by 0.1–0.3; hence it is necessary to measure the spectral and temporal slopes of the afterglow to a few percent accuracy in order to obtain a stringent test of the model. Let us take the case of the adiabatic spherical fireball as an example, and imagine we have measured an optical temporal decay index $\delta = 1.0 \pm 0.1$. We have also measured a $B-R$ color, and from this deduced that the optical spectral index is $\beta = 0.70 \pm 0.03$. Is the optical band above or below ν_c? Well, if ν_c were below the optical, we would expect $\beta = (2\delta + 1)/3 = 1.00 \pm 0.07$, whereas if it were above the optical, we would expect $\beta = 2\delta/3 = 0.67 \pm 0.07$. Thus we see that the color measurement establishes that the latter is true with fair certainty, but for the somewhat larger errors in β and δ that are often obtained in practice the question is not resolvable.

4. HIGHLIGHTS OF AFTERGLOW OBSERVATIONS

In late 1996 the BeppoSAX Team, following the derivation of an accurate (but not rapidly available) WFC error box for GRB 960720 (In't Zand et al 1997, Piro et al 1998b), was ready to quickly produce arcminute-sized WFC error boxes for subsequent follow-up observations. The first opportunity to apply this capability occurred on January 11, 1997.

The initial $10'$ radius WFC error box (Costa et al 1997a), partly cut by the BeppoSAX-Ulysses IPN annulus, contained several faint X-ray sources detected with the BeppoSAX Narrow Field Instruments (NFI), some of which are also present in the ROSAT Sky survey (Butler et al 1997, Voges et al 1997, Frontera et al 1997, Feroci et al 1998). One of these sources coincided with a variable radio source (Frail et al 1997b, Frail et al 1997a). However, an improved ($3'$ radius) WFC error box (In't Zand et al 1997) obtained some three weeks after the event contained none of these objects. Likewise, optical observations that started less than a day after the burst gave no evidence for a candidate GRB counterpart (Gorosabel et al 1998).

4.1 Solving the GRB Riddle

The next opportunity, which would lead to a breakthrough, arose on February 28, 1997. After the hard X rays from the burst were discovered with a Wide Field Camera on BeppoSAX, pointed BeppoSAX NFI X-ray observations were made $\sim$8 hours later, and revealed the presence of an unknown soft X-ray point source with a 2–10 keV flux of several 10^{-12} erg/cm^2 s in the WFC error box. Four days later, the flux of this X-ray source had decreased by a factor $\sim$20; the first X-ray afterglow of a GRB had been detected (Costa et al 1997b; Figure 4, see color insert).

In the meantime, GRB 970228 had also become the first γ-ray burst for which an optical counterpart was found, independently from the soft X-ray afterglow detection. From a comparison of (V and I band) images made with the William Herschel and Isaac Newton Telescopes 21 hours and a week after the burst, Groot et al (1997b) discovered a decaying 21st magnitude object at a position consistent with all positional information on the γ-ray burst (Van Paradijs et al 1997; Figure 5). Subsequent deep images made with the ESO New Technology Telescope (Groot et al 1997a) and the Keck Telescope (Metzger et al 1997c) showed an $\sim 1''$ extended object at the location of the optical transient, likely the host galaxy of the γ-ray burst (implying that the burst came from a distance of order Gpc).

HST observations were made in late March and early April 1997 (Sahu et al 1997) and in September 1997 (Fruchter et al 1999). These observations showed the presence of a point source whose brightness decayed according to a power law located near the edge of an extended object (diameter $\approx 0.8''$; Figure 6, see color insert). Later observations established its redshift as 0.695 (Djorgovski et al 1999), confirming that the host of GRB 970228 is a distant galaxy.

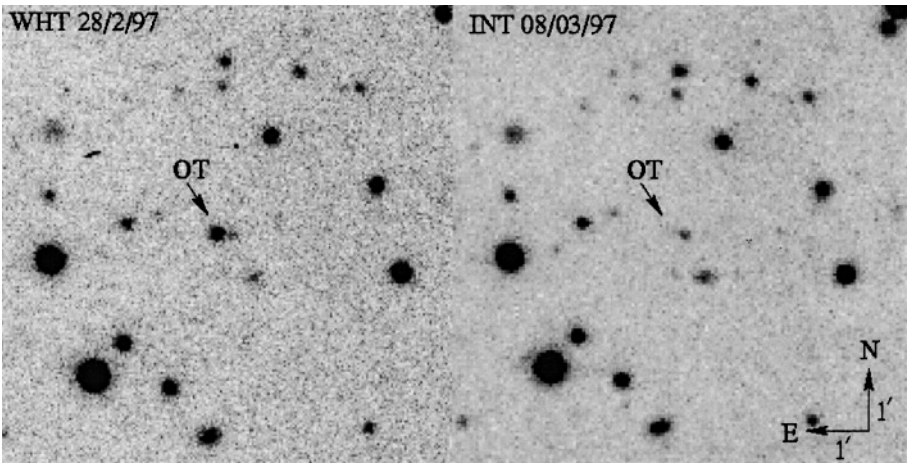

Figure 5 Discovery images of the optical afterglow of GRB 970228 at La Palma (Van Paradijs et al 1997).

The optical light curve of the afterglow of GRB 970228 showed a significant deviation from a pure power law (Galama et al 1997) about 1–2 weeks after the burst. Recently this has been interpreted as possible evidence for the presence of a supernova component in the light curve (Reichart 1999, Galama et al 2000; Figure 7), following an original suggestion for a similar deviation in GRB 980326 (Bloom et al 1999a). (See Section 4.3 for further discussion on the connection between γ-ray bursts and supernovae.)

The exponents of the power-law decay X-ray (Figure 8) and optical light curves were $\delta_{\rm X} = -1.33^{+0.12}_{-0.11}$ and $\delta_{\rm opt} = -1.46 \pm 0.16$. The exponents of the (assumed power law) spectrum of the afterglow were $\beta_{\rm X} = -1.06 \pm 0.24$ and $\beta_{\rm X\text{-}opt} = -0.78 \pm 0.02$ for the X-ray waveband and for the X-ray to R band interval, respectively. The relation between δ and β is consistent with that expected from a very simple version of the fireball model (see Section 3), and gave initial support to this model (Wijers et al 1997). However, after subtraction of the SN contribution, the temporal slope steepens and the light curve may be better fit by a blast wave propagating in a stellar wind (Chevalier & Li 1999).

The next big step forward was made with GRB 970508, whose optical counterpart (Bond 1997) initially increased in brightness from the first to the second night after the γ-ray burst and reached a maximum magnitude R $\simeq$ 19.8 two days after the burst (Pedersen et al 1998). It then started a power-law decline that could be followed for several hundred days (Galama et al 1998a, Djorgovski et al 1997, Sokolov et al 1998, Garcia et al 1998), and eventually flattened off, revealing the presence of a host (Zharikov et al 1998, Bloom et al 1998a, Fruchter et al 2000).

Optical spectroscopy obtained with the Keck telescope revealed the presence of absorption lines of Mg II, Fe II, and Mg I (Metzger et al 1997b; Figure 9) which are

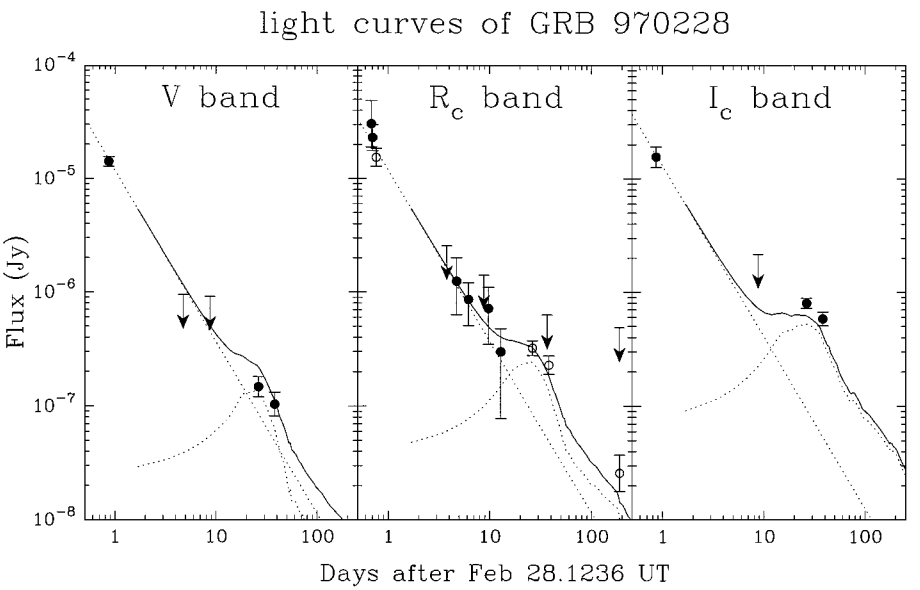

Figure 7 The *VRI* light curves of the afterglow of GRB 970228, showing the evidence of a supernova component superposed on the power-law decline at late times (Galama et al 2000).

often found in quasar spectra (Steidel & Sargent 1992), redshifted by z = 0.835 (Metzger 1997). The subsequent discovery of [O II] and [Ne III] emission lines in the spectrum at the same z = 0.835 (Metzger et al 1997a) established the presence of an underlying host galaxy. HST observations revealed that the OT was at the center of a blue, actively star-forming dwarf galaxy (Pian et al 1998, Fruchter et al 2000, Natarajan et al 1997; Figure 10, see color insert) of $L_B = 0.12L_*$ and with a star formation rate of ≤ 1 $M_\odot$/yr (Bloom et al 1998a). This result unambiguously established that GRBs originate at cosmological distances, and terminated the discussion on the GRB distance scale: it established γ-ray bursts as the most luminous photon emitters in the entire universe, with peak luminosities of order $L\gamma \simeq 10^{52}$ erg/sec. The optical afterglow of GRB 970508 reached an absolute magnitude $M_V \simeq -24$, i.e. in optical emission it became two orders of magnitude brighter than a type Ia supernova.

GRB 970508 also has the distinction of being the first γ-ray burst for which radio afterglow was detected (Frail & Kulkarni 1997). During the first month the radio flux underwent strong irregular variations, around an average value of 0.6 mJy (8.5 GHz), which damped out after about a month (Figure 11). These variations are caused by interstellar scintillation in our Galaxy. The damping of the fluctuations reflects the increase in the size of the radio emitter (analogous to the absence of twinkling of planets). From the known source distance and the properties of the interstellar medium along the line of sight, Frail et al (1997c,

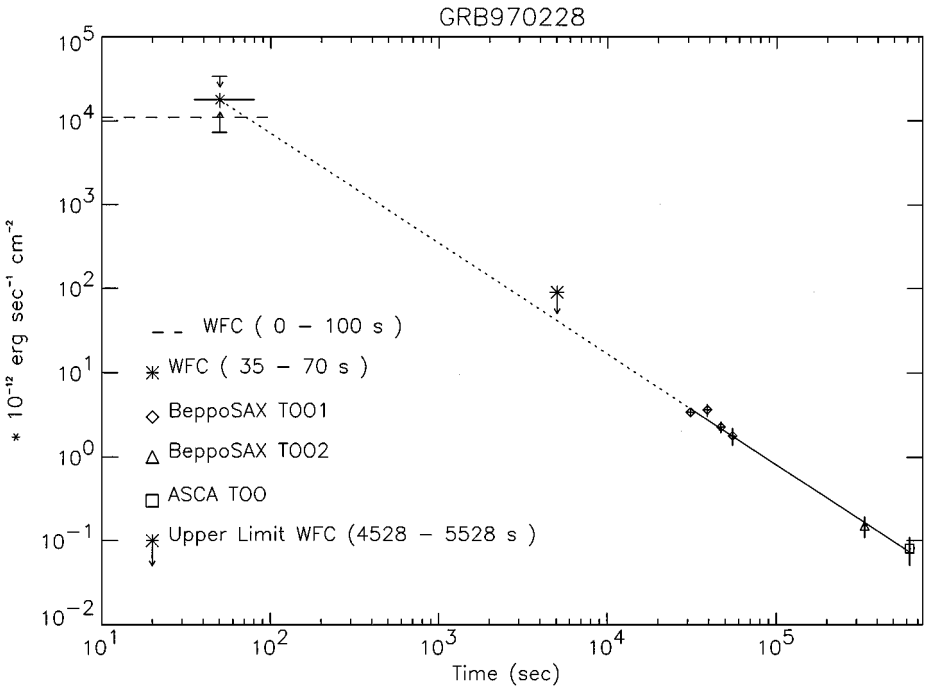

Figure 8 The X-ray afterglow light curve of GRB 970228. Note the smooth connection of the afterglow with the prompt X-ray flux from the GRB (Costa et al 1997b).

1997) inferred a value for the source size at the time the fluctuations disappeared. They concluded that the radio emitter expanded with a velocity consistent with that of light, which gives strong support to the relativistic fireball model for GRBs and their afterglows.

GRB 970508 was the first γ-ray burst for which the afterglow was observed all the way from X-rays, via optical/near IR, to mm and low-frequency radio waves (see Section 5). This allowed Galama et al (1998d) to reconstruct the X-ray to radio spectral energy distribution of the afterglow, as observed 12 days after the γ-ray burst (Figure 12). This spectrum consists of piecewise connected power-law distributions, with three clearly recognizable spectral breaks at the frequencies at which the different power laws are connected. At the low-frequency side we recognize the $\nu^{1/3}$ synchrotron low-frequency limit, which at even lower frequencies turns over because of self-absorption. The high-frequency end of the $\nu^{1/3}$ part of the spectrum connects, at the peak of the spectrum, to a power- law part whose slope depends on the power, p, of the power-law electron energy (or Lorentz factor) distribution and on particulars of the fireball synchrotron emitter (see Section 3). In the near infrared a third break is seen; this can be unambiguously identified with the cooling break, whose frequency corresponds to an electron

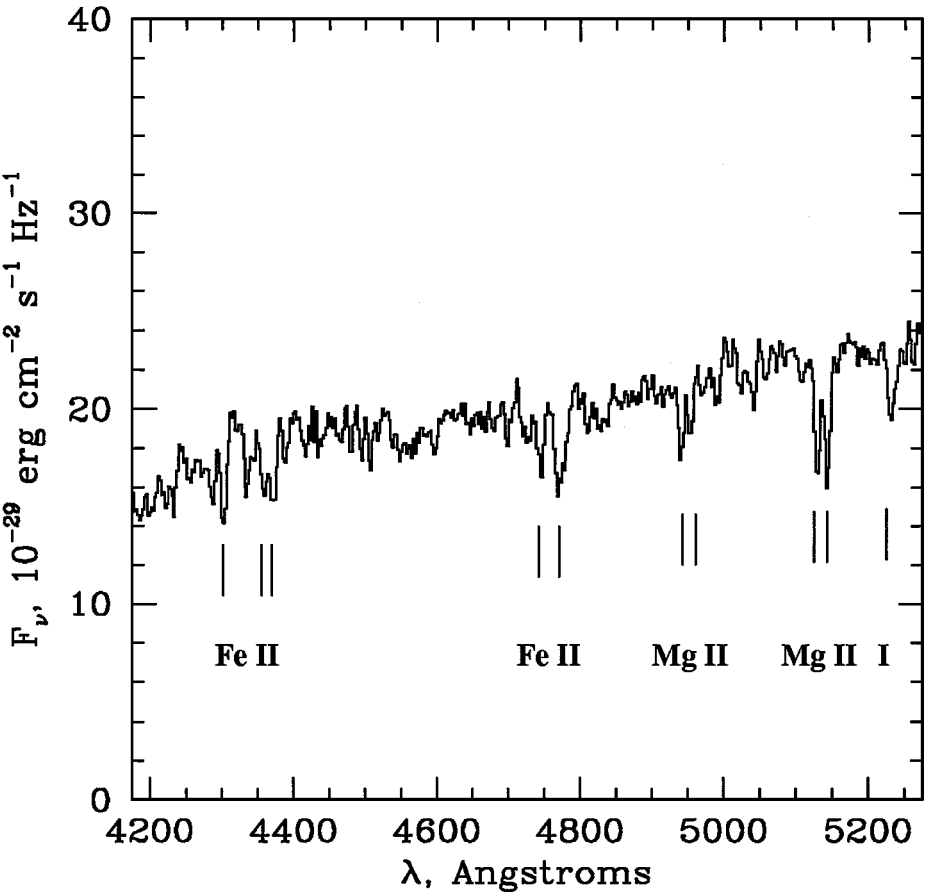

Figure 9 The spectrum of the OT of GRB 970508, showing Fe and Mg absorption lines at z = 0.835 and z = 0.77 (Metzger et al 1997b).

energy above which the synchrotron loss time is smaller than the flow timescale of the system. The identification is based on two observed facts: (1) the change in spectral slope equals 0.5 (Galama et al 1998d; Figure 12), and (2) the frequency, ν_c, of the cooling break changed with time since the burst as $\nu_c \propto t^{-1/2}$, as was evident from the progression of the spectral slope change (by 0.5) from the optical to the near-infrared passbands (Galama et al 1998a; Figure 13). These results show that relatively simple versions of the fireball model provide a reasonable description of the observed afterglow spectrum, and provide a strong argument for the idea that GRB afterglows are powered by the synchrotron emission of electrons accelerated in a relativistic shock.

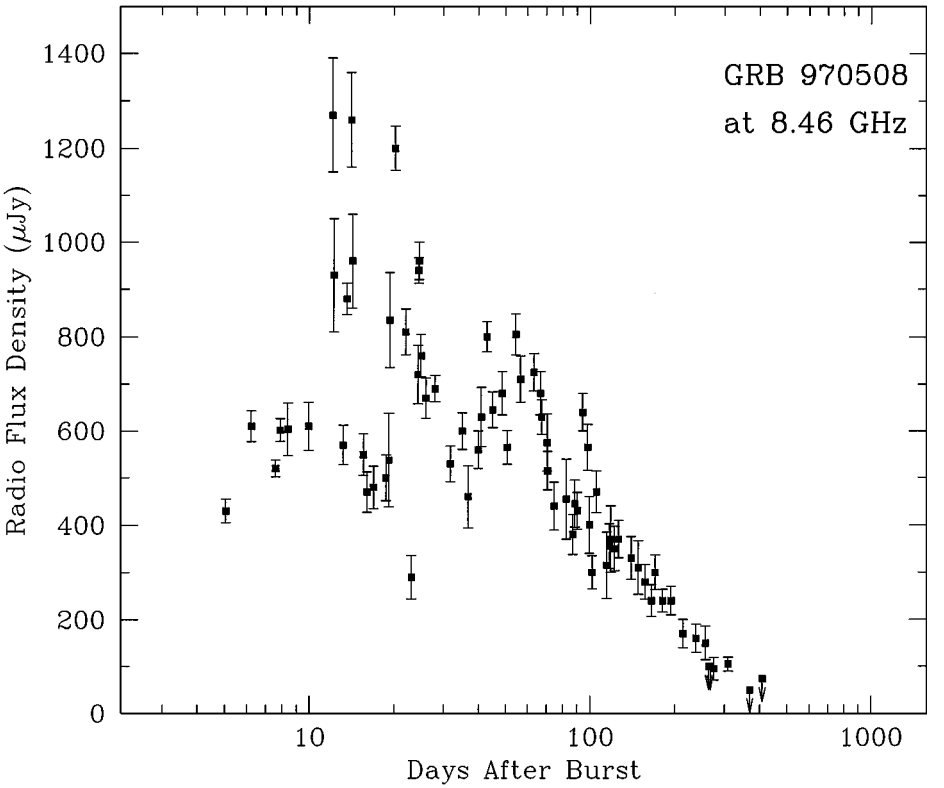

Figure 11 The 8.46 GHZ VLA light curve of the afterglow of GRB 970508 (Kulkarni et al 2000). Note the large scintillation fluctuations in the first month and their later absence, indicating that the source expanded (Frail et al 1997c).

4.2 Dark GRBs

The relative optical response in the afterglow of a γ-ray burst can vary enormously from one burst to another (for the X-ray afterglows the variations are more moderate; see Section 5). A very good example is provided by GRB 970828, a fairly strong γ-ray event for which optical observations were made within four hours after the burst and continued for eight consecutive nights after the burst. No potential optical counterpart was found to vary by more than 0.2 mag down to $R = 23.8$ (Groot et al 1998a). Compared to GRB 970508 the peak optical flux in the afterglow of GRB 970828, normalized to the fluence of the γ-ray burst, was at least a factor of 10^3 smaller. Absorption in the GRB host galaxy, by at least five magnitudes in the *R* band, may explain their large difference in optical afterglows. Note that for moderate redshifts ($z \sim 1$) the absorbed photons have wavelengths of $\sim$3000 Å, at which the interstellar extinction is a factor of $\sim$2.5 larger than in the

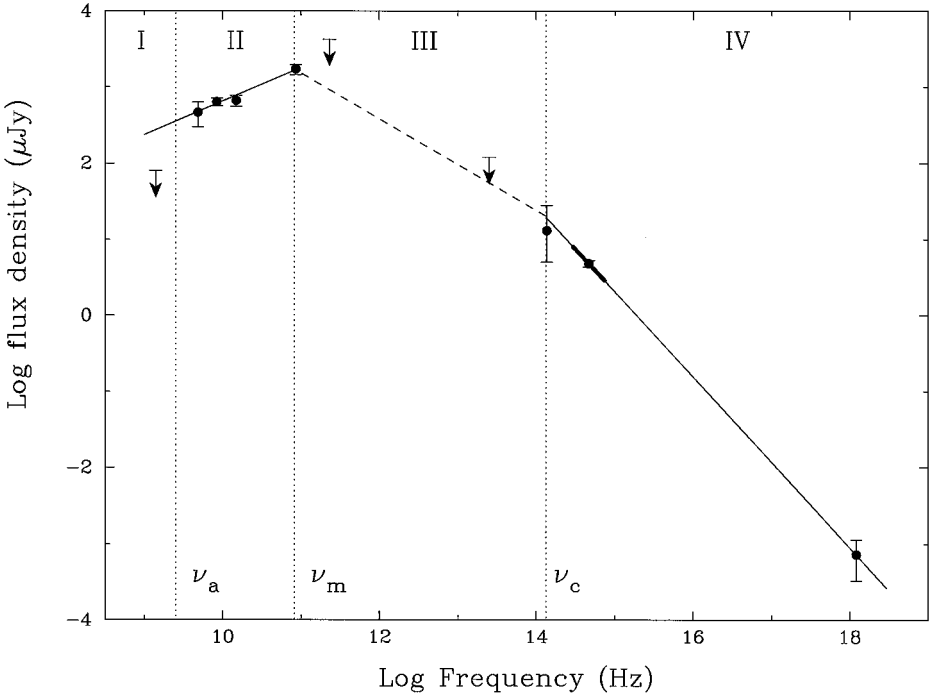

Figure 12 The radio to X-ray spectrum of the afterglow of GRB 970508, 12.1 days after trigger, showing all the characteristics of synchrotron emission (Galama et al 1998d).

R band. Therefore, with a normal dust-to-gas ratio in the host, a modest column density of $N_H \sim 10^{21}$ cm^{-2} would be sufficient to provide the large extinction. Recent results support this suggestion: at the position of GRB 970828 there is a galaxy with $z = 0.96$ (Djorgovski et al 2000) and $N_H = 4.1^{+2.1}_{-1.6} \times 10^{21}$ cm^{-2} (as measured in our rest frame by Yoshida et al 1999).

4.3 The Supernova–GRB Connection

The total energy budgets of γ-ray bursts corresponding to their cosmological distances are roughly of the same order of magnitude as those of supernovae; in γ-ray bursts, however, the energy is emitted much more rapidly than in supernovae. The reason is that in supernovae the energy (except that in neutrinos) is thermalized by a large amount of mass (several solar masses) and converted into heat and expansion at a speed of typically 10^4 km/s. In a γ-ray burst the energy cannot be shared with more than $\sim 10^{-3}\,M_\odot$ in baryons, in order not to lose the required high Lorentz factors ($\Gamma \geq 10^2$). The similar amount of total energy (10^{53} ergs) involved in both phenomena kept the possibility of their connection open, despite the very large difference in the way the energy is emitted. For instance, in one of

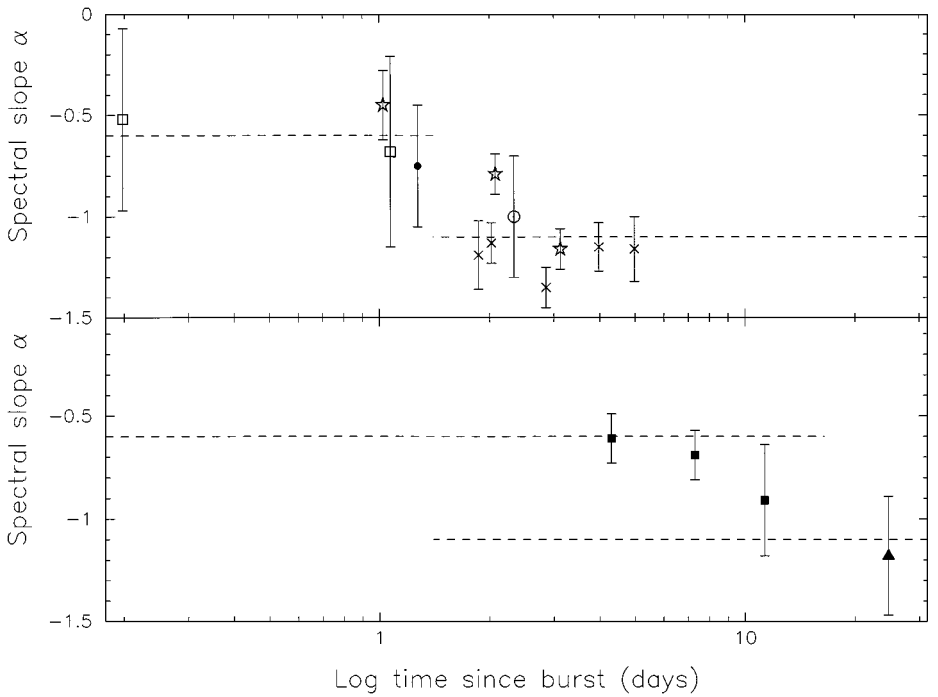

Figure 13 The evolution of the optical spectral index (top: $V - R$ and bottom: $R - K$) oft he afterglow of GRB 970508, showing the passage of a break consistent with a cooling break (Galama et al 1998a).

the main γ-ray burst models, the collapsar or failed supernova model (Woosley 1993, Paczyński 1998), a γ-ray burst is the result of a massive core collapse, with extreme parameters (e.g. extreme mass or rotation of the progenitor). However, until April 1998, direct evidence for a relation between γ-ray bursts and supernovae was totally lacking.

It therefore came as something of a surprise when Galama et al (1998c, 1998b) found that the WFC error box of GRB 980425 contained the supernova SN 1998bw (Figure 14). This supernova is located in a spiral arm of the nearby galaxy ESO 184–G82, at a redshift of 2550 km/s, corresponding to a distance of 40 Mpc. On the basis of very conservative assumptions regarding the error box and the time window in which the supernova occurred, Galama et al (1998c) determined that the probability that any supernova with peak optical flux a factor of 10 below that of SN 1998bw would be found in the error box by chance coincidence is 10^{-4}; this provides strong evidence for a physical relation between the γ-ray burst and the supernova. The WFC error box also contains two weak X-ray sources, one of which, 1SAX J1935.0-5248, coincides with SN 1998bw and GRB 980425 (Piro et al 1998a, Pian et al 1999); the second source initially faded

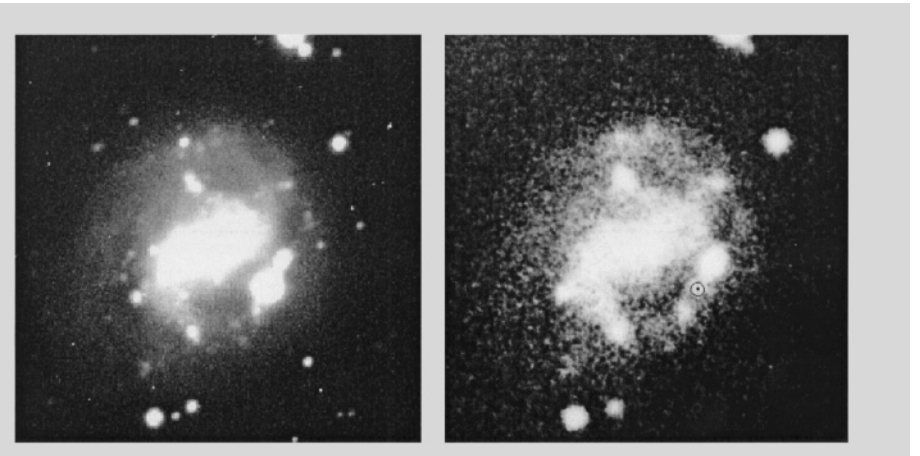

Figure 14 Image of the galaxy ESO 184-G82 with (*left*) and without (*right*) SN 1998bw (Galama et al 1998c).

but was subsequently redetected at a flux similar to the first observation (Pian et al 1999), which excludes it as a viable GRB afterglow. The case for a physical relation between the supernova and the GRB is therefore a strong one.

With respect to its apparent properties (peak flux, duration, burst profile) GRB 980425 was not remarkable. Of course, at its distance of 40 Mpc, its total energy (8×10^{47} erg/s) is some five orders of magnitude smaller than that of normal γ-ray bursts (Galama et al 1998c). The total energy in GRB 980425 is remarkably close to the value envisaged in Colgate's (1974) model.

Independent of its connection with a γ-ray burst SN 1998bw is extraordinary for its very high radio luminosity near the peak of the SN light curve (Kulkarni et al 1998b). According to the analysis of Kulkarni et al (1998b) the radio light curve requires the presence of a mildly relativistic ($\Gamma \sim 2$) outflow, which may account for the γ-ray burst emission. An analysis of the optical light curve (Galama et al 1998c; Figure 15) and its early spectra (Iwamoto et al 1998, Woosley et al 1999, Branch 1999) showed that SN 1998bw was an extremely energetic event [total explosive energy in the range $(2-6) \times 10^{52}$ erg, i.e. a factor of $\sim$30 higher than is typical for an Ib/c supernova], in which an extraordinarily large amount of ^{56}Ni (0.5–0.7 $M_\odot$) was ejected. The early expansion speed was as high as $\sim$60,000 km/s. According to Iwamoto et al (1998; see also Iwamoto 1999a, Iwamoto 1999b), the remnant mass of the core collapse exceeded 3 $M_\odot$, and a black hole was likely formed in SN 1998bw. [Note that by allowing for asymmetry in the supernova explosion, Höflich et al (1999) derive somewhat more moderate but still very large values for the energetics of this supernova.] GRB 980425 is the only γ-ray burst (out of more than 2000) for which the evidence of a connection with a supernova appears convincing. Attempts to search for further associations have not

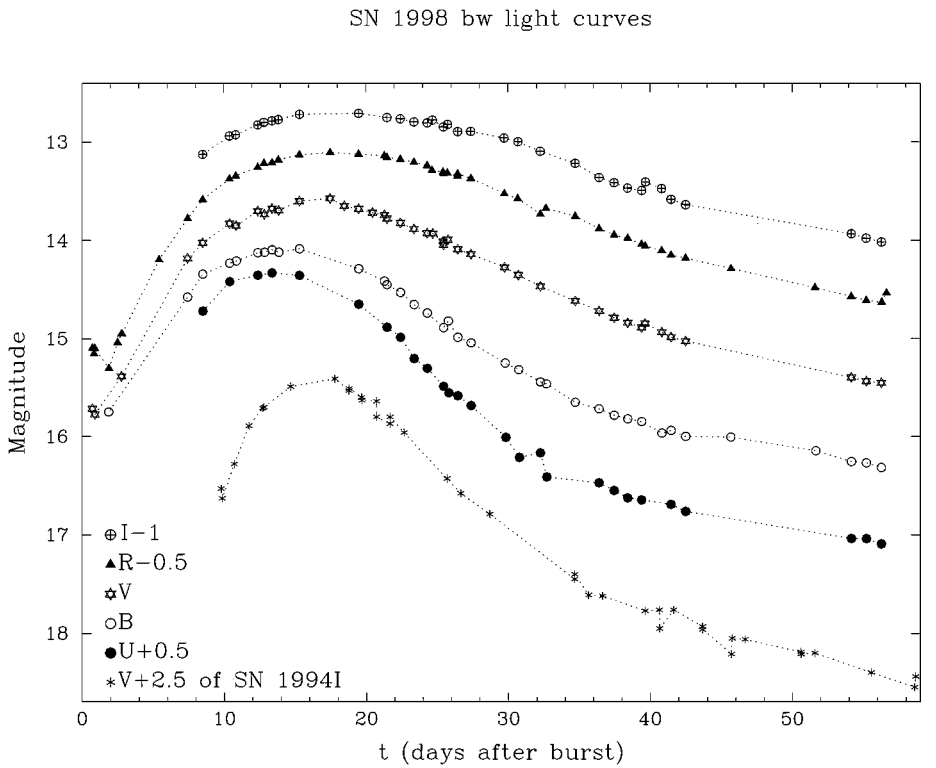

Figure 15 The optical light curve of SN 1998bw (Galama et al 1998c).

led to other strong candidates (Wang & Wheeler 1998, Woosley et al 1999, Bloom et al 1998c, Kippen et al 1998). [We consider the proposed connections between SN1997cy and GRB 970514 (Germany et al 1999) and between SN1999eb and GRB 991002 (Terlevich et al 1999) not convincing.]

Because the sampling volume for low-luminosity events such as GRB 980425 is smaller than that of the normal γ-ray bursts by a factor $\sim 10^6$, the rate (per galaxy) of the former events may well exceed those of the latter by a large factor. Because of their small distances they are expected to contribute a $P^{-3/2}$ component to the log N ($>P$) distribution. From the absence of a turn-up at the flux limit (P $\simeq$ 0.2), Kommers et al (2000a) inferred that such a Euclidean component can contribute at most 10% to the observed BATSE burst sample (99% confidence limit). With a normal GRB rate of $\sim 10^{-8}$ per galaxy per year (Wijers et al 1998), the corresponding limit on events like SN 1998bw is thus a few 10^{-4} per galaxy per year. With an observed rate for type Ib/c supernovae of a few times 10^{-3} per galaxy per year (van den Bergh & Tammann 1991), this rather weak limit serves to show that at most a fraction of the SN Ib/c produce γ-ray bursts.

The observational basis for a connection between γ-ray bursts and supernovae was greatly enriched with the discovery by Bloom et al (1999a) of a late component superposed on the power law optical light curve of GRB 980326, which they argue reflects an underlying supernova (Figure 16). A similar interpretation has been proposed by Reichart (1999) and Galama et al (2000) for the long-known deviation from a pure power-law decay of the optical afterglow of GRB 970228 (Galama et al 1997).

The optical light curve of GRB 980326 showed an initial rapid decay ($\delta_{\rm opt} = -2.0$; Groot et al 1998b); the light curve flattened after $\sim$10 days to a constant value $R = 25.5 \pm 0.5$. Such flattening has been seen in the light curves of other afterglows as well, and has been interpreted as the signature of an underlying host galaxy. Observations by Bloom et al (1999a) made $\sim$3 weeks after the burst revealed a surprising brightening of the afterglow, to a flux level 60 times above that expected from an extrapolation of the power-law decay. At the same time, the spectral energy distribution became very red. Observations made $\sim$9 months after the burst showed that any host galaxy is fainter than $R = 27.3$. Using the multicolor light curve of SN 1998bw (Galama et al 1998c) as a template, Bloom et al (1999a) found that they can reproduce the observed optical afterglow light curve of GRB 980326 by a combination of a power-law (exponent -2.0) and a bright supernova at a redshift z $\sim$ 1.

Reichart (1999) and Galama et al (2000) made the same decomposition of the optical light curve of GRB 970228 and found that this provides a good fit to the data. These results support the idea that at least a fraction of the γ-ray bursts originate from the collapse of a massive star. This confirms the models proposed by Woosley (1993) and Paczyński (1998), under various names, such as the failed supernova model or collapsar model, in which it is assumed that a black hole surrounded by a fairly massive torus is formed. It is still unclear what particular circumstances give rise to the GRB (e.g. a very high mass, rapid rotation, a particular evolutionary history), but it seems virtually certain that strong collimation of the outflow is required to accommodate both the extremely high Lorentz factor flow required for the γ-ray burst and the more sluggish flow connected with the supernova photospheric emission.

4.4 Prompt Optical Emission

Based on the fireball model, prompt optical emission simultaneous with the γ-ray burst is expected, with apparent V magnitudes ranging between 9 and 18 for typical GRB distances (Mészáros & Rees 1993, Mészáros & Rees 1997, Sari & Piran 1999, Katz 1994a). After many years of unsuccessful attempts to catch the optical signal of a γ-ray burst in progress (see e.g. McNamara et al 1995, Krimm et al 1996, Hudec & Soldan 1995, Lee et al 1997, Park et al 1997), the first such simultaneous detection was made of GRB 990123 by Akerlof et al (1999). The robotic camera ROTSE, triggered by BATSE, started a sequence of optical

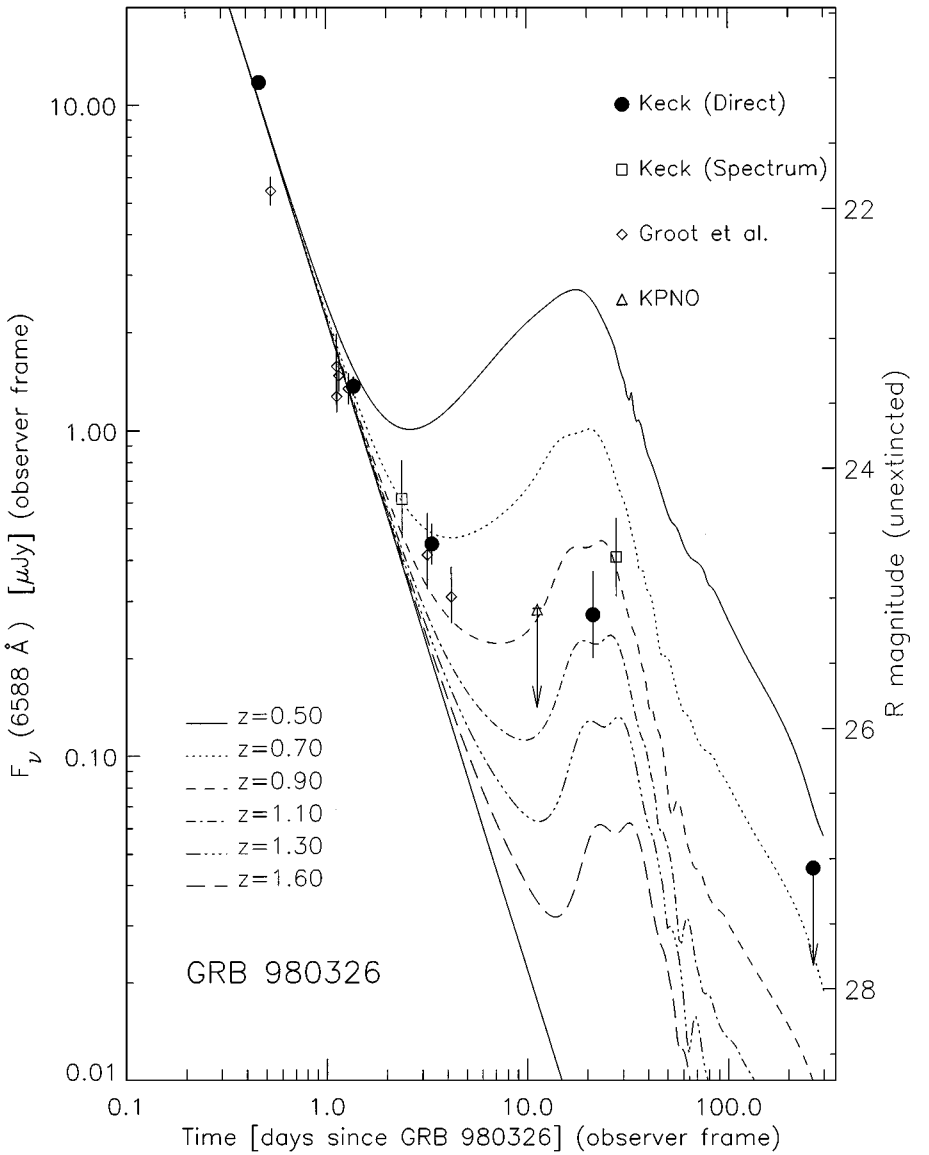

Figure 16 The *R* light curve of GRB 980326, with model curves representing the power-law decay of a relativistic afterglow superposed with the light curve of SN 1998bw, shifted to various redshifts (Bloom et al 1999a).

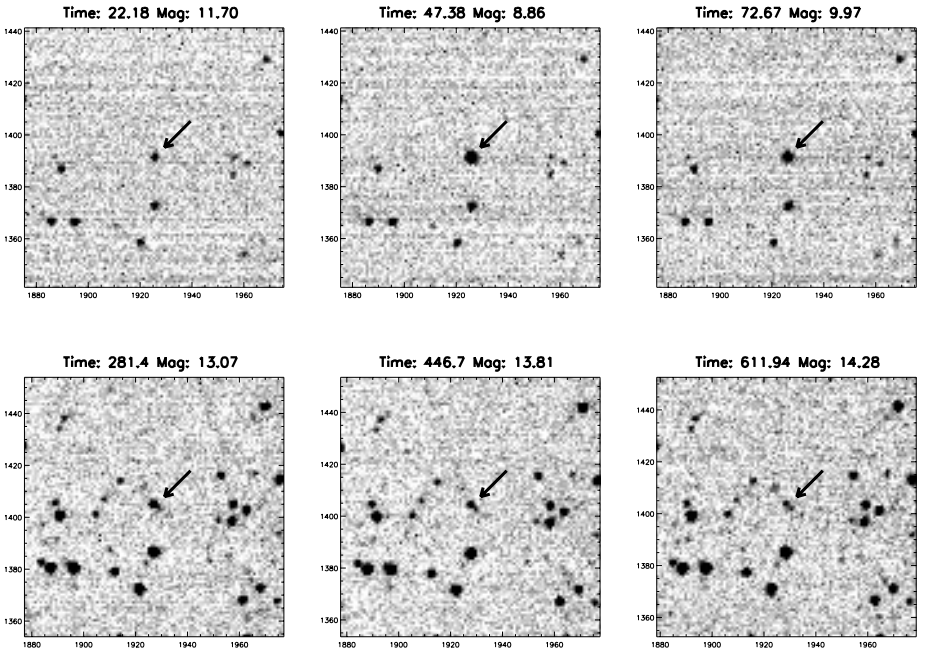

Figure 17 The ROTSE discovery images of the prompt optical emission from GRB 990123, from 22 to 800 s after trigger (Akerlof et al 1999).

images of the BATSE error box 22 seconds after the start of the burst (Figure 17). An optical transient was detected; ∼50 seconds after the start of the burst, the transient reached magnitude 8.9 and afterward decayed to $\sim 15^{\text{th}}$ mag in $\sim 10^3$ s. The slope of the prompt light curve changed after ∼300 s, and merged smoothly with the later afterglow light curve (Figure 18; Kulkarni et al 1999a, Galama et al 1999, Castro-Tirado et al 1999a). During the peak of the prompt optical emission the γ-ray burst reached an absolute magnitude $M_{\text{v}} \approx -36.5$, i.e. the event was then for a brief time interval 10 million times brighter than a Type Ia supernova.

The prompt optical emission is not proportional to the γ-ray flux; neither can it be understood as the low-energy extrapolation of the (variable) γ-ray burst spectrum (Galama et al 1999, Briggs et al 1999; see also insert of Figure 18). This indicates that the prompt optical emission and the γ rays originate from different regions in the fireball. It has been popular practice to ascribe the origin of the γ rays to internal shocks (Rees & Mészáros 1994, Kobayashi et al 1997)

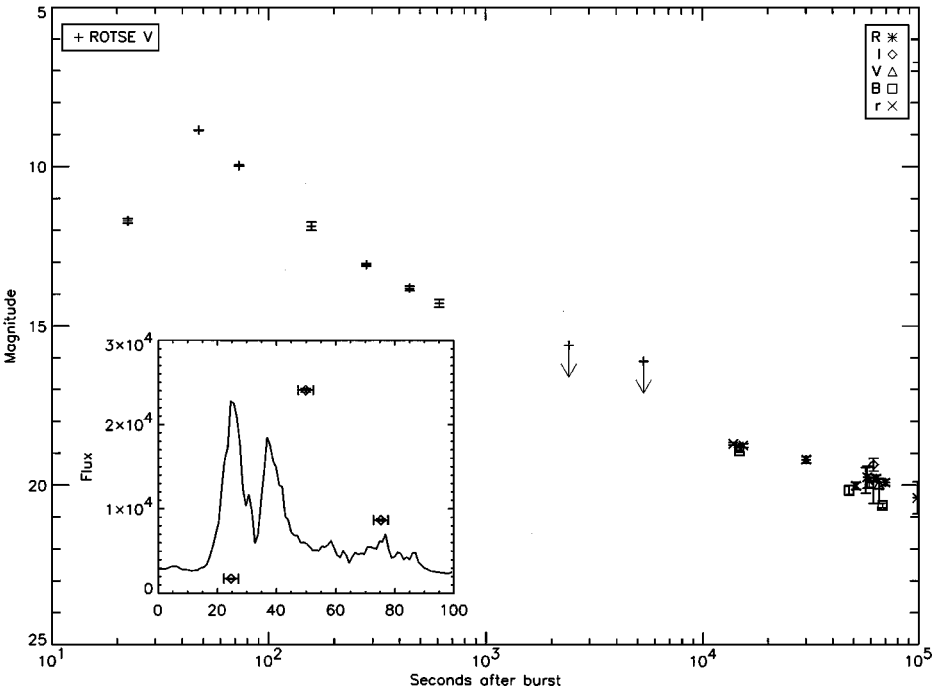

Figure 18 The R light curve of GRB 990123, showing the early emission rising above the back-extrapolated afterglow and then merging smoothly with the later afterglow light curve (Akerlof et al 1999). The γ-ray light curve of ARB 990123; the three points indicate the times during which prompt optical emission was detected with ROTSE (in an arbitrary intensity scale).

and the long-term afterglow to the external shock[2]. It has therefore been natural to ascribe the prompt optical emission to the reverse shock (Sari & Piran 1999, Mészáros & Rees 1999), which is observed only during a time interval of order of the burst duration (i.e. comparable to the time it takes for the reverse shock to travel through the ejecta). The radio afterglow properties of GRB 990123 are peculiar in that radio emission was only seen during a $\sim$ 1-day interval, about a day after the burst (Kulkarni et al 1999b, Galama et al 1999). This brief radio event has been interpreted by Kulkarni et al (1999b) as reverse-shock emission. Galama et al (1999) ascribe it to emission from the forward shock and interpret the peculiar nature of the radio emission as the result of a very low value of the

[2]Recent theoretical calculations, however, have reopened the issue: Dermer & Mitman (1999) have presented a plausible external-shock model for highly variable prompt gamma-ray emission, and Fenimore & Ramirez-Ruiz (1999) have shown that previous objections to external-shock models for the prompt emission can be circumvented.

synchrotron peak frequency one day after the burst. They suggest that differences in the afterglow properties (peak frequency, cooling frequency) reflect differences in the magnetic field strength in the afterglow-emitting regions.

4.5 GRB Polarimetry

Synchrotron radiation is highly polarized, with typical degrees of (linear) polarization for ordered magnetic fields of ~60% (Hughes & Miller 1991); one may therefore expect measurable amounts of polarization in afterglow emission. By analogy to AGNs, one might expect up to 10–20% polarization if the shock emission takes place in a collimated outflow. The strong intrinsic polarization is lowered by averaging over the unresolved source (Gruzinov 1999, Gruzinov & Waxman 1999, Medvede & Loeb 1999, Loeb & Perna 1998).

For GRB 990123, (Hjonth et al 1999) reported an upper limit to R band afterglow polarization of 2.3% (95% confidence level). The first positive detection of polarization, however, was made for GRB 990510 (Covino et al 1999, Wijers et al 1999), with polarization $\rho = 1.7 \pm 0.2$ % and 1.6 ± 0.2%, 0.77 and 0.86 days after the burst, respectively. An uncertain measurement made 1.8 days after the burst is consistent with these values (Wijers et al 1999). The angle of polarization remained constant during these observations. The rather small observed values of the polarization (compared to the high intrinsic values in the synchrotron process) may be the result of a highly tangled structure of the magnetic field, or of very symmetric field geometries.

5. TABLE OF GRB, COUNTERPART, AND HOST PROPERTIES

We have assembled here a master table of all GRBs (Table 1) that have been rapidly followed up since the launch of BeppoSAX until August 1999 (including, for completeness, GRB 960720). The reason for this selection became apparent upon collecting the relevant literature: In the last year, most of the literature is in the form of IAU and GCN circulars, making for a cumbersome and confusing literature display. For the same reason, whenever all available data were diligently collected into one or more publications, these were preferentially referenced as the main sources of literature. However, we have always referenced the discovery announcements in each wavelength.

We have used the values of the BATSE durations, fluxes, and fluences for the prompt γ-ray emission throughout the table for consistency. These were substituted by the BeppoSAX/GRBM whenever the GRB was occulted for BATSE. The prompt X-ray values were supplied predominantly by the BeppoSAX WFC, and occasionally by the RXTE/ASM; the X-ray afterglow values were consistently supplied by the BeppoSAX NFI.

Detection in a wavelength was posted when generally accepted by the community. In cases that were arguable, we preferred erring on the conservative side, as

pointed out in the relevant GRB narrative. Narratives are collections of the salient points of each event, as well as depositories of counterpart peculiarities without a place in the tabular form.

We have attempted to collect all available literature on each GRB, from trigger to manifold publication. Nevertheless, given the wealth of communication media and journals it is inevitable that we have missed some—which is unintentional, but all the same irritating for the colleagues at the other end. It would improve future versions of this table if such omissions were brought to our attention, so we would be thankful for any gentle reminders of omissions.

6. COMPLICATIONS AND EXTENSIONS OF MODELS

Although the basic principles of relativistic blast waves are now well established and have a good grounding in the body of afterglow data collected thus far, it is clear from the previous section that we can already see beyond the basic spherical adiabatic model. Many afterglows deviate so significantly from the basic predictions that we know extensions or modifications of the basic model are required. However, we seldom have enough information on a given afterglow to pin down which of the many possible modifications applies to the afterglow at hand (if there is ever only one). Therefore, different models are often found for a given afterglow by different groups, and sober evaluation of the evidence shows that the difference cannot be resolved observationally. We thus omit here most of the technical details behind the more complex models. Instead, we focus on qualitative aspects of each of the models, paying particular attention to the relevance of more complex models to the broader issues in the field, such as what causes GRBs and what their true rate is.

6.1 Collimation or jets

The importance of collimation goes beyond influencing the detailed shape of the afterglow light curve: It reveals something about the central engine and affects our estimates of how many GRB progenitors there need to be.

Consider the simplest possible jet model: two cones, of opening angle θ_c around the z-axis, have outflowing material in them. The outflows have the same Lorentz factor, γ, everywhere within the cone, and no outflow exists outside it. The shock front formed is just the part of the previous spherical shock that lies within the cones; the outflow is collimated. As long as the flow is relativistic, the emission from each part of the shock front is strongly concentrated (beamed) within an angle $\theta_b \simeq 1/\gamma$. This means that an observer only sees emission from the material that flows within an angle θ_b of her line of sight. This effect is purely relativistic, unlike collimation, which can affect any flow.[3] Beaming also affects spherical gamma-ray bursts, so in those we also see no more than a small part of the

[3]One often finds the word 'beaming' used both for true beaming and for collimation in the current GRB literature, which occasionally causes confusion.

TABLE 1: GRB, counterpart, and host properties

Name	UT trig	$(\alpha,\delta)_{2000}$			(ℓ,b)		detected $\lambda\lambda$
other names of the transient							
pr:	duration	errbox	$F_\gamma^{\rm peak}$	S_γ	$F_{\rm X}^{\rm peak}$	$S_{\rm X}$	prompt-refs
X:	$\Delta{\rm UT_X}$	$F_{\rm X}^{\rm a}$	$F_{\rm X}^{\rm a}[\mu{\rm Jy}]$	$\beta_{\rm X}$	$\delta_{\rm X}$	$N_{\rm H}$	X-refs
O:	$\Delta{\rm UT_O}$	*mag*	$F_{\rm O}$	$\beta_{\rm O}$	$\delta_{\rm O}$	A_V	O-refs
IR:	$\Delta{\rm UT_{IR}}$	*mag*	$F_{\rm IR}$	$\beta_{\rm IR}$	$\delta_{\rm IR}$		IR-refs
mm:	$\Delta{\rm UT_{mm}}$	$\nu_{\rm mm}$	$F_{\rm mm}^{\rm a}$	$\beta_{\rm mm}$	$\delta_{\rm mm}$		mm-refs
ra:	$\Delta{\rm UT_{ra}}$	$\nu_{\rm ra}$	$F_{\rm ra}^{\rm a}$	$\beta_{\rm ra}$	$\delta_{\rm ra}$		ra-refs
ho:	z	host photometry (up to 3 bands)				OT offset	host-refs
Telegram-style narrative							

960720	0.48395^{321}	$17^{\rm h}30^{\rm m}36^{\rm s}$ $+49^\circ5'49''$ $(3')^{206,\,326}$			$(75.8,+33.4)$	γ,X	
pr:	$12.5(2.5)^{13}$	~ 28	0.63(6)	$0.29(5)^{250}$	0.025	$0.008(2)^{108}$	326
X:	45.2	<0.04	$<0.002^{320,\,277}$				27, 148
O:	—						
IR:	—						
mm:	—						
ra:	49.5	1.43	$<2^{99}$				
ho:	—						

First burst with WFC signal detected during an off-line analysis 45 days after it was recorded[326]. Final ($\rho = 3'$) error box contains[148, 249, 206, 149, 326] radio-loud QSO 4C 49.29. Relation with GRB very uncertain; quoted[149, 326] probability (2×10^{-4}) does not include number of trials. No optical, mm, IR observations.

970111	0.406^{60}	$15^{\rm h}28^{\rm m}11^{\rm s}$ $+19^\circ35'54''$ $(1.8')^{186,\,84,\,125}$			$(29.6,+53.4)$	γ,X	
pr:	$31.5(2)^{231}$	~ 3	4.4(2)	$5.8(3)^{125}$	0.041(7)	$0.16(1)^{84}$	107
X:	0.6875	<0.16	$<0.008^{84}$				206
O:	0.7917	$R>22.6$	$<2.8^{146}$				125
IR:	—						
mm:	30.0	86.4	$<10^{367}$				
ra:	1.2	1.43	$<0.5^{96}$				125
ho:	—						

First attempts (unsuccessful) to find low-energy afterglows in *rapid* follow-up observations of BeppoSAX WFC error box. Initial 10′ radius[60] error box contained candidate X-ray[35, 400, 110], radio[97, 125], and optical[237] counterparts, but none of these was included in the improved ($\rho = 3'$)[206] WFC error box[96, 125]. Deep BeppoSAX NFI observations of the further improved WFC error box ($\rho = 1.8'$)[186, 84], led to upper limit to X-ray flux only[84] (weak NFI source not included in the combined IPN/NFI error box). No variable optical afterglow detected within 19 hours of the GRB[146] with $\Delta R < 0.5$ mag at $R > 22.6$ (see also [153, 125]). No mm-wave detection[367].

970228	0.123620^{58}	$05^{\rm h}01^{\rm m}46.66^{\rm s}$ $+11^\circ46'53.9''$ $(2)^{399}$			$(188.9,-17.9)$	$\gamma,X,X^{\rm a},O$	
RX J050146+1146.9[112], 1SAX J0501.7+1146[62]							
pr:	$80^{\star\,62}$	4^{200}	3.7(1)	$1.1(1)^{a\,112}$	0.14(1)	0.22^{112}	299
X:	0.3445	2.8(4)	$0.15(2)^{112}$	$1.06(24)^{112}$	$1.33^{+0.13\,112}_{-0.11}$	$3.5^{+3.3\,112}_{-2.3}$	62, 423, 28
O:	0.8679	I=20.6(1)	13.7^{399}	$0.78(2)^{136}$	$1.73^{+0.09\,136}_{-0.12}$	$0.78(12)^{357}$	159, 312, 167
IR:	18.7	$J>21.5(2)$	$<4.1^{136}$				230, 373
mm:	7.9	86.4	$<1.2^{367}$				358
ra:	3.9	4.63	$<0.07^{101}$				124
ho:	$0.695(2)^{71}$	V=25.8(2)[136]	R=25.2(2)[136]	K=22.9(3)[136]		$0.3''^{399}$	158, 269, 120

First GRB for which X-ray[59, 62] and optical[159, 399] afterglow was detected, in BeppoSAX NFI images taken 0.3 and 4 days, and in (V, I) images taken at La Palma $\sim$1 day and $\sim$1 week after the GRB, respectively. X-ray flux decays as a power-law[62, 423, 112]. Backward extrapolation of X-ray afterglow smoothly joins the late X-ray emission in the GRB tail[62]. Optical afterglow located at the edge of an extended (0.8″) optical source[399, 269, 348], which is a host galaxy at redshift 0.695[71]. Host galaxy among bluest in its magnitude range[120] suggestive of ongoing star formation with SFR$\sim$ 0.4 $M_\odot$/yr and $L_B \sim 0.05 - 0.1 L_*$[71]. Optical light curve[399, 122, 136] deviates in detail from a power-law decay; interpreted as a relatively weak supernova component superposed on the GRB afterglow[136, 338]. No optical counterpart in plate archives[142]. No radio, IR or mm detection[101, 358, 124, 367].

970402 0.9303[85]	$14^h50^m6^s$ $-69°20'0''$ $(50'')^{325}$			(313.1,−8.8)	γ, X, X^a	
1SAX J1450.1−6920[325]						
pr: 150^{*284}	$\sim 28^{183}$	0.24(7)	$0.82(9)^{a\,284}$	0.007(2)	$0.040(4)^{284}$	108
X: 0.35	0.22(6)	$0.014(3)^{284}$	0.7^{284}	$1.57(3)^{284}$	$<20^{284}$	325, 108
O: 0.77	R>21.0	<12.02[156]				303
IR: —						
mm: —						
ra: —						
ho: —						

BeppoSAX WFC ($\rho = 3'$)[183] and NFI afterglow[325] detection. Afterglow decays as a power-law[284]; spectral slope consistent with simple fireball model[284]. No variable optical counterpart within 18.5 hours of the GRB[156] with $\Delta R < 0.3$ mag at $R = 21$ (see also [303]). No radio (ΔUT = 0.703d, ν =1.43 GHz) detection[284]; observations with ISO (ΔUT = 2.3d) result in upper limits of 140 and 350 μJy in 12 and 174 μm, respectively[45].

970508 0.904[61]	$6^h53^m49.45131^s$ $+79°16'19.51312''$ (15)[388]			(135.0,+26.7)	$\gamma, X, X^a, O, IR, mm, ra$	
1SAX J0653.8+7916[323], VLA J065349.4+791619[98]						
pr: $25(4)^{231}$	$\sim 3.1^{323}$	0.61(17)	$0.37(4)^{231}$	0.059(6)	$0.033(5)^{316,\,108}$	
X: 0.2335	0.70(7)	$0.036(4)^{316}$	$1.1(6)^{108}$	$1.1(1)^{316}$	$\sim 0^{322}$	293
O: 0.236	V=21.49(21)	$9.1^{29,\,347}$	$1.11(6)^{126}$	$1.141(14)^{126}$	$<0.01^{134}$	81, 140, 309, 39, 315, 377, 426
IR: 4.3	K=18.2(1)	$33(4)^{53}$	$0.6(2)^{53}$	$1.2(1)^{53}$		271, 134, 114, 315
mm: 10.1	86.24	$2.38(51)^{32}$				366, 370, 359, 358, 165
ra: 5.056	8.46	$0.43(3)^{91,\,98}$				387, 388, 333, 133, 134
ho: $0.835(1)^{267}$	B=26.77(35)[16], R=25.7(2)[16], V=25.40(15)[117]				$<0.01''^{117}$	266, 268, 114, 140, 315, 283, 40, 98, 378

Optical counterpart[29, 347] became brighter during the first two days following the GRB. Afterglow spectrum shows redshifted interstellar absorption lines (z =0.835), unambiguously settling the GRB cosmological distance scale[268, 267]; [OII]λ 3727 detected at same redshift[266, 16] shows the absorption comes from the host galaxy. Optical afterglow coincides to within $\sim 0.01''$ with the center of the host galaxy[117] (exponential scale length 0.046″). Host is active star-forming dwarf galaxy, of $M_B = -18.55$, $L_B = 0.12 L_*$ and star formation rate $< 1\ M_\odot\ yr^{-1}$ (see [16, 378]). Two-day bump in the optical light curve[81, 126, 309, 377, 426] is reflected in the X-ray afterglow[316]. Strong Fe K_α line emission in X-ray afterglow spectrum[322]. First radio counterpart detected[98, 388, 32, 134] shows interstellar scintillation variability, which confirms the relativistically expanding fireball model; first measured linear size of the fireball (R$< 10^{17}$ cm)[98]. Detected in IR (2.16μm)[53] and mm[32] wavelengths. No sub-mm detection[370].

970616 0.7568[56]	$1^h18^m54^s$ $-5°30'00''$ $(21' \times 36')^{254}$			(141.0,−67.4)	γ, X	
pr: $66.2(5)^{13}$	$\sim 80^{204}$	5.78(49)	$4.15(19)^{231}$			
X: 0.1667	11.0	0.57^{254}				275, 151
O: —						
IR: —						
mm: —						
ra: —						
ho: —						

Search of BATSE 2° error box[56] with the RXTE/PCA 4 hours after the GRB finds an X-ray source[254]. Combined RXTE/PCA and IPN error box[204] contains four ASCA X-ray sources[275] and 11 ROSAT sources[151]. None of the X-ray sources is a convincing GRB counterpart. Optical, radio and near-IR follow-up observations focus on the four ASCA sources and do not lead to detection of transient counterpart[143, 294, 413, 154]. 2′ away from RXTE/IPN error box is a massive cluster of galaxies, probably unrelated to the GRB[143].

970815 0.5049[364] $16^h8^m43^s$ +81°30′36″ ()[364] (115.3,+32.5) γ,X

pr:	150(4)[13]	∼165[364]	2.0(3)	2.2(3)[231]	0.05	[364]	
X:	3.2	<0.1	<0.005[278]				[147]
O:	0.6	V>21.5	<9.0[155]				[180, 381, 1, 238, 41]
IR:	1.5	K>18	<42.5[41]				[180]
mm:	—						
ra:	1.14	4.6	<0.35[238]				
ho:	—						

First RXTE/ASM detection[364]. Error box does not contain ASCA sources[278]; steady ASCA source is found slightly outside the RXTE/ASM error box[278]. ROSAT/HRI field of view contains 10 sources[147], one of which lies just at the border of the error box; maybe related to the GRB. No optical[155, 180, 381, 238, 1, 41], IR[180, 41], or radio[238] detection. No mm observations.

970828 0.73931[340] $18^h8^m31.7^s$ +59°18′50″ (10″)[150] (88.2,+28.5) γ,X,X^a,ra

RX J1808.5+5918[150]

pr:	160*[340]	∼8[360]	5.5(5)	9.4(2)[231]	0.02	0.16[1340]	[196]
X:	0.15	11.5	0.6[252]	1[424]	1.44(7)[424]	$4.1^{+2.1}_{-1.6}$[424]	[280, 279, 150, 293]
O:	0.168	R>23.8	<0.91[157]				[150, 291, 43, 422, 379, 166]
IR:	12.1	K>20	<6.73[228]				
mm:	—						
ra:	3.5	8.46	0.15[103]				[69]
ho:	0.96[69]	$R = 24.2$[69]					

RXTE/PCA scan of RXTE/ASM error box[340, 368] within 3.6 hours[252], leading to detection of X-ray afterglow. ROSAT/HRI field contains 15 X-ray sources[150], one of which is inside the RXTE/IPN error box and coincides with an ASCA variable source[280, 424]. In the week following the GRB no variable optical counterpart detected in the ROSAT error box down to $R = 23.8$[157] (see also [291]). Very short-lived radio source detected within the 10″ ROSAT error box[103, 69]. Host galaxy detected at $z = 0.96$ with SFR $\simeq 1\ M_\odot/yr$[69]. Most dusty host so far ($A_V = 2.2$). No IR detection[228]. No mm observations.

971024 0.4816[363] $18^h24^m58^s$ +49°28′55″ ()[363] (77.8,+24.4) γ,X

pr:	132(8)[231]	∼13.4[363]	0.15(7)	6.5(1.5)[231]	0.001	[1363]	
X:	—						
O:	0.583	R>19	<76[274]				[406]
IR:	—						
mm:	—						
ra:	—						
ho:	—						

RXTE/ASM detection[363] of a very weak BATSE burst. Error box is large (∼13.4 arcmin^2); no X-ray follow-up and the optical follow-up is very scanty and does not lead to a counterpart detection[406, 274]. No IR, radio and mm observations.

971214 0.97272[184]	$11^h56^m26.4^s$ $+65°12'0.5''$ (0.75)[178]			(132.0,+50.9)	γ,X,X^a,O,IR	
1SAX J1156.4+6513[8]						
pr: $31(1)^{13}$	$\sim 3.2^8$	0.8(1)	$1.1(1)^{231}$	0.02^{184}	$0.019(2)^{108}$	222
X: 0.2778	0.4	0.02^8	$1.03^{+0.51}_{-0.22}{}^{293}$	$1.20(2)^{293}$	$4.3^{+6.1}_{-2.5}{}^{293}$	
O: 0.4973	I=21.30(4)	$7.2^{175,\,178}$	$2.13(4)^{337}$	$1.20(2)^{68}$		234, 67, 341, 36
IR: 0.4673	J=$20.47^{+0.21}_{-0.19}$	10.7^{68}				141, 385, 337, 145
mm: —						
ra: 0.6973	8.46	$<0.05^{92}$				337
ho: $3.418(10)^{234}$	R=$25.60(17)^{234}$ B>26.8^{234} K>22.5^{337}				$0.14(7)''^{290}$	232, 239, 290

So far the highest redshift measured ($z = 3.418$) for a host galaxy[234]. Host spectrum shows Lyα emission line; it is consistent with a star forming galaxy with SFR>5$M_\odot$ yr^{-1}, $M_B \sim -20.9$ (see [234]), L$\sim 0.2L_*$, radius= $0.16(2)''$ and e-folding scale length $0.15'' - 0.19''$ (see [290]). The burst flux[222] combined with the redshift implies an energy release of 3×10^{53} erg in γ rays, comparable to the entire energy available in a coalescing neutron star merger. Estimates[234, 290] of chance coincidence between the host and the OT are of the order of 10^{-3}. GRB detected also with the RXTE/ASM at the 470(140) mCrab level[222]. EUVE observations[26] 20 hours after the GRB provide a flux upper limit of 1.7×10^{-13} erg/cm^{2}s in 10nm; no sub-mm detection[368, 370]. No mm observations.

971227 0.34938[55]	$12^h57^m17.2^s$ $+59°24'0.2''$ (1.5')[327, 9]			(121.6,+57.7)	γ,X,X^a	
1SAX J1257.3+5924[327]						
pr: $7(2)^{13}$	$\sim 7^{327}$	0.83(4)	$1.14(15)^{231}$	0.04	0.01^9	55
X: 0.5833	0.3	0.016^{327}		$1.12^{+0.08}_{-0.05}{}^9$		
O: 0.89	R>22.8	$<2.3^{162}$				42, 123, 30, 205, 264, 336, 300, 417, 168
IR: 12.75						227
mm: —						
ra: —						
ho: —						

BATSE/BeppoSAX-WFC and NFI detections[419, 55, 327], but error box includes two BeppoSAX-NFI sources, one of which is a possible variable X-ray afterglow[327, 9]. The error box of the non-variable X-ray source contains 3 radio sources. List of optical afterglow limits and a debatable afterglow identification[42, 168] is given in[417]. For clarifications on the confusion about the optical counterparts see [30, 337, 77]. LOTIS observations starting 14 s after the GRB trigger show no simultaneous optical emission of $R > 13.2(2)$ (10 s integration time)[300, 417]. No IR detection[227]. No mm, radio observations.

980109 0.05024[208]	$0^h25^m56^s$ $-63°1'26''$ (10')[208]			(307.8,−53.9)	γ,X	
pr: $31(4)^{231}$	$\sim 314^{208}$	0.74(14)	$0.5(1)^{231}$	0.02	^{208}	
X: —						
O: 2.99	I>20	$<23.8^{349}$				397
IR: —						
mm: —						
ra: —						
ho: —						

No BeppoSAX/NFI follow-up of WFC $\rho \simeq 10'$ error box[208]. No variable optical source (>0.4 mag) seen one day [397] and three days[349] after the GRB, down to $I = 21$ and 20 mags, respectively. No IR, mm, radio observations.

980326 0.888125[51] $8^h36^m34.28^s$ $-18°51'23.9''$ (0.4″)[160] (242.4,13.0) *γ,X,O*

pr:	5^{*}[34]	∼76[202]	0.52(4)	0.22(4)[231]	0.1	0.05[51]	160
X:	0.34	<1.6	<0.08[253]				
O:	0.5319	R=21.2(1)	10.0[161, 160]	0.8(4)[22]	2.0(1)[22]		163, 164, 83, 398, 38
IR:	—						
mm:	—						
ra:	—						
ho:	≃ 1[22]	$R > 27.3$[21]					160, 73, 22

Optical transient found ∼ 0.5d after the GRB trigger[161, 160]. Light curve shows fast decline[160, 73, 22, 38]. Saturation of optical light curve initially interpreted as host galaxy at $R = 25.5(5)$[160, 73], but later observations show that $R_{\rm host} > 27.3$[21, 22]. Light curve contains a bump, about 3–4 weeks after the GRB, which is consistent with the presence of a $z \simeq 1$ type Ic supernova component[22]. The SN+PL interpretation naturally fits the collapsar model. No sub-mm detection (< 2.7mJy @ 850μm, < 30mJy @ 450μm)[370]; no IR, radio observations.

980329 0.1559[111] $7^h2^m38.0217^s$ $+38°50'44.017''$ (0.05″)[390] (178.1,+18.7) *γ,X,X*[a]*,O,IR,mm,ra*

1SAX J0702.6+3850[207],VLA J0702+3850[390]

pr:	18.9(3)[231]	∼3.1[207]	5.9(2)	5.02(8)[231]	0.14	0.07(1)[108]	111
X:	0.2931	0.4	0.02[207]	1.4(4)[209]	1.35(3)[209]	10(4)[209]	293, 152
O:	3.84	R=25.7(3)	0.16[79]		$1.21^{+0.13}_{-0.12}$[339]	0.24[339]	169, 296, 298, 144, 351, 80, 229, 304
IR:	3.84	K=20.7(2)	3.5[243]				335, 242, 265, 298, 339, 54, 298
mm:	7.0	350	5(1.5)[369]		3.0[370]		394
ra:	2.94	8.4	0.248(16)[390]	+0.9[394]			
ho:	< 3.9[69]	R=26.3(2)[69]					351, 54

Variable radio afterglow[390, 394] led the way to a decaying R to K band counterpart[79, 296, 298, 229, 54, 243, 265]. Optical/near IR light curve analysis[298, 339, 144] and host galaxy properties restrict the redshift $z < 3.9$[69] and indicate host maybe in a molecular cloud[241]; alternative models available[82, 412].

980425 0.90915[372] $19^h35^m3.316^s$ $-52°50'44.75''$ (0.07″)[236] (345.0,−27.7) *γ,X,X*[a]*,O,IR,mm,ra*

SN1998bw,1SAX J1935.0−5248[315],J195303.3−525045[236]

pr:	23(1)[231]	∼201[372]	0.30(3)	0.44(4)[231]	0.026	0.18(3)[313]	372, 314
X:	0.425	0.30(4)	0.016[313]			0.4[313]	315, 318, 282
O:	2.49	R=15.7(1)	1585[128]		1.18[262]	0.20[128]	128, 262, 302, 216, 301, 31
IR:	10.49	J=11.5	41446[246]				
mm:	11.8	150	39(11)[236]				
ra:	2.82	4.8	9[414]	0.75[236]			236, 415, 213, 212, 245
ho:	0.00841(5)[396, 219]						128, 236

BeppoSAX initial ($\rho = 8'$) error box[372] contains a bright supernova SN1998bw[128] of a peculiar Type Ib/c, located in an HII region in a spiral arm of the face-on barred spiral galaxy ESO 184−G82[128]. Probability of chance coincidence $< 10^{-4}$(see [128]). Redshift of the host is $z = 0.00841(5)$[396, 219]; linear polarization of 0.53(8)%, $\theta = 49(3)°$ detected in the spectrum of the SN[219]. SN 1998bw spectra are very unusual[302, 301]. BeppoSAX/NFI observations reveal two X-ray sources[315, 314, 313] one of which (1SAX J1935.0−5248) is found later to be consistent with the SN, after final corrections of the NFI position[318]. Very strong radio emission, indicating mildly relativistic afterglow ($\Gamma \sim 2$)[236]; IR detection[246]. Modeling of the optical light curves[128, 262] indicates SN 1998bw is extremely energetic[214, 420, 31] and may have left behind a black hole[214]. Upper limit on gravitational wave detection[4].

980515 0.708495[319] $21^h17^m25^s$ $-67°15'18''$ $(4')$[343] (326.5,−38.7) γ,X

pr:	15^{*}[343]	~ 50[343]		0.035	[343]	
X:	—					[87]
O:	—					
IR:	—					
mm:	—					
ra:	—					
ho:	—					

BeppoSAX GRBM and WFC trigger[318]. NFI follow-up observations[87] find a new X-ray source (1SAX J2116.8−6712) of $F_x = 1.6(4) \times 10^{-13}$ ergs/cm^{2}s. The source is offset by 4.9′ from the centroid of the refined[343] WFC position and does not show variability[87]; it is likely not associated with the GRB. No optical, IR, mm, radio observations.

980519 0.51410[273] $23^h22^m21.50^s$ $+77°15'43.25''$ $(0.1'')$[100] (118.0,+15.3) γ,X,X^a,O,R

1SAX J2322.3+7716[286],VLA J232221.5+771543[100]

pr:	30(2)[231]	~ 2.2[286]	2.4(1.4)	0.01(1)[231]	0.01	0.18[210]	[273]
X:	0.4059	0.38(6)	0.02[286]	$1.8^{+0.6}_{-0.5}$[285]	1.8(3)[285]	$5.6^{+10.2}_{-5.1}$[293]	[293]
O:	0.3559	I=18.5(1)	95.0[215]	1.2(3)[176]	2.05(4)[176]	0.481[170]	[402]
IR:	—						
mm:	—						
ra:	2.79	8.3	0.102(19)[106]				[103, 100]
ho:		$R = 26.05(22)$[374]					[24]

BATSE/BeppoSAX-WFC GRB with one of the fastest ($\simeq$ 2) temporal power-law decays recorded[285, 293, 402, 176]. For a complete photometry of the optical light curve see [176, 402]. Radio source detected 2.8 days after trigger with large light curve variations due to ISS[100]. The fast decline and the radio data (radio source very compact of size $< 1\mu$arcsec) indicate that the afterglow emission may originate either from a jet[176, 100] or from a blast wave propagating into the dense wind of the progenitor star[100]. No constraining mm observations[370]; no IR observations. Deep optical observations two months after the GRB detected a faint object at the OT position, presumably the host galaxy[374, 24].

980611 0.034[13] $18^h20^m7.2^s$ $+54°4'58.8''$ $(7° \times 3.5')$[194] (82.6,+26.1) γ

pr:	9.3(5)[13]	~ 1500[194]		1.1(1)[13]		
X:	—					
O:	—					
IR:	—					
mm:	—					
ra:	—					
ho:	—					

BATSE GRB (# 6816). RXTE/PCA follow-up scan finds two X-ray sources; both are shown to be substantially outside the BATSE/Ulysses IPN annulus[194] and are very likely unrelated to the GRB.

980613 0.20215[324] $10^h17^m57.82^s$ $+71°27'25.5''$ $(0.6'')$[171] (138.0,+40.8) γ,X,X^a,O

1SAX J1017.9+7127[57]

pr:	50^{*}[371]	~ 2.2[57]		0.17(3)[418]	0.014	[371]	
X:	0.3597	0.11(3)	0.006[57]				[172]
O:	0.6979	R=22.9(2)	2.1[188]		1.3[171]	0.27[70]	[49, 50, 288, 172, 66]
IR:	—						[263, 49, 50]
mm:	—						
ra:	—						[103]
ho:	1.0964(3)[70]	B=24.4(2)[70]	V=24.1(2)[70]	R=23.9(2)[70]			[74, 75, 76]

BeppoSAX GRBM and WFC triggered GRB[324]; BATSE did not trigger because of prior trigger due to intense solar flare[418]. NFI follow-up detected 2 X-ray sources, one of which is variable[57]. Optical counterpart detected 0.69 days after trigger[188]. Host galaxy was found at the OT position with $z = 1.0964$[70]; spectrum shows strong emission line interpreted as [OII] 3727 and very blue featureless continuum indicating star-forming galaxy (SFR$\simeq 3.9\ M_\odot/yr$)[70]. No IR[263, 49, 50], radio[103] detections; no mm observations.

980703 0.18247[244] $23^h59^m6.6661^s$ $+8°35'7.0939''$ $(0.0005'')$[389] (101.6,−52.1) γ, X, X^a, O, IR, R

1SAX J2359.1+0835[127]

pr:	370(10)[231]	∼30.5[365]	1.9(1)	5(2)[231]	0.04	[1244]	
X:	0.9135	0.75	0.04[127]	1.51(32)[130]	<0.91[407]	0.34[407]	
O:	1.3	R=21.2	10.0[90]	1.01(1)[407]	1.61[407]	0.188[78]	425, 18, 47
IR:	5.4	K=18.8(1)	20.3[18]		1.43(11)[47]		187, 407
mm:	7.34	220	<5.2[18]				370
ra:	1.2	4.86	0.135(26)[90]				389
ho:	0.9662(2)[78]	R=22.58$^{+0.06}_{-0.05}$[407]	V=23.04(8)[407]	K=19.62$^{+0.12}_{-0.11}$[407]		0.21(12)''[18]	74, 375, 389, 376

RXTE/ASM[244] and BATSE GRB; X-ray source detected with the BeppoSAX NFI[127, 130]. Optical counterpart detected[90, 425] following detection of a radio source[90]. Host galaxy spectrum contains emission and absorption lines allowing redshift determination at $z = 0.9662(2)$[78]. Host is the brightest so far[18, 407] with $M_B = -21.2$[18]; star-forming galaxy with SFR$\gtrsim 10\ M_\odot/yr$[78, 376]. VLBI detects source unresolved at < 0.3 mas[389]. IR detection[407, 18]; no mm detection[18, 370].

980706 0.6665[13] $11^h0^m33^s$ $+57°23'6''$ $(36' \times 1.56')$[255] (148.2,+54.0) γ

pr:	26(2)[13]	∼56[255]	5.12(5)[13]	
X:	—			255
O:	—			
IR:	—			
mm:	—			
ra:	—			
ho:	—			

RXTE/PCA scan 2.7 hours after trigger of BATSE GRB finds a 2mCrab X-ray source that is not detected at the next scan 1.5 hours later[255]. It is unclear whether the source has faded below the PCA detection limit (implying a decay index of >3) or it is not located at IPN/PCA 'best position'. Most likely, PCA source is not related to the GRB. No BeppoSAX/NFI follow-up, no optical, IR, mm, radio observations.

981220 0.91135[361] $3^h42^m33.8^s$ $+17°9'0''$ $(2.4' \times 4.5')$[199] (171.0,−29.3) γ, X

pr:	15*[89]	∼11[199]	2.4(4)	1.0(2)[1109]	0.012(1)[361]	
X:	—					
O:	2.12	V>22	<5.7[352]			401, 173, 270, 410, 12
IR:	—					
mm:	—					370
ra:	2.1	1.43	<0.2[131]			93, 95, 391
ho:	—					

RXTE/ASM, BeppoSAX, Ulysses and KONUS GRB[361, 89, 199, 109]. No optical counterpart found[352, 401, 410, 270, 12, 171]. Unusual radio variable source[131, 93] associated with a faint, slowly variable optical source[15] was later found to lie outside the refined IPN error box[201] and has a core-jet morphology in VLBA observations, strongly suggestive of a highly variable background intra-day variable (IDV) source[391]. No X-ray follow-up observations; no IR,mm observations.

981226 0.40793[65] $23^h29^m37.21^s$ $-23°55'53.8''$ (0.4″)[95] (38.2,−71.3) γ,X,X^a,R

1SAX J2329.6−2356[113],VLA 232937.2−235553[102]

pr:	20^{*65}	$\sim 3.2^{113}$		0.006	[65]		
X:	0.4701	0.30(7)	0.016^{113}				
O:	0.412	R>23	$<1.9^{247}$				95, 132, 421
IR:	—						44
mm:	3.74	350	$<0.6(3.8)^{370}$				
ra:	8.54	8.46	$0.169(28)^{95}$	$2.0(4)^{95}$			132
ho:		R=24.85(6)[95]					

BeppoSAX/WFC error box contains decaying NFI X-ray source[113]. Several suggestions for optical and IR counterpart made[132, 44, 421, 226], but none acceptable[342, 19, 356, 247]. Radio counterpart found 8.5 days after trigger[95] leads to potential host galaxy[95]. No mm detection[370].

990123 0.40759[330] $15^h25^m30.31^s$ $+44°45'59.24''$ (0.15″)[235] (73.1,+54.6) γ,X,X^a,O,IR,R

1SAX J1525.5+4446[181],VLA J152530.3+444559[235]

pr:	$63.3(3)^{135}$	$\sim 2.2^{181}$	23.7(2.3)	$27.1(5)^{231}$	0.08	[88]	33
X:	0.245	11.0	0.57^{329}		$1.44(7)^{233}$	1.2^{181}	276, 46
O:	0.169	R=18.65(4)	94.0^{289}	$0.75(23)^{135}$	$1.52(15)^{116}$	0.053^{135}	3, 2, 46, 189, 346, 292, 260
IR:	1.23	K=18.29(4)	32.5^{20}	$0.8(1)^{233}$	$1.12(11)^{233}$		46
mm:	1.27	222.0	$<2.41^{235}$				334
ra:	1.24	8.46	$0.260(32)^{94}$	$+1.4(7)^{135}$	$<0.8^{235}$		
ho:	$1.6004(8)^{220}$	V=24.20(15)[118], R=23.63(5)[118], K=21.65(30)[25]				$0.6(1)''^{25}$	189, 233, 119, 72, 116, 376, 193, 7

First detection of prompt optical emission: BATSE trigger activates the robotic telescope ROTSE, which detects the OT in 6 images between 22 s and 10 min after the burst, with V between 8.9 and 14.3 mag[2, 3]. Prompt γ emission among top 0.4% in fluence[33]; gamma-ray and optical signals do not track one another[135, 33]. Later follow-up optical observations detected the OT at $R \sim 18.6$ and smoothly declining (see [233, 135, 46, 7, 120] and references therein). Optical afterglow light-curve composed of smoothly joined power-laws; break in the light curve at $t \sim 1$ d first interpreted as beaming, but is not achromatic[233, 120]. The combined γ/optical/radio light curve[2, 135, 233, 235, 46] indicates importance of internal and external (both outward and reverse) shocks. Optical polarization not detected (<2.3%)[189]. Redshifted metal absorption and lack of the Lyα forest limit the host redshift to $1.6 < z < 2.05$[220, 233, 189]. Irregular host morphology may indicate merging galaxies[120]; spectrum indicates relatively blue, star-forming galaxy of $M_B = -20.4$, $L \simeq 0.7L_*$ and SFR>6.0 $M_\odot/yr$[25]. Three active star forming regions identified[193]. Initial detection of nearby galaxies spawned suggestions of gravitational lensing that were later refuted (see GCN Circs 219,221,234-6,238,241,242-3). First detection of radio flare 1.24 d after the trigger[94, 235]. IR detection[20, 233, 46]; no mm detection[235].

990217 0.224618[386] $3^h2^m52^s$ $-53°5'36''$ (^3I)[386] (268.9,−54.5) γ,X

pr:	25^{*6}	$\sim 28^{386}$	0.11(3)	$0.13(2)^{a6}$	0.016	[6]	386
X:	0.27	<0.1	$<0.005^{317}$		$>1.6^{317}$		
O:	0.28	R>23.5	$<1.8^{297}$				353, 311
IR:	—						
mm:	—						
ra:	1.09	4.8	$<0.28^{411}$				
ho:	—						

BeppoSAX GRBM/WFC detection with $\rho = 3'$ error box[386];NFI follow-up[317] provides only upper limit for an X-ray afterglow of 10^{-13} erg/cm^2 s. No variable optical[297, 353, 311], or radio[411] counterpart. No IR, mm, observations.

990308 0.21883[362] $12^h23^m11.44^s$ $+6°44'5.1''$ $(0.17'')$[355] (283.5,+68.5) γ,X,O

pr:	106(12)[355]	∼317[362]	0.63(14)	0.6(1)[231]	0.009	[362]
X:	—					
O:	0.1367	R=18.14(6)	246[355]	0.38(25)[355]	1.2(1)[355]	[417]
IR:	—					
mm:	—					
ra:	102.0	8.5	<0.258[355]			
ho:		R>25.7[355]	K>23.3[355]			

Near-simultaneous LOTIS and Super-LOTIS observations of BATSE error box do not reveal afterglow coincident with GRB, with $V > 12.0$ (10s integration, starting 132s after trigger), $V > 13.4$ (10 min) for LOTIS, and $V > 15.3$ for Super-LOTIS[417]. Comparison of images taken 3.28 hours and 82 days after burst show likely optical counterpart[355], which decays by 0.08 ± 0.08 mag in 7.7 min. No radio counterpart[355]. No IR, mm observations. No evidence for a host galaxy in images taken 103 days after the burst ($R > 25.7$, $K > 23.3$)[355].

990506 0.47465[223] $11^h54^m50.14^s$ $-26°40'35.2''$ $(0.8'')$[392] (287.6,+34.5) γ,X^a,R

VLA J115450.1−2640.6[392]

pr:	131.3(2)[223]	∼30[203]	7.6(6)	17.6(4)[231]		
X:	0.126	0.35	1.8[251]		1.9(6)[384]	
O:	0.616	R>23	<1.9[257]			[403, 354, 427, 404, 310, 350]
IR:	—					
mm:	—					
ra:	1.73	8.4	0.54[393, 392]			
ho:		R=24.8(2)[17]				[307]

RXTE/PCA scanning of BATSE trigger #7549[223] detects a previously unknown X-ray source of 1.5 mCrab, which decayed by a factor of 2.4 in subsequent observations[251, 384]. The source is within the refined (30 arcminsq) IPN error box[203]. No evidence for optical afterglow to $R = 23$ mag[257, 310, 403, 404, 354, 427, 350]. Radio observations detect 4 sources within the PCA/IPN error box[391], one of which fades below the VLA detection limit (0.035 mJy) sometime beween 2−16 days after the burst trigger[393]. Optical observations[17] of the radio source ∼36 days after the GRB reveal a faint, extended galaxy with irregular and possibly interacting morphology, potentially the host of the GRB. No IR, mm observations.

990510 0.36743[328] $13^h38^m7.11^s$ $-80°29'48.2''$ $(0.44'')$[190] (304.9,−17.8) γ,X,X^a,O,R

1SAX J1338.1−8030[240]

pr:	68(2)[224]	∼24[195]	4.37(13)	2.53(9)[231]	0.14	[4]	[64]
X:	0.333		[331]				[240]
O:	0.35	R=19.2(3)	92.8[408]	0.61(12)[380]	2.41(2)[380]	0.67[179]	[179, 211, 14, 190]
IR:	—						
mm:	—						
ra:	3.3	8.7	0.227(30)[179]				
ho:	1.619(2)[409]	R>27.6[14] , V>28[115]					[211]

X-ray and optical counterparts are found[331, 240, 408] in the combined WFC/IPN error box[328, 64, 195]. Later recalibration of R band measurement[218] indicates that the OT had been detected 3.5 hours after trigger[10] at $R = 17.75$ mag. Optical light curve shows clear achromatic break after ∼1.5 d, that may signify beaming; first index is −0.8 and second is −2.4[179, 380]. Radio counterpart detected in 8.7 GHz[179]. Metal absorption lines in the spectrum[409] limit the redshift above $z > 1.619(2)$; absence of Lyα forest places an upper limit $z < 2.0$[14]. First burst with detection (0.86 d after trigger) of optical linear polarization[63, 416] of 1.6(2)% and polarization angle 96(4)°, that remains constant over about three days. No host galaxy detection; no IR, mm observations.

990520 0.08539[137] $8^h35^m56^s$ $+51°18'36''$ $(3')$[137] (167.5,+36.9) γ,X

1SAX J0835.9+5118[137]

pr:	8[225]	∼28[137]		0.08(3)[225]	0.023	[137]	
X:	—						
O:	0.735	R>21.5	<11.2[248]				[256, 306, 305, 37, 177]
IR:	—						
mm:	—						
ra:	0.605	4.8	<0.125[103]				[104, 105]
ho:		R=20.75(7)[177] V=21.08(5)[256] B=21.58(8)[177]					[23]

Brief WFC transient (∼ 10 s) barely seen in GRBM data[137]. WFC error box (ρ = 3′) contains VLA source[104, 105], coincident with a non-variable optical object, which may be a galaxy[23], but could also be a point source[37, 248]. The BATSE team reports on May 24.7 UT a faint untriggered event coincident with the BeppoSAX transient, that was recorded while the onboard trigger was disabled[225]. It is uncertain whether the BeppoSAX transient and the VLA source/optical galaxy are related, but it is likely that the BeppoSAX transient is associated with a GRB. No IR, mm observations.

990527 0.58182[197] $22^h50^m27^s$ $-20°53'26''$ $(6')$[197] (39.1,−61.7) γ

pr:	20*[197]	∼100[197]		0.8[α197]			
X:	—						
O:	1.75	R>22.0	<7.0[308]				
IR:	—						
mm:	—						
ra:	—						
ho:	—						

GRB detected with Ulysses/Konus/NEAR[197]. Optical imaging of 100 arcmin^2 error box ∼1.75 d after the burst trigger does not reveal a counterpart[308] (R > 22.0). No X-ray follow-up, radio, IR, mm observations.

990627 0.20894[272] $1^h48^m27^s$ $-77°4'36''$ $(1')$[272] (298.8,−39.6) γ,X,X^a

1SAX J0148.5−7704[287]

pr:	50*[272]	∼28[272]			0.007	[272]	
X:	0.331	0.35	0.02[287]				
O:	0.929	R>21.0	<17.7[344]				
IR:	—						
mm:	—						
ra:	1.46	4.8	<0.125[383]				[103]
ho:	—						

BeppoSAX WFC error box[272] contains 4 radio sources[383], one of which coincides with a fading NFI source[287], which is a likely GRB counterpart. No variable optical counterpart is found at the R > 21.0 limit[344]. No IR, mm observations.

990704 0.7294[332] $12^h19^m27.3^s$ $-3°50'22''$ $(1')$[86] (287.7,+58.1) γ,X,X^a

1SAX J1219.5−0350[86]

pr:	40*[182]	∼154[139]			0.14	[182]	
X:	0.335	0.44	0.02[86]				[281]
O:	0.439	R>21.2	<14.7[405]				[48, 261, 259, 217]
IR:	—						
mm:	—						
ra:	1.021	4.88	<0.065[345]				
ho:	—						

BeppoSAX/WFC error box (ρ = 7′)[332, 139, 182] contains new fading X-ray source, which is the likely counterpart[86, 281]. Two radio sources in the WFC error box[345] unlikely related to GRB. Initial optical counterpart[261] later retracted[259]. No IR, mm observations.

990705 0.66765[52] $5^h9^m54.52^s$ $-72°7'53.1''$ $(0.3'')$[258] (283.5,−33.4) γ, X, X^a, O, IR

pr:	$45^{\star}$[52]	$\sim$3.5[198]		0.09	[52]	
X:	0.4744		[52, 5]		0.72[258]	
O:	0.7324	V=22.0(4)	5.7[295]	>1[258]	0.40[258]	[174]
IR:	0.272	H=16.57(5)	252.0[295]	1.68(10)[258]		
mm:	—					
ra:	0.662	4.8	<0.1[382]			[103]
ho:		V=23.80(15)[258]				

BeppoSAX/WFC detection; radio observations[382] revealed 3 sources in the WFC ($\rho = 3'$) error box[52], which are not, however, in the BeppoSAX/Ulysses/NEAR IPN/WFC intersection[198]. NFI follow-up detects a new X-ray source[138]; detection contaminated by radiation from LMC X-2, which lies 52′ off the NFI center[5]. First detection of an afterglow in NIR [295, 258] ($H = 16.57$), which decays with a power-law of index -1.68[258]. Elongated irregular, fuzzy object of $V = 23.8$ (size $2.4'' \times 0.8''$) partially superposed to the OT is suggested as the GRB host[258]. No neutrino detection ±48 hours from the GRB trigger[121]. No mm observations.

990712 0.69655[185] $22^h31^m53.1^s$ $-73°24'29''$ $(1'')$[11] (315.3,−40.2) γ, X, O

pr:	$90^{\star}$[185]	$\sim$12.6[185]			
X:	—				
O:	0.1235	R=19.4	52.5[11]	1.05[221]	[395, 191]
IR:	—				
mm:	—				
ra:	—				
ho:	0.430(5)[129]	R=21.79[192]			[221, 191]

BeppoSAX WFC error box ($\rho = 2'$)[185] contains optical counterpart[11]; its spectrum shows pronounced emission lines and absorption lines both consistent with a redshift of $z = 0.430(5)$[129]. Evidence for a host galaxy at $R = 21.76$ from the saturation of the optical light curve[191, 192, 221]. No BeppoSAX NFI follow-up; no IR, radio or mm observations.

TABLE NOTES

General notation	
[NNN]	reference for the value just to the left of it
(MM)	error in the last digits of the number just to the left of it
*	the value is not determined in the standard way adopted for this entry; see reference for details
N	the value is not determined in the standard way, but in a frequent deviation explained below in these notes
Comments on specific columns	
Name	GRB name in YYMMDD format
UT trig	time of trigger, in fractional days since start of the UT day of the burst
duration	duration, defaults to the BATSE T90, unless marked by star*.
errbox	area of prompt emission or NFI error box, in square arcmin
$F_\gamma^{\rm peak}$	prompt gamma-ray peak flux in units of $10^{-6}\,{\rm erg\,cm^{-2}\,s^{-1}}$. Defaults to BATSE flux above 20 keV
S_γ	Fluence of prompt gamma-ray emission in units of $10^{-5}\,{\rm erg\,cm^{-2}}$. Defaults to BATSE fluence above 20 keV. Reference and note are for both flux and fluence. Notes for frequent deviations: (a) SAX GRBM 40–700 keV.
$F_{\rm X}^{\rm peak}$	prompt 2–10 keV X-ray peak flux in units of $10^{-6}\,{\rm erg\,cm^{-2}\,s^{-1}}$.
$S_{\rm X}$	Fluence of prompt 2–10 keV X-ray emission in units of $10^{-5}\,{\rm erg\,cm^{-2}}$. Reference and note are for both flux and fluence
$\Delta{\rm UT_X}$	time since trigger, in days, of X-ray afterglow discovery or limit; ditto other wavelengths
$F_{\rm X}^{\rm a}$	2–10 keV X-ray afterglow discovery flux or limit, first in units of $10^{-12}\,{\rm erg\,cm^{-2}\,s^{-1}}$ and then in μJy
$F_{\rm O,\ldots,ra}$	afterglow discovery fluxes or limits, in μJy for O and IR and in mJy for mm and radio.
$\beta_{\rm X}$	X-ray afterglow flux spectral slope; ditto other wavelengths
$\delta_{\rm X}$	X-ray afterglow flux temporal slope; ditto other wavelengths
$N_{\rm H}$	H column density, from X rays, in $10^{21}\,{\rm cm^{-2}}$
mag	optical ($UBVRI$) and near-IR (JHK) discovery magnitude, with band; all else being equal, R and K were preferred
A_V	visual absorption in mags. Foreground, or total, depending on reference and method.
$\nu_{\rm mm}$	millimeter frequency in GHz. All else being equal, 90 GHz was the preferred mm frequency
$\nu_{\rm ra}$	radio frequency in GHz; All else being equal, 5 GHz was the preferred radio frequency
z	redshift; in order of preference (i) an emission-line redshift, or (ii) the redshift of the presumed host, or (iii) the highest absorption redshift in the OT spectrum. Limits sometimes from (absence of) Ly break.

Table references

[1] Adams, MT et al. 1997 IAUC 6725.
[2] Akerlof, C et al. 1999 Nat 398:400.
[3] Akerlof, CW & McKay, TA 1999 GCN 205.
[4] Amati, L et al. 1999 A&AS 138:605.
[5] Amati, L et al. 1999 GCN 384.
[6] Amati, L et al. 1999 GCN 317.
[7] Andersen, MI et al. 1999 Science 283:2075.
[8] Antonelli, LA et al. 1997 IAUC 6792.
[9] Antonelli, LA et al. 1999 A&AS 138:435.
[10] Axelrod, T et al. 1999 GCN 315.
[11] Bakos, G et al. 1999 IAUC 7225.
[12] Bartolini, C et al. 1998 GCN 175.
[13] BATSE Team. Gamma-ray burst data. http://gammaray.msfc.nasa.gov/batse/ 2000.
[14] Beuermann, K et al. 1999 A&A 352:L26.
[15] Bloom, JS et al. 1999 GCN 196.
[16] Bloom, JS et al. 1998 ApJ 507:L25.
[17] Bloom, JS et al. 1999 GCN 351.
[18] Bloom, JS et al. 1998 ApJ 508:L21.
[19] Bloom, JS et al. 1998 GCN 182.
[20] Bloom, JS et al. 1999 GCN 240.
[21] Bloom, JS & Kulkarni, SR 1998 GCN 161.
[22] Bloom, JS et al. 1999 Nat 401:453.
[23] Bloom, JS et al. 1999 GCN 335.
[24] Bloom, JS et al. 1998 GCN 149.
[25] Bloom, JS et al. 1999 ApJ 518:L1.
[26] Boer, M et al. 1997 IAUC 6795.
[27] Boller, T & Voges, W 1996 IAUC 6469.
[28] Boller, T et al. 1997 IAUC 6580.
[29] Bond, HE 1997 IAUC 6654.
[30] Bond, H et al. 1998 GCN 22.
[31] Branch, D. In Livio, M, editor, *Supernovae and Gamma Ray Bursts* in press (astro–ph/9906168) 1999.
[32] Bremer, M et al. 1998 A&A 332:L13.
[33] Briggs, MS et al. 1999 ApJ 524:82.
[34] Briggs, MS et al. 1998 IAUC 6856.
[35] Butler, RC et al. 1997 IAUC 6539.
[36] Castander, FJ et al. 1997 IAUC 6791.
[37] Castro-Tirado, A et al. 1999 GCN 336.
[38] Castro-Tirado, AJ & Gorosabel, J 1999 A&AS 138:449.
[39] Castro-Tirado, AJ et al. 1998 Science 279:1011.
[40] Castro-Tirado, AJ et al. 1998 IAUC 6848.
[41] Castro-Tirado, AJ et al. 1997 IAUC 6744.
[42] Castro-Tirado, AJ et al. 1997 IAUC 6800.
[43] Castro-Tirado, AJ et al. 1997 IAUC 6730.
[44] Castro-Tirado, AJ et al. 1998 GCN 173.
[45] Castro-Tirado, AJ et al. 1998 A&A 330:14.
[46] Castro-Tirado, AJ et al. 1999 Science 283:2069.
[47] Castro-Tirado, AJ et al. 1999 ApJ 511:L85.
[48] Castro-Tirado, A et al. 1999 GCN 362.
[49] Castro-Tirado, AJ et al. 1998 GCN 102.
[50] Castro-Tirado, AJ et al. 1998 GCN 103.
[51] Celidonio, G et al. 1998 IAUC 6851.
[52] Celidonio, G et al. 1999 IAUC 7218.
[53] Chary, R et al. 1998 ApJ 498:L9.
[54] Cole, DM et al. 1998 IAUC 6866.
[55] Coletta, A et al. 1997 IAUC 6796.
[56] Connaughton, V et al. 1997 IAUC 6683.
[57] Costa, E et al. 1998 IAUC 6939.
[58] Costa, E et al. 1997 IAUC 6572.
[59] Costa, E et al. 1997 IAUC 6576.
[60] Costa, E et al. 1997 IAUC 6533.
[61] Costa, E et al. 1997 IAUC 6649.
[62] Costa, E et al. 1997 Nat 387:783.
[63] Covino, S et al. 1999 A&A 348:L1.
[64] Dadina, M et al. 1999 IAUC 7160.
[65] di Ciolo, L et al. 1998 IAUC 7074.
[66] Diercks, A et al. 1997 GCN 108.
[67] Diercks, A et al. 1997 IAUC 6791.
[68] Diercks, AH et al. 1998 ApJ 503:L105.
[69] Djorgovski, SG & et al. Hosts of GRB 970828 and GRB 980329. in preparation 2000.
[70] Djorgovski, SG et al. 1998 GCN 189.
[71] Djorgovski, SG et al. 1999 GCN 289.
[72] Djorgovski, SG et al. 1999 GCN 256.
[73] Djorgovski, SG et al. 1998 GCN 57.
[74] Djorgovski, SG et al. 1998 GCN 139.
[75] Djorgovski, SG et al. 1998 GCN 114.
[76] Djorgovski, SG et al. 1998 GCN 117.
[77] Djorgovski, SG et al. 1998 GCN 25.
[78] Djorgovski, SG et al. 1998 ApJ 508:L17.
[79] Djorgovski, SG et al. 1998 GCN 41.
[80] Djorgovski, SG et al. 1998 GCN 38.
[81] Djorgovski, SG et al. 1997 Nat 387:876.
[82] Draine, BT 2000 ApJ 532:273.
[83] Eichelberger, AC et al. 1998 GCN 33.
[84] Feroci, M et al. 1998 A&A 332:L29.
[85] Feroci, M et al. 1997 IAUC 6610.
[86] Feroci, M et al. 1999 IAUC 7217.
[87] Feroci, M et al. 1998 IAUC 6909.
[88] Feroci, M et al. 1999 IAUC 7095.
[89] Feroci, M et al. 1998 GCN 159.
[90] Frail, DA et al. 1998 GCN 128.
[91] Frail, DA & Kulkarni, SR 1997 IAUC 6662.
[92] Frail, DA & Kulkarni, SR 1997 GCN 7.
[93] Frail, DA & Kulkarni, SR 1998 GCN 170.
[94] Frail, DA & Kulkarni, SR 1999 GCN 211.
[95] Frail, DA et al. 1999 ApJ 525:L81.
[96] Frail, DA et al. 1997 ApJ 483:L91.
[97] Frail, DA et al. 1997 IAUC 6545.
[98] Frail, DA et al. 1997 Nat 389:261.
[99] Frail, DA et al. 1996 IAUC 6472.
[100] Frail, DA et al. 2000 ApJ 534:559.
[101] Frail, DA et al. 1998 ApJ 502:L119.

[102] Frail, DA et al. 1999 GCN 269.
[103] Frail, DA et al. In Kippen, RM et al., editors, *Gamma-Ray Bursts* in press 2000.
[104] Frail, DA et al. 1999 GCN 334.
[105] Frail, DA et al. 1999 GCN 337.
[106] Frail, DA et al. 1998 GCN 89.
[107] Frontera, F et al. In Meegan, C et al., editors, *Gamma-Ray Bursts* 446 New York 1998. AIP.
[108] Frontera, F et al. 2000 ApJS 127:59.
[109] Frontera, F et al. 1998 GCN 167.
[110] Frontera, F et al. 1997 IAUC 6567.
[111] Frontera, F et al. 1998 IAUC 6853.
[112] Frontera, F et al. 1998 A&A 334:L69.
[113] Frontera, F et al. 1998 IAUC 7078.
[114] Fruchter, A et al. 1997 IAUC 6674.
[115] Fruchter, A et al. 1999 GCN 386.
[116] Fruchter, A et al. 1999 GCN 354.
[117] Fruchter, AS et al. 2000 ApJ submitted (astro-ph/9903236).
[118] Fruchter, AS et al. 1999 ApJ 519:L13.
[119] Fruchter, A et al. 1999 GCN 255.
[120] Fruchter, AS et al. 1999 ApJ 516:683.
[121] Fulgione, W 1999 GCN 390.
[122] Galama, T et al. 1997 Nat 387:479.
[123] Galama, T et al. 1997 GCN 21.
[124] Galama, T et al. 1997 IAUC 6574.
[125] Galama, TJ et al. 1997 ApJ 486:L5.
[126] Galama, TJ et al. 1998 ApJ 497:L13.
[127] Galama, TJ et al. 1998 GCN 127.
[128] Galama, TJ et al. 1998 IAUC 6895.
[129] Galama, TJ et al. 1999 GCN 388.
[130] Galama, TJ et al. 1998 GCN 145.
[131] Galama, TJ et al. 1998 GCN 168.
[132] Galama, TJ et al. 1998 GCN 183.
[133] Galama, TJ et al. 1998 ApJ 500:L101.
[134] Galama, TJ et al. 1998 ApJ 500:L97.
[135] Galama, T et al. 1999 Nat 398:394.
[136] Galama, T et al. 2000 ApJ 536:185.
[137] Gandolfi, G et al. 1999 IAUC 7174.
[138] Gandolfi, G 1999 GCN 373.
[139] Gandolfi, G 1999 GCN 366.
[140] Garcia, MR et al. 1998 ApJ 500:L105.
[141] Garcia, MR et al. 1997 IAUC 6792.
[142] Gorosabel, J & Castro-Tirado, AJ 1998 A&A 333:417.
[143] Gorosabel, J et al. 1999 A&AS 138:455.
[144] Gorosabel, J et al. 1999 A&A 347:L31.
[145] Gorosabel, J et al. 1998 A&A 335:L5.
[146] Gorosabel, J et al. 1998 A&A 339:719.
[147] Greiner, J 1997 IAUC 6742.
[148] Greiner, J et al. 1996 IAUC 6487.
[149] Greiner, J et al. 1997 IAUC 6570.
[150] Greiner, J et al. 1997 IAUC 6757.
[151] Greiner, J et al. 1997 IAUC 6722.
[152] Greiner, J et al. 1998 GCN 59.
[153] Groot, PJ et al. 1997 IAUC 6574.
[154] Groot, PJ et al. 1997 IAUC 6723.
[155] Groot, PJ et al. 1997 IAUC 6723.
[156] Groot, PJ et al. 1997 IAUC 6616.
[157] Groot, PJ et al. 1998 ApJ 493:L27.
[158] Groot, PJ et al. 1997 IAUC 6588.
[159] Groot, PJ et al. 1997 IAUC 6584.
[160] Groot, PJ et al. 1998 ApJ 502:L123.
[161] Groot, PJ et al. 1998 IAUC 6852.
[162] Groot, P et al. 1997 GCN 27.
[163] Grossan, B et al. 1998 GCN 34.
[164] Grossan, B et al. 1998 GCN 35.
[165] Gruendl, RA et al. In Meegan, C et al., editors, *Gamma-Ray Bursts* 576 New York 1998. AIP.
[166] Guarnieri, A et al. 1997 IAUC 6733.
[167] Guarnieri, A et al. 1997 A&A 328:L13.
[168] Guarnieri, A et al. 1999 A&AS 138:457.
[169] Guarnieri, A et al. 1998 IAUC 6855.
[170] Hakkila, J et al. 1997 AJ 114:2043.
[171] Halpern, J & Fesen, R 1998 GCN 134.
[172] Halpern, J et al. 1998 GCN 106.
[173] Halpern, J et al. 1998 GCN 163.
[174] Halpern, J et al. 1999 GCN 381.
[175] Halpern, J et al. 1997 IAUC 6788.
[176] Halpern, JP et al. 1999 ApJ 517:L105.
[177] Halpern, JP et al. 1999 GCN 343.
[178] Halpern, JP et al. 1998 Nat 393:41.
[179] Harrison, FA et al. 1999 ApJ 523:L121.
[180] Harrison, TE et al. 1997 IAUC 6721.
[181] Heise, J et al. 1999 IAUC 7099.
[182] Heise, J et al. 1999 IAUC 7217.
[183] Heise, J et al. 1997 IAUC 6610.
[184] Heise, J et al. 1997 IAUC 6787.
[185] Heise, J et al. 1999 IAUC 7221.
[186] Heise, J et al. In Meegan, C et al., editors, *Gamma-Ray Bursts* 397 New York 1998. AIP.
[187] Henden, AA et al. 1998 GCN 140.
[188] Hjorth, J et al. 1997 GCN 109.
[189] Hjorth, J et al. 1999 Science 283:2073.
[190] Hjorth, J et al. 1999 GCN 320.
[191] Hjorth, J et al. 1999 GCN 389.
[192] Hjorth, J et al. 1999 GCN 403.
[193] Holland, S & Hjorth, J 1999 A&A 344:L67.
[194] Hurley, K 1998 GCN 100.
[195] Hurley, K & Barthelmy, S 1999 GCN 309.
[196] Hurley, K et al. 1997 IAUC 6728.
[197] Hurley, K & Cline, T 1999 GCN 347.
[198] Hurley, K et al. 1999 GCN 380.
[199] Hurley, K et al. 1998 GCN 160.
[200] Hurley, K et al. 1997 ApJ 485:L1.
[201] Hurley, K & Feroci, M 1999 GCN 270.
[202] Hurley, K et al. 1998 GCN 53.
[203] Hurley, K et al. 1999 GCN 298.
[204] Hurley, K et al. 1997 IAUC 6687.
[205] Ilovaisky, SA & Chevalier, C 1998 IAUC 6803.
[206] In 't Zand, J et al. 1997 IAUC 6569.
[207] in 't Zand, J et al. 1998 IAUC 6854.
[208] in 't Zand, J et al. 1998 IAUC 6805.

[209] in 't Zand, JJM et al. 1998 ApJ 505:L119.
[210] in 't Zand, JJM et al. 1999 ApJ 516:L57.
[211] Israel, GL et al. 1999 A&A 348:L5.
[212] Iwamoto, K 1999 ApJ 517:L67.
[213] Iwamoto, K 1999 ApJ 512:L47.
[214] Iwamoto, K et al. 1998 Nat 395:672.
[215] Jaunsen, AO et al. 1998 GCN 78.
[216] Jeffery, D 1999 astro-ph/ 9907015.
[217] Jensen, BL et al. 1999 GCN 371.
[218] Kałuzny, J et al. 1999 IAUC 7164.
[219] Kay, LE et al. 1998 IAUC 6969.
[220] Kelson, DD et al. 1999 IAUC 7096.
[221] Kemp, J & Halpern, J 1999 GCN 402.
[222] Kippen, MR et al. 1997 IAUC 6789.
[223] Kippen, RM 1999 GCN 306.
[224] Kippen, RM 1999 GCN 322.
[225] Kippen, RM et al. 1999 GCN 344.
[226] Klose, S 1998 GCN 186.
[227] Klose, S 1998 GCN 28.
[228] Klose, S et al. 1997 IAUC 6756.
[229] Klose, S et al. 1998 IAUC 6864.
[230] Klose, S et al. 1997 IAUC 6611.
[231] Koshut, T 2000 ApJ in preparation.
[232] Kulkarni, SR et al. 1998 GCN 29.
[233] Kulkarni, SR et al. 1999 Nat 398:389.
[234] Kulkarni, SR et al. 1998 Nat 393:35.
[235] Kulkarni, SR et al. 1999 ApJ 522:L97.
[236] Kulkarni, SR et al. 1998 Nat 395:663.
[237] Kulkarni, SR et al. 1997 IAUC 6559.
[238] Kulkarni, SR et al. 1997 IAUC 6723.
[239] Kulkarni, SR et al. 1998 GCN 27.
[240] Kuulkers, E et al. 1999 GCN 326.
[241] Lamb, DQ et al. 1999 A&AS 138:479.
[242] Larkin, J et al. 1998 GCN 44.
[243] Larkin, J et al. 1998 GCN 51.
[244] Levine, A et al. 1998 IAUC 6966.
[245] Li, ZY & Chevalier, RA 1999 ApJ 526:716.
[246] Lidman, C et al. 1998 IAUC 6895.
[247] Lindgren, B et al. 1999 GCN 190.
[248] Luginbuhl, C et al. 1999 GCN 341.
[249] Luginbuhl, C et al. 1996 IAUC 6526.
[250] Mallozzi, R. priv. commun. 2000.
[251] Marshall, F & Takeshima, T 1999 GCN/RXTE_PCA burst position notice Thu 06 May 99 17:27:37 UT.
[252] Marshall, FE et al. 1997 IAUC 6727.
[253] Marshall, FE & Takeshima, T 1998 GCN 58.
[254] Marshall, FE et al. 1997 IAUC 6683.
[255] Marshall, FE et al. 1998 GCN 138.
[256] Masetti, N et al. 1999 GCN 345.
[257] Masetti, N et al. 1999 GCN 327.
[258] Masetti, N et al. 2000 A&A 354:473.
[259] Maury, A 1999 IAUC 7217.
[260] Maury, A et al. 1999 GCN 220.
[261] Maury, A et al. 1999 IAUC 7214.
[262] McKenzie, EH & Schaefer, BE 1999 PASP 111:964.
[263] McMahon, RG et al. 1998 GCN 101.
[264] Mendez, J et al. 1998 IAUC 6806.
[265] Metzger, MR 1998 IAUC 6874.
[266] Metzger, MR et al. 1997 IAUC 6676.
[267] Metzger, MR et al. 1997 Nat 387:879.
[268] Metzger, MR et al. 1997 IAUC 6655.
[269] Metzger, MR et al. 1997 IAUC 6588.
[270] Metzger, MR et al. 1999 GCN 191.
[271] Morris, M et al. 1997 IAUC 6666.
[272] Muller, JM et al. 1999 IAUC 7211.
[273] Muller, JM et al. 1998 IAUC 6910.
[274] Munn, JA et al. 1997 GCN 4.
[275] Murakami, T et al. 1997 IAUC 6687.
[276] Murakami, T et al. 1999 GCN 228.
[277] Murakami, T et al. 1996 IAUC 6481.
[278] Murakami, T et al. 1997 IAUC 6722.
[279] Murakami, T et al. 1997 IAUC 6729.
[280] Murakami, T et al. 1997 IAUC 6732.
[281] Murakami, T et al. 1999 GCN 372.
[282] Nakamura, T 1999 ApJ 522:L101.
[283] Natarajan, P et al. 1997 New Astron. 2:471.
[284] Nicastro, L et al. 1998 A&A 338:L17.
[285] Nicastro, L et al. 1999 A&AS 138:437.
[286] Nicastro, L et al. 1998 IAUC 6912.
[287] Nicastro, L et al. 1999 IAUC 7213.
[288] Odewahn, S et al. 1998 GCN 105.
[289] Odewahn, SC et al. 1999 IAUC 7094.
[290] Odewahn, SC et al. 1998 ApJ 509:L5.
[291] Odewahn, SC et al. 1997 IAUC 6735.
[292] Offutt, W 1999 IAUC 7098.
[293] Owens, A et al. 1998 A&A 339:L37.
[294] Pahre, MA et al. 1997 IAUC 6691.
[295] Palazzi, E et al. 1999 GCN 377.
[296] Palazzi, E et al. 1998 GCN 48.
[297] Palazzi, E et al. 1999 GCN 262.
[298] Palazzi, E et al. 1998 A&A 336:L95.
[299] Palmer, DM et al. In Meegan, C et al., editors, *Gamma-Ray Bursts* 304–308 New York 1998. AIP.
[300] Park, HS et al. 1997 GCN 19.
[301] Patat, F et al. 1999 IAUC 7215.
[302] Patat, F et al. 1998 IAUC 7017.
[303] Pedersen, H et al. 1997 IAUC 6628.
[304] Pedersen, H et al. 1998 GCN 52.
[305] Pedersen, H et al. 1999 GCN 348.
[306] Pedersen, H et al. 1999 GCN 340.
[307] Pedersen, H et al. 1999 GCN 352.
[308] Pedersen, H et al. 1999 GCN 349.
[309] Pedersen, H et al. 1998 ApJ 496:311.
[310] Pedersen, H et al. 1999 GCN 342.
[311] Pedersen, K et al. 1999 GCN 267.
[312] Pedichini, F et al. 1997 A&A 327:L36.
[313] Pian, E et al. 1999 A&AS 138:463.
[314] Pian, E et al. 1998 GCN 69.
[315] Pian, E et al. 1998 ApJ 492:L103.
[316] Piro, L et al. 1998 A&A 331:L41.
[317] Piro, L et al. 1999 IAUC 7111.
[318] Piro, L et al. 1998 GCN 155.
[319] Piro, L & Costa, E 1998 GCN 99.

[320] Piro, L et al. 1996 IAUC 6480.
[321] Piro, L et al. 1996 IAUC 6467.
[322] Piro, L et al. 1999 ApJ 514:L73.
[323] Piro, L et al. 1997 IAUC 6656.
[324] Piro, L & Feroci, M 1998 GCN 72.
[325] Piro, L et al. 1997 IAUC 6617.
[326] Piro, L et al. 1998 A&A 329:906.
[327] Piro, L et al. 1997 IAUC 6797.
[328] Piro, L 1999 GCN 304.
[329] Piro, L 1999 GCN 203.
[330] Piro, L 1999 GCN 199.
[331] Piro, L 1999 GCN 311.
[332] Piro, L 1999 GCN 360.
[333] Pooley, G & Green, D 1997 IAUC 6670.
[334] Pooley, G 1999 GCN 244.
[335] Quashnock, JM et al. 1998 IAUC 6860.
[336] Ramaprakash, AN et al. 1998 GCN 24.
[337] Ramaprakash, AN et al. 1998 Nat 393:43.
[338] Reichart, DE 1999 ApJ 521:L111.
[339] Reichart, DE et al. 1999 ApJ 517:692.
[340] Remillard, R et al. 1997 IAUC 6726.
[341] Rhoads, J & Halpern, J 1997 IAUC 6793.
[342] Rhoads, J et al. 1998 GCN 181.
[343] Ricci, R et al. 1998 IAUC 6910.
[344] Rol, E et al. 1999 GCN 358.
[345] Rol, E et al. 1999 GCN 374.
[346] Sagar, R et al. 1999 Bull. Astron. Soc. India 27:3.
[347] Sahu, K et al. 1997 ApJ 489:L127.
[348] Sahu, KC et al. 1997 Nat 387:476.
[349] Sahu, KC & Sterken, C 1998 IAUC 6808.
[350] Sargent, WLW et al. 1999 GCN 297.
[351] Schaefer, BE 1998 IAUC 6865.
[352] Schaefer, BE 1998 GCN 165.
[353] Schaefer, BE 1999 GCN 259.
[354] Schaefer, BE 1999 GCN 293.
[355] Schaefer, BE et al. 1999 ApJ 524:L103.
[356] Schaefer, BE et al. 1998 GCN 185.
[357] Schlegel, DJ et al. 1998 ApJ 500:525.
[358] Shepherd, DS et al. 1998 ApJ 497:859.
[359] Shepherd, DS et al. 1997 IAUC 6664.
[360] Smith, D et al. 1997 IAUC 6728.
[361] Smith, DA 1998 GCN 159.
[362] Smith, DA et al. 1999 GCN 275.
[363] Smith, DA et al. 1999 ApJ 526:683.
[364] Smith, DA et al. 1997 IAUC 6718.
[365] Smith, DA et al. 1998 GCN 126.
[366] Smith, IA & Gruendl, RA 1997 IAUC 6663.
[367] Smith, IA et al. 1997 ApJ 487:L5.
[368] Smith, IA & Tilanus, RPJ 1997 GCN 15.
[369] Smith, IA & Tilanus, RPJ 1998 IAUC 6868.
[370] Smith, IA et al. 1999 A&A 347:92.
[371] Smith, MJS et al. 1998 IAUC 6938.
[372] Soffitta, P et al. 1998 IAUC 6884.
[373] Soifer, B et al. 1997 IAUC 6619.
[374] Sokolov, V et al. 1998 GCN 148.
[375] Sokolov, V et al. 1998 GCN 147.
[376] Sokolov, VV et al. 2000 Bull. Special Astrophys. Obs. submitted (astro-ph/0001357).
[377] Sokolov, VV et al. 1998 A&A 334:117.
[378] Sokolov, VV et al. 1999 A&A 344:43.
[379] Stanek, KZ et al. 1997 IAUC 6735.
[380] Stanek, KZ et al. 1999 ApJ 522:L39.
[381] Stanek, KZ et al. 1997 IAUC 6721.
[382] Subrahmanyan, R et al. 1999 GCN 376.
[383] Subrahmanyan, R et al. 1999 GCN 357.
[384] Takeshima, T & Marshall, F 1999 GCN/RXTE_PCA burst position notice Fri 07 May 99 02:31:42 UT.
[385] Tanvir, N et al. 1997 IAUC 6796.
[386] Tarei, G et al. 1999 IAUC 7110.
[387] Taylor, GB et al. 1997 IAUC 6670.
[388] Taylor, GB et al. 1997 Nat 389:263.
[389] Taylor, GB et al. 1998 GCN 152.
[390] Taylor, GB et al. 1998 GCN 40.
[391] Taylor, GB et al. 1999 GCN 168.
[392] Taylor, GB et al. 1999 GCN 350.
[393] Taylor, GB et al. 1999 GCN 308.
[394] Taylor, GB et al. 1998 ApJ 502:L115.
[395] Thompson, I et al. 1999 GCN 391.
[396] Tinney, C et al. 1998 IAUC 6896.
[397] Udalski, A. priv. comm. 1998.
[398] Valdes, F et al. 1998 GCN 56.
[399] van Paradijs, J et al. 1997 Nat 386:686.
[400] Voges, W et al. 1997 IAUC 6539.
[401] Vrba, FJ 1999 GCN 194.
[402] Vrba, FJ et al. 2000 ApJ 528:254.
[403] Vrba, FJ et al. 1999 GCN 294.
[404] Vrba, FJ et al. 1999 GCN 300.
[405] Vrba, FJ et al. 1999 GCN 365.
[406] Vrba, FJ & Munn, JA 1997 GCN 2.
[407] Vreeswijk, PM et al. 1999 ApJ 523:171.
[408] Vreeswijk, P et al. 1999 GCN 310.
[409] Vreeswijk, P et al. 1999 GCN 324.
[410] Wagner, RM & Starrfield, S 1998 GCN 162.
[411] Wark, R et al. 1999 GCN 266.
[412] Waxman, E & Draine, BT 2000 ApJ 537:796.
[413] Wheeler, JC et al. 1997 IAUC 6697.
[414] Wieringa, M et al. 1998 IAUC 6896.
[415] Wieringa, MH et al. 1999 A&AS 138:467.
[416] Wijers, RAMJ et al. 1999 ApJ 523:L33.
[417] Williams, GG et al. 1999 ApJ 519:L25.
[418] Woods, P et al. 1998 GCN 112.
[419] Woods, PM et al. 1997 IAUC 6798.
[420] Woosley, SE et al. 1999 ApJ 516:788.
[421] Wozniak, PR 1998 GCN 177.
[422] Yanagisawa, K et al. 1997 IAUC 6731.
[423] Yoshida, A et al. 1997 IAUC 6593.
[424] Yoshida, A et al. 1999 A&AS 138:433.
[425] Zapatero Osorio, MR et al. 1998 IAUC 6967.
[426] Zharikov, SV et al. 1998 A&A 337:356.
[427] Zhu, J & Zhang, HT 1999 GCN 295.

outflow. This means that we expect at least one transition to occur in a collimated outflow; as long as $\theta_b \sim 1/\gamma$ is less than θ_c, the observer sees a smaller part of the outflow than the cone, and therefore cannot distinguish between a spherical and a collimated flow. When $\theta_b = \theta_c$, which happens when the Lorentz factor becomes low enough ($\gamma \lesssim \gamma_b = 1/\theta_b$), the observer begins to see the edge of the cone and thus becomes aware of the collimated nature of the flow. When this happens, the falloff of the light curve becomes steeper; at early times, the decline of the afterglow is a balance between a very steep drop of the surface brightness of the shock and an increase in the observed emitting area proportional to $1/\gamma^2 \propto t^{3/4}$. When $\gamma < 1/\theta_b$, the emitting area, limited by the size of the cone, stays constant; hence, a drop in the exponent of the power law decline by $t^{-3/4}$ is expected.

Because the pressure is very high behind the shock, this decreases the likeliness of a pressure on the edge able to confine it, so one may well ask how long the flow can stay collimated. Here, relativity comes to the rescue: The jet expands sideways no faster than its internal speed of sound ($c/\sqrt{3}$ in the ultrarelativistic limit). Because to an external observer the apparent sideways expansion of the jet is superluminal with speed γc, the angular size of a region of the jet that is causally connected is only of order $1/\gamma$, and the angle by which the jet expands sideways is similar. Therefore, sideways expansion of the jet is unimportant as long as the total jet opening angle is larger than $\theta_b > 1/\gamma$. When the sideways expansion does become important, simple scaling suggests that the radius of the shock front stops expanding, and the energy is lost in one place. More detailed considerations show that in fact the shock Lorentz factor decreases exponentially with radius (Rhoads 1999). However, changes in the area and relativistic kinematics also take place at the same time, and the net result is that an external observer still sees a power-law decline of the brightness, albeit much steeper.

Since the critical angles for the end of collimation and the fanning-out of the emission are of the same order, it is unclear whether the collimation break of $t^{-3/4}$ (Mészáros & Rees 1999) would ever be seen. The detailed calculations by Rhoads (1999) only show a very broad transition between the initial spherical evolution and the steep (t^{-p}) late-time behavior, in which the beaming break is presumably hidden (see also Panaitescu & Mészáros 1999). More recent detailed calculations even suggest that complicating effects cause the collimation break to be much weaker (Kumar & Panaitescu 2000) or even absent (Huang et al 2000), though a jet may manifest itself via a steep break in the transition to non-relativistic evolution. An important aspect of the break resulting from a jet collimation transition is that it is expected to be achromatic, i.e. of the same strength and occurring at the same time in all wavelengths.

The first claim for a possible collimated burst came for GRB 980519 (Halpern et al 1999), which had a very sharply declining afterglow. In this burst, however, the break was not seen (it would have occurred before the first observation), and the data are also consistent with a spherical afterglow expanding into a $1/r^2$ stellar wind (Halpern et al 1999). When a break was seen in the afterglow of GRB 990123, starting about a day after the burst, this was again attributed to a jet (Kulkarni et al

1999a,b). However, closer investigation shows that the break is not nearly strong enough to be caused by a jet, even if only the beaming break occurs and is not seen in *K* band, which is contrary to expectation. Also, the optical data of Castro-Tirado et al (1999) indicate an achromatic decline possibly consistent with a cooling break moving through optical frequencies between days 1 and 3. The short radio afterglow of this source has also been advanced as support for a jet (Kulkarni et al 1999b), but can be interpreted without using a jet as well (Galama et al 1999). The afterglow of GRB 990510 appears to be the first in which the evidence for beaming is strong and has not been the subject of controversy: All optical data from *U* to *K* can be fit with a single transition time and the same asymptotic power-law indices, perhaps with some evidence of deviations in *B*. The values of the pre- and post-break power-law agree with the calculations of Rhoads (1999). In addition, polarization has been detected in this source (Wijers et al 1999; see Section 6.2), which may be related to its jet-like character.

In summary, some clear predictions from collimated outflows are strong enough to rule out certain sources as being beamed, and make at least one source a good candidate. Also, in some well-studied cases significant collimation is ruled out (e.g. GRB 970228 and GRB 970508). The implications for the physics of GRB are considerable: If a burst has a collimation angle of even 10° (very wide by the standard of AGN jets), then only 1.5% of the sky is illuminated by the burst. This means that when making the usual assumption of isotropy, we would overestimate the energy requirements of the central engine by a factor of 100, and at the same time underestimate the formation rate of GRB progenitors by that same factor of 100. This establishes the investigation of the reality of collimation in GRB, and any correlations between collimation and brightness, as one of the more pressing challenges in afterglow research.

6.2 Rings and Polarization

The beaming of the GRB emission has further consequences for the appearance of the afterglow. Because the Lorentz factor of the burst is continually declining, the surface we see at a given observer time is not perfectly elliptical as in the constant-γ case (Rees 1964), nor is it uniform in surface brightness. The point on the line of sight is closest to us, which means that among all the points we see at any given time, the light from that particular point left the surface the latest, so that point is oldest in the frame of the afterglow. Therefore, it has the lowest γ and lowest surface brightness. Consequently, the point approaching us is less bright than those immediately around it. Furthermore, the edge of the afterglow in our observer frame is only of order $1/\gamma$ away in angle from the center. The net result is that the observed surface brightness has a maximum away from the line of sight (by about an angle of $1/\gamma$), i.e. it appears as a ring (Panaitescu & Mészáros 1998b, Sari 1998, Waxman 1997a). At very low frequencies, the less steep dependence of the surface brightness on the Lorentz factor makes this effect nearly go away (Granot et al 1999a).

Because the angular size of the ring is usually too small to resolve and does not change any major scalings, the observable effects are small at best. However, it does offer the chance of an asymmetry that brings about net polarization of the afterglow.

Since the afterglow is synchrotron radiation, its intrinsic polarization will be 60–70%; therefore, rather than asking why it is polarized, we should ask why it is not. Two reasons have been advanced: First, the magnetic field is generated by some instability, and thus should be highly tangled in nature. If the coherence length of the field is much less than the size of the observable afterglow surface, then we expect greatly reduced polarization, to a value of about $60/\sqrt{N}\%$ for N independent patches (Gruzinov & Waxman 1999). Second, there could be net direction to the magnetic field even if it is generated by instability, especially if one accounts for aberration effects in the ring of emission (Medvedev & Loeb 1999, Gruzinov 1999, Ghisellini & Lazzati 1999). If the ring is perfect, the symmetry ensures zero net polarization, but any imperfections would give a net polarization.

In the latter case, beaming and collimation may combine to give a net polarization that varies with time. Initially, when a collimated outflow still has a very high Lorentz factor, we see a complete ring, and the symmetry precludes any net polarization. At very late times, we see the entire outflow, of which the symmetry once again precludes net polarization. At intermediate times, when the beaming cone is similar to the collimation angle and the afterglow light curve is breaking to a steeper decline, we can see part of a ring if our line of sight is offset from the center of the outflow. During this phase the polarization does not average to zero, since we do not get emission from the complete ring.

After a first attempt by Hjorth et al (1999) on GRB 990123, which set an upper limit of 2.3% on polarization, an actual detection was made with the ESO VLT for GRB 990510 (Wijers et al 1999, Covino et al 1999). The polarization was measured as 1.7% around the time of the jet break. The data are consistent both with a symmetry-breaking origin of the polarization and with the random-patch model. Much earlier and later data, during the power-law parts of the light curve, would be needed to distinguish between the two (Wijers et al 1999). Sari (1999) has calculated a toy model of the polarization in the jet case. He showed that the period of maximum polarization near the jet break contains considerable fine structure, with a few minima possible as a result of polarization sign changes. The other burst with measured polarization to date is GRB 990712 (Rol et al 2000). Curiously, this burst does not show any signs of a beaming break, and the middle of three polarization measurements has the lowest value, whereas the polarization angle is constant. It is possible that a beaming break is hidden by the effects of a bright host in this burst, but even so, a minimum in the polarization is not easy to obtain without changes in the polarization angle. Likewise, the random-patch model would predict large angle changes in the polarization as the value changes, so neither model provides a convincing interpretation of this event. The observational difficulties of improving the situation are clear: To detect polarization of 1%, one needs the object to be 5 or 6 magnitudes above the detection limit, and therefore

measurements of polarization can only be made within the first few days after trigger.

6.3 External Density Profiles and Late Evolution

Depending on the type of progenitor, a burst may occur in more or less average interstellar medium, or it may be surrounded by a large amount of circumstellar medium. Consequently, it is not trivial that the ambient medium should have a uniform density. Specifically, the stellar-wind case of a $1/r^2$ density falloff has received some attention since the discovery of a GRB-supernova association (Sections 4 & 7).

Aside from providing smooth changes, circumstellar media also offer the possibility of strong inhomogeneities. For example, a wind has a termination shock where it encounters the older wind pressed up against the interstellar medium, and a forward shock driven into the ISM by the wind pressure. When the blast wave meets these, sudden density changes will lead to jumps and non–self-similar behavior in the afterglows. The maximum in the light curve of GRB 970508 after 1.5 days could represent such a situation. At a shock interface, instabilities may also lead to finger formation and other small-scale irregularity. Dermer & Mitman (1999) and Dermer et al (1999) have suggested that the irregular light curves of gamma-ray bursts may be caused by an encounter of the forward shock with these irregularities. Most recent work has attributed the gamma-ray burst proper to internal shocks in the relativistic outflow (Rees & Mészáros 1994, Kobayashi et al 1997); however, objections to the external shock model seem to be circumvented by this new model, so this has again become an open question (Fenimore et al 1999, Fenimore & Ramirez-Ruiz 1999).

What density structures an observable afterglow will meet depends on its energy; not long after it turns non-relativistic, it declines fast enough to become unobservable, so in broad terms we can define the afterglow phase as lasting from $t_{\rm dec}$ to $t_{\rm NR}$ (Section 3). The non-relativistic phase starts when a mass equal to E/c^2 has been swept up, since at that point the energy per particle is comparable to the rest mass energy, i.e. $M_{\rm NR} = 0.05 E_{52} M_\odot$. This is small compared to the total wind mass ejected by a massive star, so indeed massive stars may produce GRB whose afterglows are entirely within their old wind (Chevalier & Li 1999). However, most of that wind is in a shocked, nearly uniform bubble, so it does not follow that all massive-star GRBs have rapidly fading afterglows characteristic of a $1/r^2$ density profile. This is even more true if the star moves with even a few tens of km/s, because then most of the ejected mass during its life is left far behind and plays no role when the star's life ends.

6.4 Finite Optical Depths, Prompt Emission, and Lines

Except at radio wavelengths, the optical depth of the afterglow to its own emission is negligible. Nonetheless, a variety of observations or other considerations have inspired observers to look for effects of finite optical depth. The oldest concern

is that the peak frequency in a synchrotron model should be very strongly dependent on the Lorentz factor of the blast wave. Combined with the narrow range of observed peak frequencies in GRBs, this raises concerns about the required narrowness of the Lorentz factor distribution. Brainerd et al (1998) has proposed his Compton attenuation model specifically for this: Compton scattering by the external, non-moving medium imposes a signature at a fixed source-frame photon energy of 0.5 MeV. A problem with this model is the large required optical depth, which implies even larger energies for GRB than more conventional models, but also makes it difficult to understand why we generally see little or modest reddening in the optical afterglow. More recent suggestions achieve a signature of a non-moving medium in the spectrum by interaction of the GRB flux with previously emitted and scattered GRB photons, or with external sources of soft radiation (Madau & Thompson 2000, Madau et al 2000, Dermer et al 1999).

The optical depth to MeV photons during the burst has also been rediscussed recently, after the long-held belief that it must be small lest the spectrum become thermalized (the compactness problem; Section 1). It appears that the effects must be mostly small (Lazzati et al 2000, Mészáros & Rees 2000; but see Liang et al 1999), but some unexpected effects did turn up: Granot et al (2000) discovered that the optical depth at the earliest times in a burst could be large enough to cause self-absorption in X-rays. This may answer a long-standing issue that a significant fraction of burst spectra, especially early in the burst, rises more steeply than optically thin synchrotron spectra can account for (Preece et al 1998, Tavani et al 2000). It is important to note that low optical depths do not necessarily imply that any other emission process is energetically unimportant. For example, inverse Compton scattering may have a luminosity as large as $\gamma_e^2\tau$ times the primary luminosity, whereas the random electron Lorentz factor, γ_e, can be hundreds of times the already large shock Lorentz factor. Therefore, even at $\tau \sim 10^{-6}$ this could still produce an important fraction of the energy output (Waxman 1997b, Mészáros et al 1994).

Another effect of finite optical depth (or rather, finite emission measure) is the possibility of emission and absorption lines in the spectra of GRB. An iron line was reported in BeppoSAX NFI X-ray spectra of GRB 970508 (Piro et al 1999). Since this line is not highly blueshifted, it must come from material that does not participate in the relativistic outflow. It may therefore signal the presence of high-density colder material that is being illuminated by the energetic radiation from the GRB, such as the remains of an exploding star (Böttcher 1999, Lazzati et al 1999).

7. HOSTS, COSMOLOGY, AND CENTRAL ENGINE

It has become clear that GRBs lie in star-forming galaxies and are associated with supernovae, and that their great brightness allows us in principle to observe them at high redshifts, perhaps up to $z = 20$ (Wijers et al 1998, Lamb & Reichart 2000). This has greatly increased the interest in gamma-ray bursts as tools for cosmology

and laboratories of high- energy astrophysics, so we will briefly touch upon these subjects here.

7.1 The Association of GRB with Star Formation and Host Galaxies

Prior to 1997 there appeared to be a systematic dearth of sufficiently bright galaxies in the best determined error boxes of γ-ray bursts. This became known as the no host problem (e.g. Band et al 1999). However, as the first afterglows were found, it rapidly became clear that almost all detected counterparts lie in a host galaxy. Furthermore, the large energies required also pointed to source models involving stellar collapses and mergers. This prompted a number of attempts to associate the GRB rate in the universe with the star formation rate (Totani 1997, Wijers et al 1998). It was shown that the observed peak flux distribution of gamma-ray bursts (Figure 19) is consistent with the assumption that the GRB rate in the universe is directly proportional to the star formation rate. Recent discoveries of supernovae associated with GRBs (Section 4) have lent further support to this conclusion.

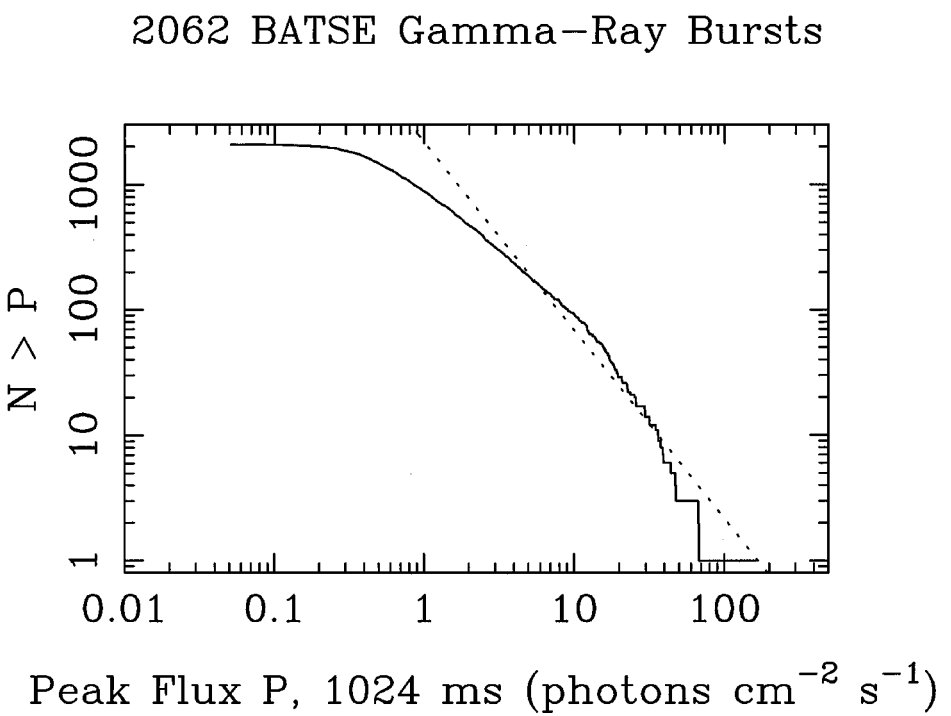

Figure 19 The cumulative peak flux distribution of gamma-ray bursts detected with BATSE. The dotted line (a $-3/2$ power-law) indicates the expected distribution for a uniform density of GRBs in a Euclidean space (M Briggs, private communication).

In star formation-related models, the GRB rate is only 10^{-8} per galaxy per year in the universe at present but was much higher at $z \sim 1$, and the characteristic peak luminosity is 10^{52} erg/s (Wijers et al 1998). Typical GRBs at the BATSE threshold would be at $z \simeq 4$. These results are quite different from those of earlier fits to the peak flux distribution, which assumed standard candles and no evolution of the GRB rate; they typically placed the dimmest BATSE bursts at $z \sim 1$ (e.g. Fenimore et al 1993, Paczyński 1992; but see Fenimore & Bloom 1995).

With a small dozen redshifts and a somewhat greater number of hosts known, it has become clear that GRB luminosities in all wavelengths range widely (Section 5), so the results of standard-candle fits to the flux distribution should be taken with a grain of salt (see e.g. Kommers et al 2000a, Krumholz et al 1998, Schmidt 1999). However, the bursts with known OTs are a much brighter group than the BATSE bursts as a whole, and their median redshift is about 1, making it likely that the dimmest GRBs are very far away indeed. This opens the prospect of using GRBs to study the early universe, e.g. by investigating absorption line forests in their spectra, as is done with quasars up to $z = 5$ (Wijers et al 1998, Lamb & Reichart 2000).

In Figure 20 we have assembled images of the known GRB hosts; measured properties of the hosts are assembled in the summary table (Section 5). They are rather diverse in nature, but share some important characteristics: all are blue, indicating the presence of an abundant number of young stars. In virtually all cases, the OT does not coincide with the center of the galaxy, but does lie within its detectable light distribution (e.g. Bloom et al 1999b). Many of the hosts are subluminous, but the wide range of values includes L_* galaxies (e.g. Hogg & Fruchter 1999). Star formation rates in several hosts have been estimated (Section 5). While they are not particularly high in many cases, the star formation rate per unit luminosity in some is quite substantial (e.g. in the small host of GRB 970508; Natarajan et al 1997). These average properties support the notion that GRBs occur where massive stars are born and die in the Universe.

7.2 Progenitors and Central Engines

The association of GRBs with supernovae and blue host galaxies, as well as the supernova-like energies, clearly suggest an origin of GRBs in some type of stellar death. The most popular among these have been mergers of neutron stars (Paczyński 1986, Goodman et al 1987, Eichler et al 1989, Mochkovitch et al 1993) and massive-star collapses (Woosley 1993, Paczyński 1998). The location of GRB counterparts within the blue parts of galaxies argues against high-velocity progenitors, such as merging neutron stars (Bloom et al 1999c, Bulik et al 1999).

Figure 20 The known host galaxies of GRBs, imaged with HST (0228, 0508, 1214, 0123, 0510), Keck (0828, 0326, 0329, 0519, 0613, 0703, 1226, 0506; courtesy Caltech GRB collaboration), and NTT (0425). Images are $14''$ on a side except 0828, 0123, and 1214, which are $7''$, and 0425 ($2'$ on a side).

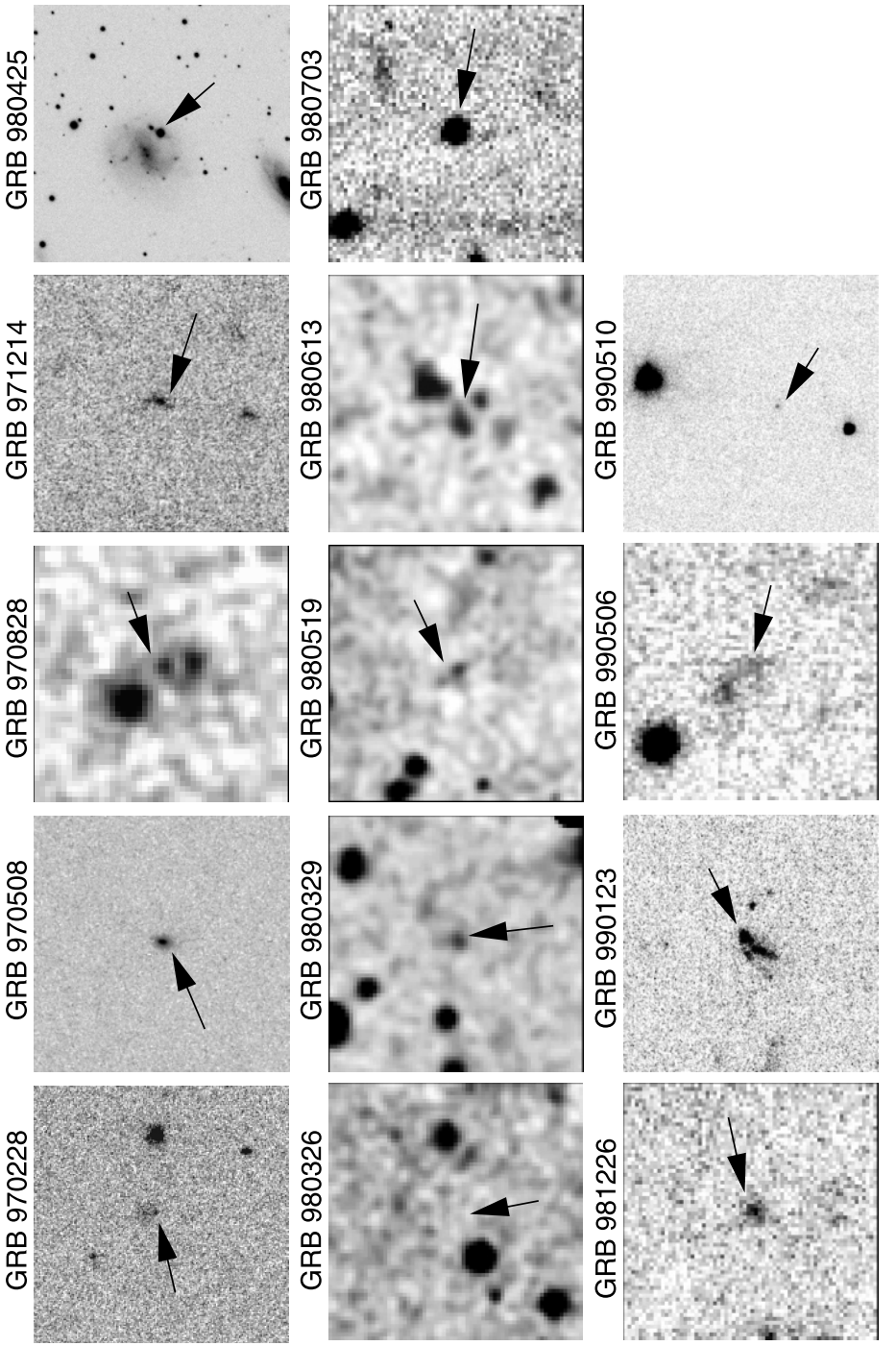
GRB 980425
GRB 980703
GRB 971214
GRB 980613
GRB 990510
GRB 970828
GRB 980519
GRB 990506
GRB 970508
GRB 980329
GRB 990123
GRB 970228
GRB 980326
GRB 981226

While this is true for the bursts thus far located accurately, it should be noted that those are all long-duration bursts. The short bursts (Kouveliotou et al 1993) have not yet been followed up, so it is possible that these represent another type of central engine (e.g. Fryer et al 1999).

The energies provided by many possible central engines are quite similar, since all eventually lead to the formation of a rotating compact object surrounded by debris (Mészáros et al 1999). For some bursts, such as GRB 971214 and GRB 990123, the implied isotropic energy is large $\sim 10^{54}$ erg (Kulkarni et al 1998a, Ramaprakash et al 1998, Halpern et al 1998, Kulkarni et al 1999a, Galama et al 2000). While still within the realm of the possible for the stellar-death models, the efficiency of converting the original energy to gamma rays could be low, so some collimation and beaming of the outflows may be necessary (Kumar 1999, Kumar & Piran 1999).

Two mechanisms have been suggested for the extraction of energy from the central engine. Both use a disk-like configuration around a compact object, and therefore naturally lead to some amount of collimation. First, neutrino annihilation can provide a large energy input while the central object is still hot and accreting rapidly. Because it depends steeply on the neutrino luminosity, it is not expected to last for more than a few to ten seconds (see e.g. Ruffert & Janka 1999). This suffices to push a jet through a helium-star envelope in a collapsar model (MacFadyen & Woosley 1999), but not to power bursts at the long end of the duration distribution (100–1000 s). Second, electromagnetic extraction of rotation energy from a central black hole (Blandford & Znajek 1977) has been proposed. This mechanism has the potential of lasting much longer and extracting somewhat higher energies. Its efficacy is not yet universally accepted (Li 1999, Livio et al 1999), but has recently been discussed in detail by Lee et al (2000a,b), who conclude that it is a viable central-engine model.

8. CONCLUDING REMARKS

In the last three years we have witnessed a tremendous observational breakthrough in our understanding of GRBs. This, in turn, has led to a new generation of GRB models, ironically both based on very old initial concepts: the 1978 fireball model (Cavallo & Rees 1978) and the 1968 and 1974 supernova model (Colgate 1968, Colgate 1974). Over 30 GRBs have provided believable afterglows, and in at least a dozen of these a galaxy host has been clearly identified: The GRB cosmological distance scale is established beyond reasonable doubt. Also among the hard GRB afterglow facts, one should count the following (see Section 5): (1) temporal and spectral power-law decays for all wavelengths, varying between -1.1 and -2.1, and between -0.8 and -2.0, respectively; (2) initial source sizes of the order of μarcsecs (defined by VLA radio scintillation observations); (3) the existence of dark afterglows, i.e. cases where we observe the X-ray but not the optical counterpart; they are thought to lie in dense molecular clouds or have

much steeper decay rates; (4) in some cases, an association between a GRB and a peculiar type of supernova has been established; (5) in almost all cases where a host has been identified, it is a rather blue and actively star-forming galaxy; and (6) given their peak luminosities and their distance scales, GRBs are the most powerful photon emitters in the Universe.

We are still seeking the answers to some major questions on gamma-ray bursts. What is the meaning of dark, afterglow-less bursts? What is the true energy output of GRBs, and how does the central engine deliver it? How high a redshift can we go to in chasing these cosmic explosions? In addition, the mystery of how the prompt gamma-ray emission is precisely produced is still with us.

As the GRB afterglow stamp collection grows, new evidence will emerge and fill in the puzzle. As we pointed out in the introduction to this article, none of this would have been achieved without the dedication of the scientific team of BeppoSAX; they deserve a major part of the credit. Another generous part of the credit should go to the GRB hunters, the tireless observers who scan enormous amounts of data for the elusive counterpart detection, quite often without reward.

The situation will dramatically change with the advent of the new GRB satellites, HETE-2 and SWIFT. Through them, fast and accurate GRB positions will be delivered automatically to the ground for subsequent follow-ups. Although the nature of the hunt may change, following up already identified counterparts instead of searching for them, the existing shortage of observing facilities will become more severe. A good ground-based observatory infrastructure therefore needs to be built and maintained to cope with the (predicted) future deluge of GRB observations. Monitoring, however, should be done in all wavelengths and with high-resolution capability, to further advance the field. GRBs have by now brought together multiple astrophysical disciplines, including early star formation and cosmology. It is a very healthy sign in a field when the excitement of discovery alternates between theorists and observers.

ACKNOWLEDGMENTS

We would like thank the many people whose invaluable help made the completion of this review possible, despite the unusually difficult circumstances. Ed van den Heuvel in Amsterdam and Jerry and Nancy Fishman in Huntsville provided unlimited support despite their own grief. In Amsterdam, Erica Veenhof and Jane Ayal helped with typing the text, and Paul Vreeswijk, Paul Groot, and Evert Rol gave invaluable practical support. We thank Astrid Havinga for keeping our bodies and souls together during the final writing, and Geoff Burbidge for his great patience and encouragement. The compilation of the enormous amount of literature would not have been possible without the authors of the IAU Circular Service, NASA's Astrophysics Data System, the Los Alamos Preprint Server, and Scott Barthelmy's GCN Circular Service. Jochen Greiner's web page (http://www.aip.de:8080/People/JGreiner/grbgen.html) served as an invaluable cross-check reference for Section 5. We are indebted to many colleagues for

their helpful advice and cooperation—especially George Djorgovski, Dale Frail, Andy Fruchter, Tom Koshut, and Shri Kulkarni for sharing unpublished results with us, and Tim Giblin and Michael Briggs for preparing figures for this paper. We wish to thank Valerie Connaughton, Titus Galama, Ed van den Heuvel, Chip Meegan, Peter Mészáros, Elena Pian, Alan Sandage and Re'em Sari for valuable comments on the manuscript. To Titus Galama and Josh Bloom, who prepared one of the most beautiful figures of this review (host galaxies), we would like to say thank you for a job well done.

LITERATURE CITED

Akerlof C, Balsano R, Barthelmy S, Bloch J, Butterworth P, et al. 1999. *Nature* 398:400–2

Atkins R, Benbow W, Berley D, Chen ML, Coyne DG, et al. 2000. *Ap. J.* 533:L119–22

Band DL, Hartmann DH, Schaefer BE. 1999. *Ap. J.* 514:862–68

BATSE Team. 2000. URL http://gammaray.msfc.nasa.gov/batse/

Blandford RD, McKee CF. 1976. *Phys. Fluids* 19:1130–38

Blandford RD, Znajek RL. 1977. *MNRAS* 179:433–56

Bloom JS, Djorgovski SG, Kulkarni SR, Frail DA. 1998a. *Ap. J.* 507:L25–28

Bloom JS, Frail DA, Kulkarni SR, Djorgovski SG, Halpern JP, et al. 1998b. *Ap. J.* 508:L21–24

Bloom JS, Kulkarni SR, Djorgovski SG, Eichelberger AC, Cote P, et al. 1999a. *Nature* 401:453–56

Bloom JS, Kulkarni SR, Harrison F, Prince T, Phinney ES, Frail DA. 1998c. *Ap. J.* 506:L105–8

Bloom JS, Odewahn SC, Djorgovski SG, Harrison SRKFA, Koresko C, et al. 1999b. *Ap. J.* 518:L1–4

Bloom JS, Sigurdsson S, Pols OR. 1999c. *MNRAS* 305:763–69

Boella G, Butler RC, Perola GC, Piro L, Scarsi L, Bleeker JAM. 1997. *Astron. Astrophys. Suppl. Ser.* 122:299–307

Bond HE. 1997. *IAU Circ.* 6654

Böttcher M. 1999. *Ap. J.* In Press (astro–ph/9912030)

Brainerd JJ. 1992 *Nature* 355:552–4

Brainerd JJ, Preece RD, Briggs MS, Pendleton GN, Paciesas WS. 1998. *Ap. J.* 501:325–38

Branch D. 1999. In *Supernovae and Gamma Ray Bursts*, ed. M Livio. In Press (astro–ph/9906168)

Briggs MS. 1999. In *Gamma-Ray Bursts: The First Three Minutes*, ed. J Poutanen, R Svensson, p. 133–50. San Francisco: ASP

Briggs MS, Band DL, Kippen RM, Preece RD, Kouveliotou C, et al. 1999. *Ap. J.* 524:82–91

Briggs MS, Paciesas WS, Pendleton GN, Meegan CA, Fishman GJ, et al. 1996. *Ap. J.* 451:40–63

Bulik T, Belczynski K, Zbijewski W. 1999. *Astron. Astrophys. Suppl. Ser.* 138:483–84

Bulik T, Lamb DQ, Coppi PS. 1998. *Ap. J.* 505:666–87

Burenin RA, Vikhlinin AA, Gilfanov MR, Terekhov OV, Tkachenko AY, et al. 1999. *Astron. Astrophys.* 344:L53–56

Butler RC, Piro L, Costa E, Feroci M, Frontera F, et al. 1997. *IAU Circ.* 6539

Castro-Tirado AJ, Rosa Zapatero-Osorio M, Caon N, Marina Cairos L, Hjorth J, et al. 1999a. *Science* 283:2069–73

Castro-Tirado AJ, Zapatero-Osorio MR, Gorosabel J, Greiner J, Heidt J, et al. 1999b. *Ap. J.* 511:L85–88

Cavallo G, Rees MJ. 1978. *MNRAS* 183:359–65

Chevalier RA, Li ZY. 1999. *Ap. J.* 520:L29–32
Chiang J, Dermer CD. 1999. *Ap. J.* 512:699–710
Cohen E, Piran T, Sari R. 1998. *Ap. J.* 509:717–27
Colgate SA. 1968. *Can. J. Phys.* 46:S476–80
Colgate SA. 1974. *Ap. J.* 187:333–36
Condon JJ. 1999. *Proc. Nat. Acad. Sci. USA* 96:4756–58
Connaughton V. 2000, in preparation
Connors A, Huether GJ. 1998 *Ap. J.* 501:307–24
Costa E, Feroci M, Piro L, Frontera F, Zavattini G, et al. 1997a. *IAU Circ.* 6533
Costa E, Frontera F, Heise J, Feroci M, in't Zand J, et al. 1997b. *Nature* 387:783–85
Covino S, Lazzati D, Ghisellini G, Saracco P, Campana S, et al. 1999. *Astron. Astrophys.* 348:L1–4
Dermer CD, Böttcher M, Chiang J. 1999. *Ap. J.* 515:L49–52
Dermer CD, Mitman KE. 1999. *Ap. J.* 513:L5–8
Djorgovski SG, et al. 2000. in preparation
Djorgovski SG, Kulkarni SR, Bloom JS, Frail DA. 1999. GCN 289
Djorgovski SG, Metzger MR, Kulkarni SR, Odewahn SC, Gal RR, et al. 1997. *Nature* 387:876–78
Eichler D, Livio M, Piran T, Schramm DN. 1989. *Nature* 340:126–28
Fenimore EE, Bloom JS. 1995. *Ap. J.* 453:25–36
Fenimore EE, Conner JP, Epstein RI, Klebesadel RW, Laros JG, et al. 1988. *Ap. J.* 335:L71–74
Fenimore EE, Epstein RI, Ho C, Klebesadel RW, Lacey C, et al. 1993. *Nature* 366:40–42
Fenimore EE, Ramirez-Ruiz E. 1999. *Ap. J.* pp submitted (astro–ph/9909299)
Fenimore EE, Ramirez-Ruiz E, Wu B. 1999. *Ap. J.* 518:L73–76
Feroci M, Antonelli LA, Guainazzi M, Muller JM, Costa E, et al. 1998. *Astron. Astrophys.* 332:L29–33
Feroci M, Frontera F, Costa E, dal Fiume D, Amati L, et al. 1997. *Proceedings of SPIE* 3114:186–97
Fishman GJ, Meegan CA. 1995. *Annu. Rev. Astron. Astrophys.* 33:415–58
Fishman GJ, Meegan CA, Watts JW, Derrickson JH. 1978. *Ap. J.* 223:L13–15
Frail DA, Bloom JS, Kulkarni SR, Sari R, Taylor GB. 2000. in preparation
Frail DA, Kulkarni SR. 1995. *Astrophys. Space Sci.* 231:277–80
Frail DA, Kulkarni SR. 1997. *IAU Circ.* 6662
Frail DA, Kulkarni SR, Costa E, Frontera F, Heise J, et al. 1997a. *Ap. J.* 483:L91–94
Frail DA, Kulkarni SR, Nicastro L, dal Fiume D, Orlandini M, et al. 1997b. *IAU Circ.* 6545
Frail DA, Kulkarni SR, Nicastro L, Feroci M, Taylor GB. 1997c. *Nature* 389:261–63
Frontera F, Costa E, Piro L, Antonelli LA, Voges W, et al. 1997. *IAU Circ.* 6567
Fruchter AS, Pian E, Gibbons R, Thorsett SE, Ferguson H, et al. 2000. *Ap. J.* submitted (astro-ph/9903236)
Fruchter AS, Pian E, Thorsett SE, Bergeron LE, González RA, et al. 1999. *Ap. J.* 516:683–92
Fryer CL, Woosley SE, Hartmann DH. 1999. *Ap. J.* 526:152–77
Galama T, Briggs M, Wijers RAMJ, Vreeswijk PM, Rol E, et al. 1999. *Nature* 398:394–99
Galama T, Groot PJ, van Paradijs J, Kouveliotou C, Robinson CR, et al. 1997. *Nature* 387:479–81
Galama T, Tanvir N, Vreeswijk P, Wijers R, Groot P, et al. 2000. *Ap. J.* 536:185–94
Galama TJ, Groot PJ, van Paradijs J, Kouveliotou C, Strom RG, et al. 1998a. *Ap. J.* 497:L13–16
Galama TJ, Vreeswijk PM, Pian E, Frontera F, Doublier V, Gonzalez JF. 1998b. *IAU Circ.* 6895
Galama TJ, Vreeswijk PM, van Paradijs J, Kouveliotou C, Augusteijn T, et al. 1998c. *Nature* 395:670–72
Galama TJ, Wijers RAMJ, Bremer M, Groot PJ, Strom RG, et al. 1998d. *Ap. J.* 500:L97–100
Gallant YA, Achterberg A. 1999. *MNRAS* 305:L6–10
Gallant YA, Achterberg A, Kirk JG. 1999. *Astron. Astrophys. Suppl. Ser.* 138:549–50

Garcia MR, Callanan PJ, Moraru D, McClintock JE, Tollestrup E, Willner SP, et al. 1998. *Ap. J.* 500:L105–8

Germany LM, Reiss DJ, Sadler EM, Schmidt BP, Stubbs CW. 1999. *Ap. J.* 533:320–28

Ghisellini G, Lazzati D. 1999. *MNRAS* 309:L7–11

Giblin T, VanParadijs J, Kouveliotou C, Connaughton V, Wijers RAMJ, Fishman GJ. 1999. *Ap. J.* 524:L41–50

Goodman J, Dar A, Nussinov S. 1987. *Ap. J.* 314:L7–10

Gorosabel J, Castro-Tirado AJ, Wolf C, Heidt J, Seitz T, et al. 1998. *Astron. Astrophys.* 339:719–28

Granot J, Piran T, Sari R. 1999a. *Ap. J.* 513:679–89

Granot J, Piran T, Sari R. 1999b. *Ap. J.* 527:236–46

Granot J, Piran T, Sari R. 2000. *AP. J.* 534:L163–6

Greiner J, Wenzel W, Degel W. 1990. *Astron. Astrophys.* 234:251–61

Greiner J, Wenzel W, Hudec R, Pravec P, Rezek T, et al. 1993. In *Compton Gamma-Ray Observatory*, ed. M Friedlander, N Gehrels, DJ Macomb, pp. 828–32. New York: AIP

Groot PJ, Galama TJ, van Paradijs J, Kouveliotou C, Wijers RAMJ, et al. 1998a. *Ap. J.* 493:L27

Groot PJ, Galama TJ, van Paradijs J, Melnick G, vander Steene G, et al. 1997a. *IAU Circ.* 6588

Groot PJ, Galama TJ, van Paradijs J, Strom RG, Telting J, et al. 1997b. *IAU Circ.* 6584

Groot PJ, Galama TJ, Vreeswijk PM, Wijers RAMJ, Pian E, et al. 1998b. *Ap. J.* 502:L123–26

Gruzinov A. 1999. *Ap. J.* 525:L29–31

Gruzinov A, Waxman E. 1999. *Ap. J.* 511:852–61

Hakkila J, Meegan CA, Pendleton GN, Fishman GJ, Wilson RB, et al. 1994. *Ap. J.* 422:659–70

Halpern JP, Kemp J, Piran T, Bershady MA. 1999. *Ap. J.* 517:L105–8

Halpern JP, Thorstensen JR, Helfand DJ, Costa E. 1998. *Nature* 393:41–43

Hjorth J, Bjornsson G, Andersen MI, Caon N, Marina Cairos L, et al. 1999. *Science* 283:2073

Höflich P, Wheeler JC, Wang L. 1999. *Ap. J.* 521:179–89

Hogg DW, Fruchter AS. 1999. *Ap. J.* 520:54–58

Huang YF, Dai ZG, Lu T. 1999. *MNRAS* 309:513–16

Hudec R, Ceplecha Z, Spurny P, Florián J, Kolá A, et al. 1999. *Astron. Astrophys. Suppl. Ser.* 138:591–92

Hudec R, Soldan J. 1995. *Astrophys. Space Sci.* 231:311–14

Hughes PA, Miller L. 1991. In *Beams and Jets in Astrophysics*, ed. PA Hughes, 19:1–51, Cambridge:CUP

Hurley K. 1986. In *Gamma-ray Burst and Neutrino Star Physics*, ed. EP Liang, V Petrosian, 141:1. New York: AIP

Hurley K, Cline T, Mazets E, Aptekar R, Golenetskii S, et al. 2000a. *Ap. J.* 534: L23–5

Hurley K, Feroci M, Cinti M, Costa E, Preger B, et al. 2000b. *Ap. J.* 534:258–64

Hurley K, Hartmann D, Kouveliotou C, Fishman G, Laros J, et al. 1997. *Ap. J.* 479:L113–16

In't Zand, J, Heise J, Hoyng P, Jager R, Piro L, et al. 1997. *IAU Circ.* 6569

Iwamoto K. 1999a. *Ap. J.* 517:L67–67

Iwamoto K. 1999b. *Ap. J.* 512:L47–50

Iwamoto K, Mazzali PA, Nomoto K, Umeda H, Nakamura T, et al. 1998. *Nature* 395:672–74

Jager R, Heise J, In't Zand J, Brinkman AC. 1995. *Adv. Space Res.* 13:315–18

Katz JI. 1994a. *Ap. J.* 432:L107–9

Katz JI. 1994b. *Ap. J.* 422:248–59

Katz JI, Piran T. 1997. *Ap. J.* 490:772

Kippen RM, Briggs MS, Kommers JM, Kouveliotou C, Hurley K, et al. 1998. *Ap. J.* 506:L27–30

Klebesadel RW, Strong IB, Olson RA. 1973. *Ap. J.* 182:L85–88

Kobayashi S, Piran T, Sari R. 1997. *Ap. J.* 490:92
Kolatt T, Piran T. 1996. *Ap. J.* 467:L41–44
Kommers JM, Lewin WHG, Kouveliotou C, van Paradijs J, Pendleton GN, et al. 2000a. *Ap. J.* 533:696–709
Kommers JM, Lewin WHG, Kouveliotou C, van Paradijs J, Pendleton GN, et al. 2000b. *Ap. J.* In preparation
Kouveliotou C, Meegan CA, Fishman GJ, Bhat NP, Briggs MS, et al. 1993. *Ap. J.* 413:L101–4
Krimm HA, Vanderspek RK, Ricker GR. 1996. *Astron. Astrophys. Suppl. Ser.* 120:251
Krumholz MR, Thorsett SE, Harrison FA. 1998. *Ap. J.* 506:L81–84
Kulkarni SR, Berger E, Bloom JS, Chaffee F, Diercks A, et al. 2000. In *Gamma-Ray Bursts*, ed. Kippen RM, RS Mallozzi, GJ Fishman. In press
Kulkarni SR, Djorgovski SG, Odewahn SC, Bloom JS, Gal RR, et al. 1999a. *Nature* 398:389–94
Kulkarni SR, Djorgovski SG, Ramaprakash AN, Goodrich R, Bloom JS, et al. 1998a. *Nature* 393:35–39
Kulkarni SR, Frail DA, Moriarty-Schieven GH, Shepherd DS, Udomprasert P, et al. 1999b. *Ap. J.* 522:L97–100
Kulkarni SR, Frail DA, Wieringa MH, Ekers RD, Sadler EM, et al. 1998b. *Nature* 395:663–69
Kumar P. 1999. *Ap. J.* 523:L113–16
Kumar P, Panaitescu A. 2000. *Ap. J. Lett.* Submitted (astro-ph/0003264)
Kumar P, Piran T. 2000. *Ap. J.* 535: 152–57
Lamb DQ. 1995. *Publ. Astron. Soc. Pac.* 107:1152
Lamb DQ, Reichart D.2000. *Ap. J.* 536:1–18
Larson SB, McLean IS, Becklin EE. 1996. *Ap. J.* 460:L95–98
Lazzati D, Campana S, Ghisellini G. 1999. *Astron. Astrophys. Suppl. Ser.* 138:547–48
Lazzati D, Ghisellini G, Celotti A, Rees MJ. 2000. *Ap. J.* 529:L17–20
Lee B, Akerlof C, Band D, Barthelmy S, Butterworth P, et al. 1997. *Ap. J.* 482:L125
Lee HK, Brown GE, Wijers RAMJ. 2000a. *Ap. J.* 536:416–19
Lee HK, Wijers RAMJ, Brown GE. 2000b. *Phys. Rep.* 325:83–114
Li LX. 1999. *Phys. Rev. D* 61:084016
Liang EP, Crider A, Böttcher M, Smith IA. 1999. *Ap. J.* 519:L21–24
Livio M, Ogilvie GI, Pringle JE. 1999. *Ap. J.* 512:100–4
Loeb A, Perna R. 1998. *Ap. J.* 495:597–603
MacFadyen AI, Woosley SE. 1999. *Ap. J.* 524:262–89
Madau P, Blandford RD, Rees MJ. 2000. *Ap. J.* In press
Madau P, Thompson C. 2000. *Ap. J.* 534:239–47
Mazets EP, Golenetskii SV, Aptekar RL, Gurian IA, Ilinskii VN. 1981. *Nature* 290:378–82
McNamara BJ, Harrison TE, Williams CL. 1995. *Ap. J.* 452:L25–28
Medvedev MV, Loeb A. 1999. *Ap. J.* 526:697–706
Meegan CA, Fishman GJ, Wilson RB, Paciesas WS, Pendleton GN, et al. 1992. *Nature* 355: 143–45
Mészáros P, Laguna P, Rees MJ. 1993. *Ap. J.* 415:181–90
Mészáros P, Rees MJ. 1993. *Ap. J.* 418:L59–62
Mészáros P, Rees MJ. 1997. *Ap. J.* 476:232–37
Mészáros P, Rees MJ. 1999. *MNRAS* 306:L39–43
Mészáros P, Rees MJ. 2000. *Ap. J.* 530:292–98
Mészáros P, Rees MJ, Papathanassiou H. 1994. *Ap. J.* 432:181–93
Mészáros P, Rees MJ, Wijers RAMJ. 1998. *Ap. J.* 499:301–8
Mészáros P, Rees MJ, Wijers RAMJ. 1999. New Astron. 4:303–12
Metzger MR, Cohen JG, Chaffee FH, Blandford RD. 1997a. *IAU Circ.* 6676
Metzger MR, Djorgovski SG, Steidel CC, Kulkarni SR, Adelberger KL, Frail, DA. 1997b. *IAU Circ.* 6655

Metzger MR, Kulkarni SR, Djorgovski SG, Gal R, Steidel CC, Frail DA. 1997c. *IAU Circ.* 6588

Mochkovitch R, Hernanz M, Isern J, Martin X. 1993. *Nature* 361:236–38

Murakami T, Fujii M, Hayashida K, Itoh M, Nishimura J. 1988. *Nature* 335:234–5

Natarajan P, Bloom JS, Sigurdsson S, Johnson RA, Tanvir NR, et al. 1997. *New Astron.* 2:471–75

Norris JP, Marani GF, Bonnell JT. 2000. *Ap. J.* 534:248–57

Norris JP, Nemiroff RJ, Scargle JD, Kouveliotou C, Fishman GJ, et al. 1994. *Ap. J.* 424:540–545

Paciesas WS, Meegan CA, Pendleton GN, Briggs MS, Kouveliotou C, et al. 1999. *Astrophys. J. Suppl. Ser.* 122:465–95

Paczyński B. 1986. *Ap. J.* 308:L43–46

Paczyński B. 1992. *Nature* 355:521

Paczyński B. 1995. *Publ. Astron. Soc. Pac.* 107:1167

Paczyński B. 1998. *Ap. J.* 494:L45–48

Paczyński B, Rhoads JE. 1993. *Ap. J.* 418:L5–8

Panaitescu A. Mészáros P. 1998a. *Ap. J.* 501: 772–9

Panaitescu A. Mészáros P. 1998b. *Ap. J.* 493: L31–34

Panaitescu A. Mészáros P. 1999. *AP. J.* 526: 707–15

Park HS, Ables E, Band DL, Barthelmy SD, Bionta RM, et al. 1997. *Ap. J.* 490:99–108

Pedersen H, Jaunsen AO, Grav T, Ostensen R, Andersen MI, et al.1998. *Ap. J.* 496: 311–5

Pendleton GN, Hakkila J, Meegan CA. 1998. In *Gamma-Ray Bursts*, ed. C Meegan, R Preece, T Koshut, p. 899. New York: AIP

Pian E, Amati L, Antonelli LA, Butler RC, Costa E, et al. 1999. *Astron. Astrophys. Suppl. Ser.* 138:463–64

Pian E, Fruchter AS, Bergeron LE, Thorsett SE, Frontera F, et al. 1998. *Ap. J.* 492:L103–6

Piran T. 1999. *Phys. Rep.* 314:575–667

Piro L, Butler R, Fiore F, Antonelli A, Pian E. 1998a. *GCN 155*

Piro L, Costa E, Feroci M, Frontera F, Amati L, et al. 1999. *Ap. J.* 514:L73–77

Piro L, Heise J, Jager R, Costa E, Frontera F, et al. 1998b. *Astron. Astrophys.* 329:906–10

Podsiadlowski P, Rees MJ, Ruderman M. 1995. *MNRAS* 273:755–71

Preece RD, Briggs MS, Mallozzi RS, Pendleton GN, Paciesas WS, Band DL. 1998. *Ap. J.* 506:L23–26

Ramaprakash AN, Kulkarni SR, Frail DA, Koresko C, Kuchner M, et al. 1998. *Nature* 393:43–46

Ramirez-Ruiz E, Fenimore EE. 2000. In *Gamma-Ray Bursts* ed. RM Kippen, RS Malliozzi, GJ Fishman. In press

Rees MJ. 1964. PhD thesis. University of Cambridge

Rees MJ, Mészáros P. 1992. *MNRAS* 258:L41–43

Rees, MJ Mészáros P. 1994. *Ap. J.* 430:L93–96

Reichart DE. 1999. *Ap. J.* 521:L111–15

Rhoads JE. 1999. *Ap. J.* 525:737–49

Rol E, Wijers RAMJ, Vreeswijk PM, Galama TJ, Van Paradijs J, Kouveliotou C, et al. 2000. *Ap. J.* In press

Ruffert M, Janka HT. 1999. *Astron. Astrophys.* 344:573–606

Rybicki GB, Lightman AP. 1979. *Radiative Processes in Astrophysics.* New York: Wiley & Sons

Sahu KC, Livio M, Petro L, Macchetto FD, van Paradijs J, et al. 1997. *Nature* 387:476–78

Sari R. 1998. *Ap. J.* 494:L49–52

Sari R. 1999. *Ap. J.* 524:L43–46

Sari R, Piran T. 1999. *Ap. J.* 517:L109–12

Sari R, Piran T, Narayan R. 1998. *Ap. J.* 497:L17–20

Schaefer BE. 1981. *Nature* 294:722–24

Schaefer BE. 1990. *Ap. J.* 364:590–600

Schaefer BE. 1992. In *Gamma-Ray Bursts—Observations, Analyses and Theories.* ed. C Ho, RI Epstein, EE Fenimore, pp. 107–12. Cambridge, UK: Cambridge Univ. Press

Schaefer BE. 1998. In *Gamma-Ray Bursts*, ed. Meegan CA, Preece RD, Koshut TM. pp. 595–99. New York: AIP

Schaefer BE, Bradt HV, Barat C, Hurley K, Niel M, Vedrenne G, et al. 1984. *Ap. J.* 286:L1–L4
Schmidt M. 1999. *Ap. J.* 523:L117–20
Schmidt WKH. 1978. *Nature* 271:525–27
Sedov L. 1969. *Similarity and Dimensional Methods in Dynamics*. New York: Academic
Shklovskii IS, Mitrofanov IG. 1985. *MNRAS* 212:545–51
Sokolov VV, Kopylov AI, Zharikov SV, Feroci M, Nicastro L, Palazzi E. 1998. *Astron. Astrophys.* 334:117–23
Steidel CC, Sargent WLW. 1992. *Astrophys. J. Suppl. Ser.* 80:1–108
Stern B, Tikhomirova Y, Stepanov M, Kompaneets D, Berezhnoy A, Svensson R. 1999. *Astron. Astrophys. Suppl. Ser.* 138:413–14
Takeshima T, Marshall FE, Corbet RHD, Cannizzo JK, Valinia A, et al. 1998. In *Gamma-Ray Bursts.* ed. CA Meegan, RD Preece, TM Koshut, pp. 414–19. New York: AIP
Tavani M, Band D, Ghirlanda G. 2000. In *Gamma-Ray Bursts.* ed. RM Kippen, RS Mallozzi, GJ Fishman. In press
Taylor GB, Frail DA, Beasley AJ, Kulkarni SR. 1997. *Nature* 389:263–65
Taylor GI. 1950. *Proc. R. Soc. London, Ser. A* 201:159
Terlevich R, Fabian A, Turatto M. 1999. *IAU Circ.* 7269
Totani T. 1997. *Ap. J.* 486:L71–74
Usov VV, Chibisov GV. 1975. *Sov. Astron.* 19:115–16
van den Bergh S, Tammann GA. 1991. *Annu. Rev. Astron. Astrophys.* 29:363–407
van Paradijs J, Groot PJ, Galama T, Kouveliotou C, Strom, RG, et al. 1997. *Nature* 386: 686–89
Voges W, Boller T, Greiner J. 1997. *IAU Circ.* 6539
Vreeswijk PM, Galama TJ, Owens A, Oosterbroek T, Geballe TR, et al. 1999. *Ap. J.* 523:171–76
Wang L, Wheeler JC. 1998. *Ap. J.* 504:L87–90
Waxman E. 1997a. *Ap. J.* 491:L19–22
Waxman E. 1997b. *Ap. J.* 489:L33–36
Waxman E. 1997c. *Ap. J.* 485:L5–8
Wijers RAMJ, Bloom JS, Bagla JS, Natarajan P. 1998. *MNRAS* 294:L13–17
Wijers RAMJ, Galama TJ. 1999. *Ap. J.* 523:177–86
Wijers RAMJ, Rees MJ, Mészáros P. 1997. *MNRAS* 288:L51–56
Wijers RAMJ, Vreeswijk PM, Galama TJ, Rol E, van Paradijs J, et al. 1999. *Ap. J.* 523:L33–36
Woosley SE. 1993. *Ap. J.* 405:273–77
Woosley SE, Eastman RG, Schmidt BP. 1999. *Ap. J.* 516:788–96
Yoshida A, Namiki M, Otani C, Kawai N, Murakami T, et al. 1999. *Astron. Astrophys. Suppl. Ser.* 138:433–34
Zharikov SV, Sokolov VV, Baryshev YV. 1998. *Astron. Astrophys.* 337:356–62
Żytkow AN. 1990. *Ap. J.* 359:138–54

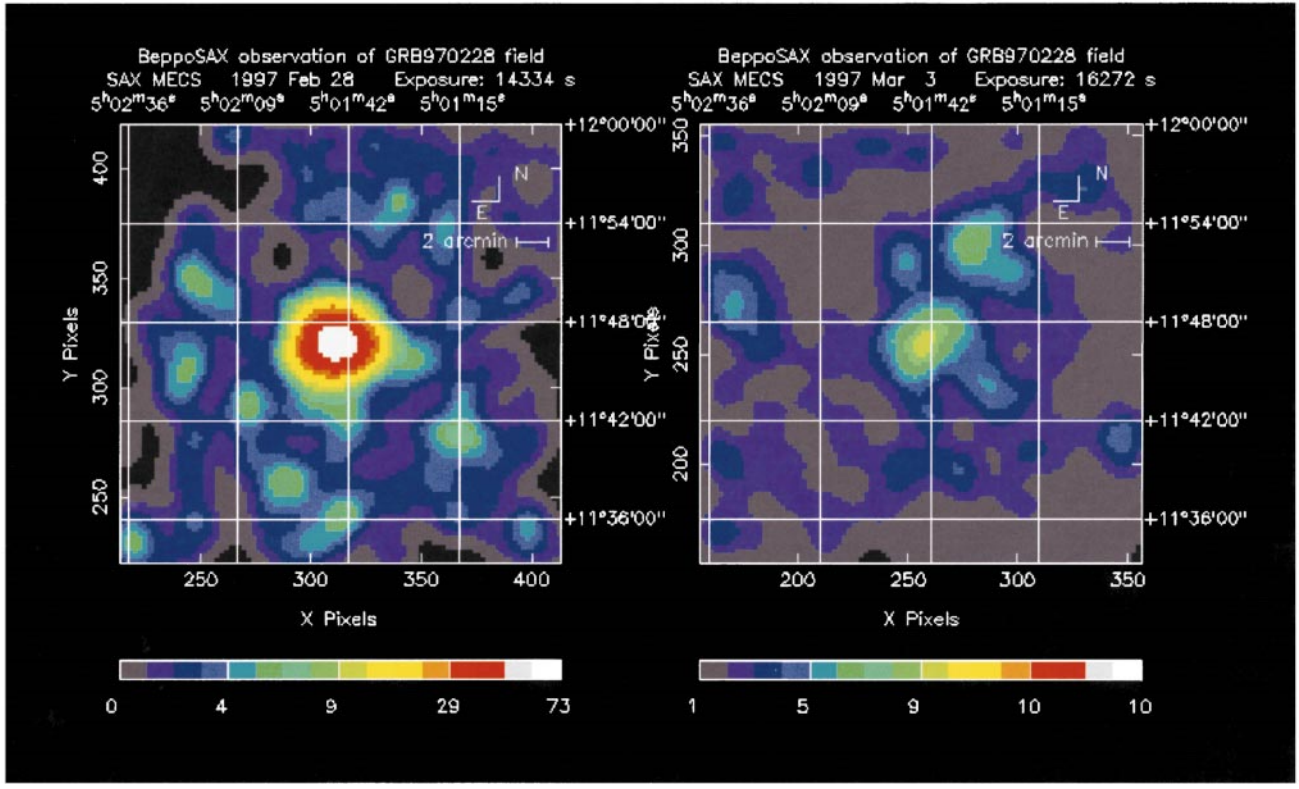

Figure 4 Discovery images of the X-ray afterglow of GRB 970228 with the BeppoSAX NFI (Costa et al 1976).

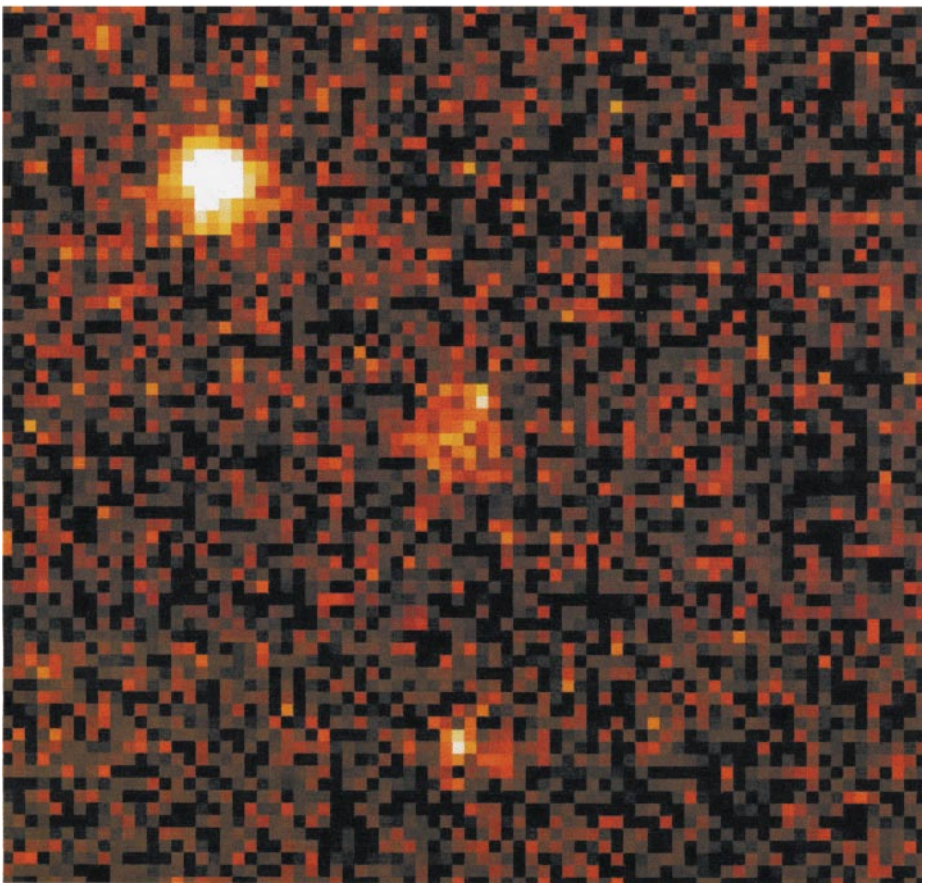

Figure 6 The host galaxy of GRB 970228 (*center*), imaged with HST. The six-month-old afterglow is still visible (*bright pixel*) at the top right edge of the host (Fruchter et al 1999).

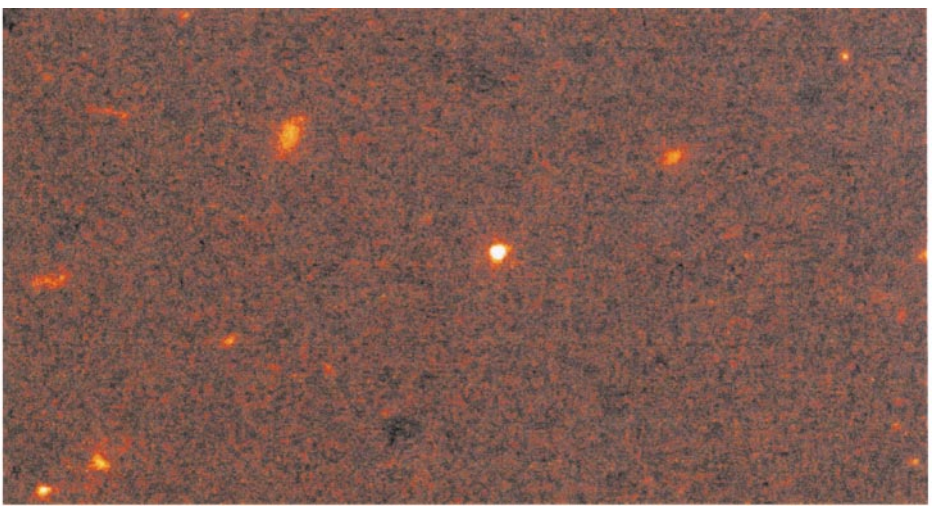

Figure 10 HST/STIS image of the OT of GRB 970508 (Pian et al 1998). The faint host only became visible after the OT had faded.